

Statistical methods for the estimation of pollutant loads from monitoring data

Final Project Report

Petra Kuhnert, You-Gan Wang, Brent Henderson, Lachlan Stewart and Scott Wilkinson
CSIRO Mathematical and Information Sciences



Burdekin Falls Dam, February 2007 (Lachlan Stewart / CSIRO)



Australian Government

**Department of the Environment,
Water, Heritage and the Arts**

Supported by the Australian Government's
Marine and Tropical Sciences Research Facility
Project 3.7.7 Analysis and synthesis of information for reporting credible
estimates of loads for compliance against targets and tracking trends in loads

© CSIRO Mathematical and Information Sciences: To the extent permitted by law, all rights are reserved and no part of this publication covered by copyright may be reproduced or copied in any form or by any means except with the written permission of the CSIRO.

CSIRO advises that the information contained in this publication comprises general statements based on scientific research. The reader is advised and needs to be aware that such information may be incomplete or unable to be used in any specific situation. No reliance or actions must therefore be made on that information without seeking prior expert professional, scientific and technical advice. To the extent permitted by law, CSIRO (including its employees and consultants) excludes all liability to any person for any consequences, including but not limited to all losses, damages, costs, expenses and any other compensation, arising directly or indirectly from using this publication (in part or in whole) and any information or material contained in it.

This report should be cited as:

Kuhnert, P., Wang, Y-G., Henderson, B., Stewart, L. and Wilkinson, S. (2009) *Statistical methods for the estimation of pollutant loads from monitoring data. Final project report.* Report to the Marine and Tropical Sciences Research Facility. Reef and Rainforest Research Centre Limited, Cairns (92pp.).

The Australian Government's Marine and Tropical Sciences Research Facility (MTSRF) supports world-class, public good research. The MTSRF is a major initiative of the Australian Government, designed to ensure that Australia's environmental challenges are addressed in an innovative, collaborative and sustainable way. The MTSRF investment is managed by the Department of the Environment, Water, Heritage and the Arts (DEWHA), and is supplemented by substantial cash and in-kind investments from research providers and interested third parties. The Reef and Rainforest Research Centre Limited (RRRC) is contracted by DEWHA to provide program management and communications services for the MTSRF.

The views and opinions expressed in this publication are those of the authors and do not necessarily reflect those of the Australian Government or the Minister for the Environment, Water, Heritage and the Arts or Minister for Climate Change and Water.

While reasonable effort has been made to ensure that the contents of this publication are factually correct, the Commonwealth does not accept responsibility for the accuracy or completeness of the contents, and shall not be liable for any loss or damage that may be occasioned directly or indirectly through the use of, or reliance on, the contents of this publication.

This report is available for download from the Reef and Rainforest Research Centre Limited website:
http://www.rrrc.org.au/mtsr/theme_3/project_3_7_7.html



August 2009

Contents

List of Figures.....	ii
List of Tables.....	v
Executive Summary	viii
1. Introduction	1
2. Importance of a credible loads calculation.....	4
2.1 Measurement uncertainty	6
2.2 Stochastic uncertainty	7
2.3 Knowledge uncertainty	9
3. Loads methodology	9
3.1 Regression based methodology	9
3.2 Important system processes for GBR catchments	11
3.2.1 Phenomena 1: First flush.....	11
3.2.2 Phenomena 2: Rising / falling limb sampling biases.....	12
3.2.3 Phenomena 3: Exhaustion.....	14
3.2.4 Phenomena 4: Hysteresis.....	16
3.2.5 Phenomena 5: Overbank flow	18
3.3 The generalised rating curve approach	19
3.4 Estimating pollutant loads from the regression model.....	20
3.5 Estimating load uncertainty	20
4. Case Study 1: Burdekin Catchment.....	21
4.1 Catchment characteristics	21
4.2 Inkerman Bridge	23
4.2.1 Total suspended sediment (TSS)	24
4.2.2 Oxidised nitrogen (NOx)	29
4.3 Bowen River	33
4.4 Mistake Creek.....	40
4.5 Summary of results for the Burdekin Catchment.....	43
5. Case Study 2: Tully Catchment.....	45
5.1 Catchment characteristics	45
5.2 Tully River.....	45
6. Validation of the method.....	50
6.1 Simulation study	52
6.1.1 Simulations of a wet site	54
6.1.2 Simulations of a dry site.....	54
6.2 Conclusions	62
7. Discussion	63

- 8. Conclusions and future work..... 64**
- 9. References 65**
- A. Model estimates for the Burdekin Catchment 70**
- B. Loads estimates for Inkerman Bridge, Burdekin Catchment.....**
- C. Model estimates for the Tully River at Euramo 70**
- D. Loads estimates for the Tully River at Euramo 75**

List of Figures

1	Overview of Project 3.7.7	1
2	Demonstrating the difference between bias and the true value.	5
3	Tully river at Euramo site showing measured flow and total suspended sediment (TSS) from 2000-2008.	8
4	A snapshot from Inkerman Bridge in the Burdekin showing the concept of a "flush" in m ³ /L which is determined using the 90th percentile for each financial year.	13
5	A snapshot from Inkerman Bridge in the Burdekin showing an event and the rising/falling limb corresponding to that event.	14
6	Depth-turbidity relationship in the Bowen river at Myuna for four events in the 2006/07 wet season.	15
7	Implications of the discount factor in the calculation of the discounted flow term when (a) $d = 0.1$, (b) $d = 0.5$, (c) $d = 0.95$ and (d) $d = 0.99$	17
8	Plot showing flow, TSS and NO _x captured at the Inkerman Bridge site along the Burdekin River.	23
9	Plots showing the predictive contribution of $\log(D)$ with respect to TSS for the Inkerman Bridge site.	25
10	Residual plots examining the fit of the final model for TSS for the Inkerman Bridge site.	26
11	Summary and comparison of loads estimates for Inkerman bridge for TSS under the 4 different error structures.	28
12	Plots showing the predictive contribution of $\log(D)$ with respect to NO _x at the Inkerman Bridge site.	30
13	Periodic term fit in the generalised additive model for the Inkerman Bridge site across a water year.	30
14	Residual plots examining the fit of the final model for NO _x recorded at the Inkerman Bridge site.	31
15	Summary and comparison of loads estimates for Inkerman bridge for NO _x	32

16	Plot showing flow, TSS and NO _x captured at the Myuna site along the Bowen river.	34
17	Plots showing the predictive contribution of $\log(D)$ with respect to TSS and NO _x for the Myuna site along the Bowen River.	35
18	Periodic term fitted to the Myuna dataset showing the contribution to NO _x on the y -axis (log-scale) and time on the x -axis.	37
19	Residual plots for the model fit to (a) TSS and (b) NO _x at the Myuna site in the Bowen River.	38
20	Summary of loads estimates for the Myuna site for (a) TSS and (b) NO _x	39
21	Plot showing (a) flow, (b) TSS and (c) NO _x captured at the Mistake Creek site along the Bowen river.	40
22	Residual plots for the model fit to (a) TSS and (b) NO _x at the Mistake Creek site in the Burdekin catchment.	41
23	Summary of loads estimates for Mistake Creek for (a) TSS and (b) NO _x	42
24	Plot showing (a) flow and (b) TSS captured at the Euramo site along the Tully river.	46
25	Residual plots for the final GAM model fit to the tully dataset.	47
26	Plots showing the predictive contribution of $\log(D)$ with respect to NO _x for the Euramo site along the Tully River.	47
27	Periodic term fit in the generalised additive model for the Euramo site in the Tully River	48
28	Summary and comparison of loads estimates for the Euramo site along the Tully river for TSS	49
29	Plots for a wet site (Station 9368000) extracted from the USGS database which show (a) flow and concentration for the last 5 years and (b) the relationship between concentration and flow.	51
30	Plots for a dry site (Station 11046550) extracted from the USGS database which show (a) flow and concentration for the last 5 years and (b) the relationship between concentration and flow.	52
31	Sampling scenarios generated for a wet catchment site using the USGS data based on (a) stratified (80/10), (b) event only, (c) stratified (50/50) and (d) ambient only sampling.	55
32	Sampling scenarios generated for (a) a wet catchment site and (b) a dry catchment site using the USGS data based on community sampling	56

33	Plots showing the MSE (on the log scale) from all models fitted in (a) the stratified (80/10), (b) event only, (c) stratified (20/20) and (d) ambient only scenarios for the wet catchment.	57
34	Plots showing the MSE (on the log scale) from all models fitted in the community sampling scenario for the wet catchment.	58
35	Sampling scenarios generated for a dry catchment site using the USGS data based on (a) stratified 80/10, (b) event only, (c) stratified 50/50 and (d) ambient only sampling.	59
36	Plots showing the MSE (on the log scale) from all models fitted in (a) the stratified (80/10), (b) event only, (c) stratified (50/50) and (d) ambient only scenarios for the dry catchment.	60
37	Plots showing the MSE (on the log scale) from all models fitted in the community sampling scenario for the wet catchment.	61

List of Tables

1	Primary issues related to loads estimation.	6
2	Illustration of bias in the sampling regime for the Euramo site located along the Tully river.	8
3	A summary of the primary hydrological processes affecting the calculation of loads	11
4	Parameter estimates from the optimal model fit to TSS at the Inkerman Bridge site using 14 years worth of data.	24
5	Estimates of the total TSS load (Mt) for the average, extrapolation, ratio and Beale estimators for the Inkerman Bridge site.	27
6	Parameter estimates from the optimal model fit to NO _x at the Inkerman Bridge site using 14 years worth of data.	29
7	Estimates of the total NO _x load (t) for the average, extrapolation, ratio and Beale estimators computed at the Inkerman Bridge site.	33
8	Parameter estimates from the optimal model fit to TSS and NO _x respectively at the Myuna site in the Bowen River using data collected during the 2005/06 water year.	36
9	Estimates of the total TSS load (Mt) and NO _x load (t) calculated for the Myuna site in the Bowen River	38

10	Estimates of the total TSS load (Mt) and NOx load (t) for the Myuna site in the Bowen River for the average, extrapolation, ratio and Beale estimators.	39
11	Estimates of the total TSS load (Mt) and NOx load (t) in Mistake Creek under four different error structures.	42
12	Estimates of the total TSS load (Mt) and NOx load (t) at the Myuna site in the Bowen River for the average, extrapolation, ratio and Beale estimators.	43
13	Summary of results for TSS and NOx for the Burdekin catchment	44
14	A summary of models fit to the Burdekin data in terms of the % deviance explained.	44
15	Parameter estimates from the optimal model fit to TSS at the Euramo site along the Tully river using 8 years worth of data.	48
16	Estimates of the total TSS load (Mt) for the average, extrapolation, ratio and Beale estimators.	50
17	Summary of generalised additive models (GAM) fit in the simulation study. A tick indicates that the term was fit in the model.	53
18	Parameters used to simulate the five different scenarios investigated in the simulation study. .	53
19	Summary of results by year from the wet catchment scenarios where we highlight the <i>best models</i> representing those with low mean square errors reported from the simulation study. Models are grouped into 3 types: GAM (G), Ratio (R) and Average (A).	56
20	Summary of results by year from the dry catchment scenarios where we highlight the <i>best models</i> representing those with low mean square errors reported from the simulation study. Models are grouped into 3 types: GAM (G), Ratio (R) and Average (A).	61
21	Estimates of (a) the total TSS load (Mt) and (b) NOx load (t) assuming error structure 1 ($\alpha_1 = 0, \alpha_2 = 0$).	71
22	Estimates of (a) the total TSS load (Mt) and (b) NOx load (t) assuming error structure 2 ($\alpha_1 = 0.1, \alpha_2 = 0.05$).	72
23	Estimates of (a) the total TSS load (Mt) and (b) NOx load (t) assuming error structure 3 ($\alpha_1 = 0.3, \alpha_2 = 0.1$).	73
24	Estimates of (a) the total TSS load (Mt) and (b) NOx load (t) assuming error structure 4 ($\alpha_1 = 0.5, \alpha_2 = 0.2$).	74

25	Estimates of the total TSS load (Mt) assuming error structure 1 ($\alpha_1 = 0, \alpha_2 = 0$).	75
26	Estimates of the total TSS load (Mt) assuming error structure 2 ($\alpha_1 = 0.1, \alpha_2 = 0.05$).	76
27	Estimates of the total TSS load (Mt) assuming error structure 3 ($\alpha_1 = 0.3, \alpha_2 = 0.1$).	76
28	Estimates of the total TSS load (Mt) assuming error structure 4 ($\alpha_1 = 0.5, \alpha_2 = 0.2$).	76

EXECUTIVE SUMMARY

Quantifying the amount of sediment, nutrients and pesticides (via a *load*) entering into the Great Barrier Reef (GBR) is a primary focus for Water Quality Improvement Plans that aim to halt or reverse the decline in reef health over the next 5 years. Although substantial work has been undertaken in the literature to define a load under varying conditions and assumptions, the methods currently available do not adequately address all aspects of *uncertainty* surrounding the load estimate. This reduces the ability to usefully inform future monitoring activities and to report on the status of, or trends in, loads.

The approach we present in this report is an extension to the regression or rating curve methodology, which incorporates three primary aspects of uncertainty specific to the calculation of riverine loads. These represent

- Measurement Error, the uncertainty in the measured flow and concentration observed at a particular site or at different spatial locations within a site;
- Stochastic Uncertainty, arising from the fact that not all flow and concentration data are collected; and
- Knowledge Uncertainty, arising from our lack of understanding of the underlying hydrological processes and the ensuing choice of load estimation algorithm.

The loads methodology that we propose takes on a 4 step process.

1. Estimation steps for flow
2. Estimation steps for concentration
3. Estimation of the load
4. Calculation of the standard error of the load

The first step involves predicting flow at regular time intervals using a time series model such that the model captures all of the peak flows. The predicted flow is then matched to concentration sampling times and used only when flow was not collected at that specific time interval. The second step involves the prediction of concentration using a generalised additive model (GAM) that incorporates all important covariates in an attempt to capture the underlying hydrological processes concerned with the flow and transportation of sediment and nutrient loads in an attempt to account for knowledge uncertainty. These predictions are made at regular time intervals and matched with the predicted flow at the first stage ensuring that flow is capped at the maximum flow observed and extrapolation from the model does not occur. Predicting at regular time intervals is the key to accounting for stochastic uncertainty. We refer to this part of the

estimation process as the *generalised rating curve approach*. We then obtain an estimate of the load in the third step using the predicted concentration and predicted flow and incorporating a unit-conversion constant for time interval used. Standard errors are then computed during the fourth step of this process which incorporate both measurement error and errors due to the spatial location of sampling sites.

The generalised rating curve approach is novel as it seeks to represent a number of important system processes for GBR catchments to account for expected or implied system behaviours:

1. First Flush, the first significant channelised flow in a water year accompanied by high concentrations (represented as a percentile of flow and used in the calculation of other system processes).
2. Rising/Falling Limb, which allows higher or lower concentrations on the rising limb when runoff energies are higher and sediment supply may also be higher. This is usually represented at shorter time-scales than exhaustion, which is parameterised for between-event variations. This covariate is based on the flush (process 1) defined for that period.
3. Exhaustion, representing the limited supply of sediments and nutrients due to previous events (represented by a discounted flow term).
4. Hysteresis, representing complex interactions between flow and concentration with strong historical effects and dependence captured by non-linear terms for flow and incorporating hydrological processes 1-3.
5. Overbank Flow, described as flow that goes overbank in flood events (represented by a correction factor, which is used to adjust the calculation). This is work currently investigated by (Wallace et al., 2008).

The methodologies are applied to two real case studies and a simulation study to evaluate the method, make inferences and compare the results to standard loads based estimators. The first case study discusses 3 sites within the Burdekin catchment, representing data collected at three different spatial scales: Inkerman Bridge (daily sampling at the end of catchment), Myuna station (automatic depth based sampling at the end of sub-catchment) and Mistake Creek (intermittent manual sampling from community groups). The second case study investigates the Euramo site along the Tully River. In both investigations we found that the standard ratio estimators (e.g Beale) matched closely with our modelled estimates and in most cases fell within the 95% confidence intervals calculated, particularly when the defined measurement and spatial errors were larger.

Specific modelling results for the Burdekin and Tully catchments are summarised as follows:

1. Inkerman Bridge (1989-2000 time series)

- 24.2% of TSS on average can be attributed to the rise of an event, while 14.5% are associated with the fall compared with no samples appearing on the rise or the fall.
- Exhaustion appears strongly linked with the movement of TSS in the system while a dilution effect is evident with the movement of NO_x during frequent and large events.
- A subtle seasonal effect associated with NO_x in the system where decreases are indicated between October and January, increases between January and May followed by another slight decrease from May through to September are indicated.

2. Myuna Station, Bowen River (2005/06 Water Year)

- A preliminary indication of sediment accumulation stabilising with multiple large events requiring further exploration.
- Increases in flow are indicative of increases in both TSS and NO_x.
- A strong seasonal term exhibiting increases in NO_x from November through to January in a typical water year.

3. Mistake Creek (2005/06 Water Year)

- Models fit to this data are similar to the average type estimators as they include a constant term.

4. Euramo Site, Tully River (2000-2008)

- Progressive increases in TSS concentration as flow increases during wetter periods.
- A possible dilution effect of TSS occurring during large events.
- Low estimated TSS concentration across the 8 years compared to estimates produced from the Burdekin. When compared with the average and ratio estimators, modelled estimates were considerably lower, which could be attributed to the irregular sampling conducted at this site.

For the simulation study, we investigated the performance of our methodology and compared it to four standard loads estimators: Average, Extrapolation, Beale and Ratio estimators. We based the simulation study on 5 years worth of data and investigated a range of generalised additive models. Scenarios that were investigated consisted of stratified sampling, event only monitoring, equal rates of ambient and event based monitoring, ambient only monitoring and community based sampling. Simulations from both a wet and dry site using a long term United States Geological Survey dataset was conducted under these scenarios and

summary statistics were obtained. The advantages of the USGS data set is that it is high frequency and thus provides a natural gold standard measure of the true load. We found the following:

- **Conclusions from a wet site**

- The results show some variability between years, sampling scenarios and methods however, it is clear that across most years the generalised additive models investigated perform reasonably well and in fact, for event only scenarios outperform the ratio and average based estimators suggesting that their capacity in predicting loads using event based data only is promising.

- **Conclusions from a dry site**

- The results for the dry catchment are quite contrasting to the wet catchment. Little variability in estimates is indicated between years, sampling scenarios and methods, apart from the event only and community sampling scenarios. Overall, the majority of methods perform well. In event only situations however, the GAM and ratio methods performed the best, indicating that for dry sites, where fewer events have been recorded, both the GAM and ratio estimators are promising.

There are clear advantages from modelling multiple years worth of data. The first and most important advantage is that it builds in history, a time series of flow and concentration characteristics that can be used to predict across the entire time frame. This approach also has the capacity to incorporate trends through time (whether seasonal or long term) and it aids in the understanding of concentration and flow relationships and how they might differ for different types of concentrations we are interested in. We could of course fit models to each water year separately and in some circumstances we are limited to this because of the nature of the sampling. In doing so we may find that a much simpler model is supported because the seasonal and long term patterns of flow and concentration are not apparent in a shorter time series.

We conclude with the following observations regarding the methodology presented in this report.

1. Depending on the nature of the sampling and assumptions about measurement and spatial error, the coefficient of variation (CV)¹ can be as low as 5% (heavily sampled) and as high as 80% (community based datasets).
2. We found that loads estimates were similar to standard ratio based estimators at sites where sampling bias was minimal (e.g. Inkerman Bridge, Burdekin) but much smaller when the bias was large (e.g. Tully). The regression based methodology offers a novel way of capturing all forms of bias and uncertainty that we believe leads to a more robust estimate of the load compared to other estimators.

¹The coefficient of variation is a normalised measure of precision and is given by the ratio of the standard deviation to the mean (load estimate). Low CVs have a small standard deviation relative to the mean and are seen to be more precise.

The average based estimators consistently estimated a higher load compared to the modelled based estimators except when samples were taken at regularly based intervals and the only significant term fitted in the model was the constant term (e.g. Mistake Creek).

3. The generalised regression based approach is general enough to incorporate a range of different models from models involving just flow to more complicated models that incorporate other covariates (e.g. rising/falling limb, discounted cumulative flow) and possibly interaction terms. Different covariates may be important in different catchments because the underlying hydrological and catchment processes vary and their contribution in a model can be graphically explored to determine the reason why a large load has been estimated in any particular water year. This represents a novel feature of the regression based approach not offered by standard load based estimators.
4. Serial correlation may also be an issue and needs to be accounted for where appropriate as high correlations can lead to larger standard errors.
5. Sites with small numbers of concentration samples can also be modelled, although the number and type of covariates incorporated into the model are limited. At worst, the model defaults to the popular average type estimator.
6. Stochastic uncertainty is adequately dealt with by predicting concentration at regular flow intervals and estimating the load accordingly. This eliminates unwanted bias effectively.
7. The regression approach allows us to borrow strength across years to characterise relationships better and improve the estimation of loads, particularly in years where sampling is poor.
8. The framework presented here is general enough to be applied to all GBR catchments.

We have targeted a number of areas of future work which will help to operationalise the methodology presented here. These are outlined below.

- **[TASK1]** Further validation of the methodology through simulation is required. We have performed a preliminary investigation of the methodology through a simulation exercise in this report but some further fine tuning of parameters are required (e.g. choice of discounting, percentile for defining a "flush", evaluating redundancy and whether all process representations are required, additional covariates). Selection of suitable datasets for simulation also requires discussion with key stakeholders (QDERM and JCU) to ensure they are representative of catchments in the GBR and whether other Australian longterm datasets are available may be more suitable, or whether "true load" measurements are available with which to validate the sample-based modelling methods (eg continuous turbidity for sediment).

- **[TASK2]** Investigate how new data consisting of new sites over other monitoring years can be incorporated into the analysis and how well existing models can predict concentration at these sites.
- **[TASK3]** Investigate computational issues for the standard error calculation. Currently for large datasets, the standard error calculation involves inverting a large matrix. Approaches that speed up the calculation of the standard error are of interest.
- **[TASK4]** Expand the simulation approach to investigate and inform current sampling regimes with the aim of having direct input into future monitoring schemes in the GBR.
- **[TASK5]** Operationalise methods through workshops and interactions with key stakeholders (QDERM and JCU) using case studies in the GBR (e.g. Burdekin & Tully).
- **[TASK6]** Focus on the interpretation of the model outputs and the reporting of loads.
- **[TASK7]** Publishing results in a number of applied and theoretical publications to provide greater confidence in the methods via peer review. Currently we have one publication in the Modelling and Simulation (MODSIM) conference and a second paper in the pipeline that outlines the methodology intended for submission into *Water Resources Research*.

1 INTRODUCTION

Quantifying the amount of sediment, nutrients and pesticides (via a *load*) entering into the Great Barrier Reef (GBR) is a primary focus for water quality improvement plans that aim to halt or reverse the decline in reef health over the next 5 years (SOQ, 2003). Although substantial work has been undertaken to define a load under varying conditions and assumptions (see Kuhnert et al. (2008) for a comprehensive overview of loads methodologies and related papers on the topic), the methods do not adequately address all aspects of *uncertainty* which can be useful to inform future monitoring activities and reporting on the status of trends in loads (Figure 1).

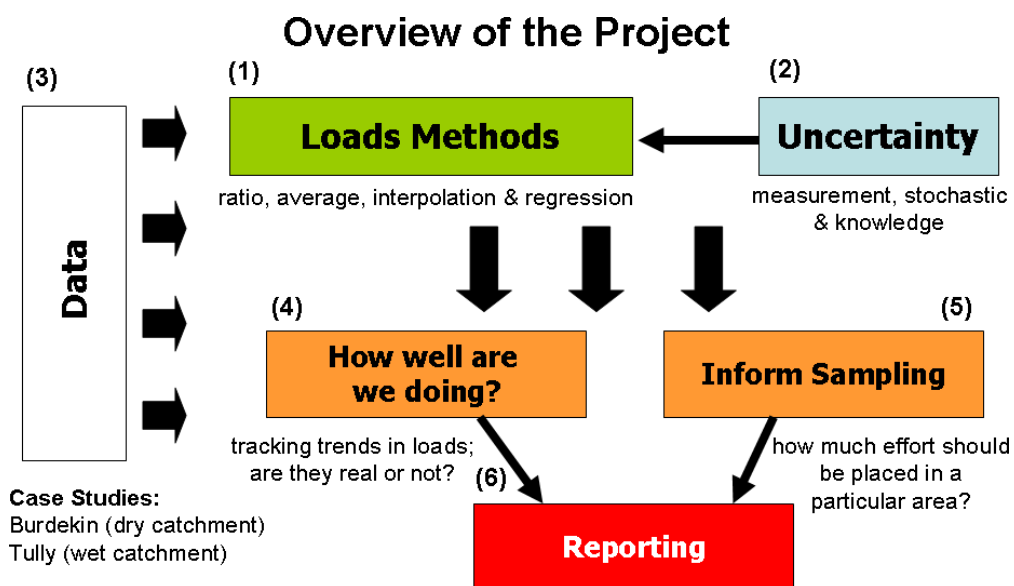


Figure 1: Overview of Project 3.7.7: *Analysis and synthesis of information for reporting credible estimates of loads for compliance against targets and tracking trends in loads* and its relevant components.

There are numerous methods for estimating pollutant loads as described by Kuhnert et al. (2008) and references therein, Degens & Donohue (2002); Fox (2005) and Letcher et al. (2002). The approaches described in these publications range from the class of simple average based estimators, ratio estimators, infilling or interpolation approaches and the rating curve approaches. The approach we focus in this report is the regression or rating curve method, which seeks to *infill* the missing concentration data according to a regression model. Once the missing concentrations are predicted the load is calculated as shown in Equation 1 where \hat{c}_i represents the predicted concentration at the i -th discharge point, q_i represents the discharge, n represents the number of sampling points and K is a constant that depends on the frequency

of measurements and units that the load is reported in.

$$\hat{L}_1 = K \sum_{i=1}^n \hat{c}_i q_i \quad (1)$$

Regression approaches are frequently used to define a so-called *pollutant rating curve*, which represents a relationship between pollutant concentration and discharge. The relationship is often defined on the log scale as

$$\log c_i = \beta_0 + \beta_1 \log q_i + \epsilon_i \quad (2)$$

although this does not have to be the case. Here, β_0 and β_1 are the regression coefficients, c_i and q_i represent the concentration and discharge, respectively, and ϵ_i represents the error due to measurement and other sources e.g. spatial error. Linear regression is often the first choice for modelling log-transformed responses in environmental applications because of its simplicity and ease of implementation (Thomas & Lewis, 1995). However, the accuracy of the approach relies heavily on the strength and consistency of the linear relationship. The effectiveness of this method is also known to depend on the sampling regime, both the frequency of sample collection and the adequacy of the samples to reflect a broad range of conditions.

A generalized approach proposed by Cohn et al. (1992) adopts a 7 parameter model that includes seasonal and temporal terms, along side a quadratic adjustment for discharge. This model takes the form

$$\begin{aligned} \log c_i = & \beta_0 + \beta_1 \log(q_i/\bar{q}) + \beta_2 \log(q_i/\bar{q})^2 + \beta_3(t_i - \bar{t}) + \beta_4(t_i - \bar{t})^2 \\ & + \beta_5 \sin(2\pi t_i) + \beta_6 \cos(2\pi t_i) + \epsilon_i \end{aligned} \quad (3)$$

where c_i is the concentration and q_i the discharge at time t_i , \bar{q} and \bar{t} are centering variables and the sine and cosine terms capture seasonal effects. Despite working reasonably well in practice it does not attempt to capture any underlying system processes that may be driving river systems nor does it incorporate any temporal dependencies which can have an impact on the prediction standard error if they are large and significant. We believe these to be key components that are often overlooked in the modelling process and can contribute heavily to the uncertainty surrounding loads.

In this report, we are primarily interested in quantifying the uncertainty in loads, where uncertainty is comprised into three components: measurement error, stochastic uncertainty and knowledge uncertainty (See Figure 1 for an overview of the project and areas of focus). Many approaches in the literature do not incorporate uncertainty. Those that do, focus on some aspects of uncertainty but not all. For example, there are many simulation based approaches that tackle uncertainty by examining the variability amongst load methodologies (Guo et al., 2002; Etchells et al., 2005; Fox, 2005; Tan et al., 2005), while others develop an approximation for various loads estimation approaches (Baun, 1982; Fox, 2004; 2005). Tarras-Wahlberg &

lane (2003) use Monte Carlo simulation to generate alternative log concentration values for their regression model and thus enable a family of curves to be generated, while Rustomji & Wilkinson (2008) use bootstrap resampling to place confidence intervals around estimates of load, based on a non-linear regression approach.

The approach we present in this report attempts to address the three primary aspects of uncertainty related to the calculation of riverine loads. This is achieved using a regression based estimator to predict concentration given flow, temporal terms and attributes of flow that mimic hydrological phenomena related to the riverine system under investigation. The prediction is performed at regular time intervals to account for sampling bias, and correlation is introduced into the modelling process to account for serial dependence between sampling intervals. The load is calculated by computing the sum of the products of the flow and concentration predicted at the regular time intervals and the corresponding error is estimated, where the error incorporates two sources: measurement and spatial error. The latter corresponds to the location of samples taken in the river.

We begin with a summary and overview of the three components of uncertainty that lead to the formation of a credible loads estimate and describe how we intend to address each of these in the context of loads in Section 2. Section 3 proposes a new loads methodology which represents an extension of the regression approach by Cohn et al. (1992). Sections 4 and 5 applies the methodology to two case studies, the Burdekin and Tully catchments respectively and compares the results to 4 standard load estimation techniques that are widely implemented in the hydrology literature:

- Average based estimators
 - Average²: $\hat{L}_A = K\bar{c}\bar{q}$
 - Extrapolation³: $\hat{L}_E = K \sum_{i=1}^n cq/n$
- Ratio based estimators
 - Ratio⁴: $\hat{L}_R = \hat{L}_E\bar{Q}/\bar{q}$
 - Beale: $\hat{L}_B = \hat{L}_R \times BC, BC = \text{bias correction}^5$

Section 6 investigates a validation approach for testing the effectiveness of the methodology using simulation applied to a comprehensive dataset from the United States Geological Survey (USGS) database.

²Referred to as the flow \times concentration estimator in the Loads Tool. Available from: <http://www.wqonline.info/products/tools.html>

³Referred to as the *average* estimator in the Loads Tool.

⁴Referred to as the flow weighted concentration estimator in the Loads Tool.

⁵See Kuhnert et al. (2008) for details regarding *BC*.

Finally in Sections 7 and 8 we provide some discussion around the methodology, its application to GBR catchments in general, possible implications for future sampling and a summary of future work that focuses on operationalising the methodology, informing monitoring programs and reporting. These represent supplementary stages in Figure 1.

2 IMPORTANCE OF A CREDIBLE LOADS CALCULATION

There are numerous loads estimation techniques available. Each varies according to how they characterise the relationship between flow and concentration over a particular sampling frame. Although often overlooked, uncertainty plays a key role in evaluating a load and providing a credible loads estimate. Other than providing some indication of the precision around the load estimate, uncertainty is important for being able to track trends in loads and determining whether an observed trend is real or not. If the uncertainty around an estimated load is large to begin with, and remains large over the course of monitoring, then it will be extremely difficult to detect a decline. Improving the error around these estimates may be more of a focus in these instances and this will usually result in placing more effort towards sampling.

Uncertainty has a number of different meanings and it can be confused with what is sometimes referred to as "bias". To avoid confusion here, we provide a formal definition for the two terms. Bias is what we would refer to as a difference between what is measured and the truth. Take the example shown in Figure 2, where the estimate of the truth is represented by a Normal distribution, which is centred on 2 (the blue dotted line) with some error. The truth is represented by the red solid line and is well outside our estimated range, resulting in a bias that reflects the difference between the truth and that which is estimated. Uncertainty is a general term that people tend to use interchangeably with bias to represent different sources of error. Experimental or measurement error is the most common form that is addressed by this term but often stochastic uncertainty and knowledge uncertainty are described under this general heading as well. Both stochastic uncertainty and knowledge uncertainty is what we would refer to as bias. Knowledge uncertainty tends to correspond to a lack of system understanding that comes about from not being able to capture system processes in a model while stochastic uncertainty can lead to a bias from the sampling regime. The key difference between bias and uncertainty is that even though you can have the most precise estimate from a model which you believe captures the system processes, you still might have a large bias. Incorporating these biases into estimates of load is therefore an important part of a credible loads calculation and should not be overlooked.

There are several issues relating to incorporating uncertainty into loads. We highlight these issues in

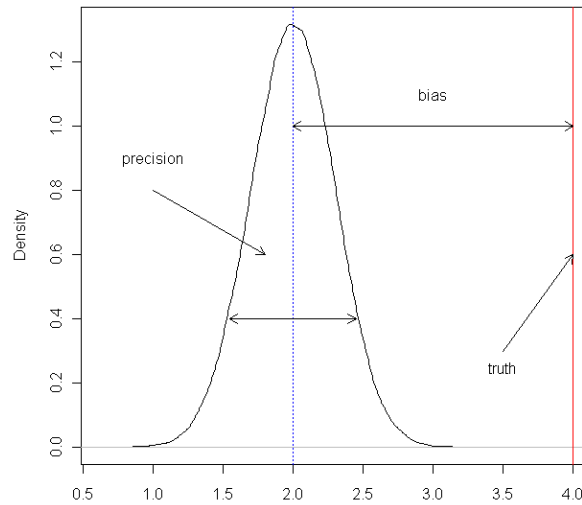


Figure 2: Demonstrating the difference between bias (difference between mean - dotted blue line) and the true value (solid red line).

Table 1. The first and probably most prominent is the issue around sampling. Flow and concentration are collected at different temporal frequencies. Most often, flow is measured near continuously (e.g. once every hour), while concentration is measured at less frequent time intervals, and often only during an event. Community based sampling typically results in very few concentration measurements and in some instances, flow is only recorded when concentration is measured or not at all. A second issue involves the relationship between discharge and concentration, which is often reported on the log-scale and assumed to be linear. In many instances, a linear relationship is not appropriate and quite often, a model incorporating just flow has poor predictive power. Furthermore, appropriate back transformations need to be implemented when using the predicted concentration to calculate a load and care must be taken when using such a relationship for prediction as extrapolation beyond the range of the data may cause spurious results. A third issue relates to the difficulty in capturing hydrological phenomena such as the concept of a *first flush*, *depletion* or *rising/falling limb*, which are present in some riverine systems. Although recognised as having an impact on load calculations, they are often ignored because of the difficulty in incorporating these into a model, or the limited data with which to calibrate empirical models to represent these processes. Finally, a fourth issue is accounting for spatial and temporal errors in the collection of discharge and concentration measurements. Often these are known subjectively, but never incorporated formally into a model. We address each of these issues in the following sections where we describe the three main sources of uncertainty inherent in loads

estimation and mechanisms for incorporating these in the modeling of riverine systems.

Table 1: Primary issues related to loads estimation.

No.	Issue	Impact	Type of Uncertainty
1	Flow and concentration collected at different temporal frequencies e.g. event based, community	Bias	Stochastic
2	Adequately forming a relationship between flow and concentration	poor prediction, bias, extrapolation	Knowledge
3	Difficulty in capturing hydrological phenomena	poor prediction	Knowledge
4	Accurately measuring flow and concentration	bias	Measurement

2.1 Measurement Uncertainty

Measurement uncertainty or measurement error as it is more commonly termed, represents the uncertainty in the measured flow and concentration observed at a particular site or at different spatial locations within a site. The latter corresponds to sampling conducted at different spatial locations along a river, e.g. left or right bank or towards the centre of the river for concentration measurements and downstream, upstream for discharge. The uncertainty will vary according to the data collection method used. For example, routine discharge measurements are collected using 15 minute intervals of flow depth, which is then converted to a discharge through empirical relationships. The uncertainty in discharge can vary with stage, with the common situation indicating smaller errors for flow contained within the river banks and larger errors identified above bankfull stage due to the greater difficulty in estimating flow velocity across floodplains, the relatively infrequent nature of such events, and practical difficulties in gauging under such conditions. For events, the coefficient of variation (CV) can be as high as 20%. However, in most cases, the CV is estimated at around 10% (Olsen et al., 2004). Measured concentration can be more variable however and depends on the type of water quality parameter being measured, how the parameter has been measured (cross-channel or spatial variation), its storage, preservation and laboratory analysis. Work by Harmel et al. (2006) indicates that a CV of 50% is achievable for most parameters but this can be as low as 5% and as high as 80%.

Although discussing the different sources of uncertainty at a recent workshop (Bainbridge, 2006), currently

no formal quantification of measurement (or spatial) error for flow and concentration has been undertaken for riverine systems in the GBR. It is believed that both forms of error can be as low as 5% and as high as 20% or 30% in some rivers (Jon Brodie, *pers. comm.*) and that these range of errors should be considered in the calculation of loads for the GBR.

2.2 Stochastic Uncertainty

Stochastic uncertainty arises from the fact that not all flow and concentration data are collected. Flow tends to be measured at regularly spaced intervals but concentration can be measured much less frequently, with a natural bias towards events because events are generally the focus in these types of calculations. We therefore will have uncertainty in loads for the periods we do not have data.

There is a substantial body of literature showing that the sampling regime can have strong impacts on the accuracy of pollutant loads (Walling & Webb, 1981; Johnes, 2007). Many have approached the problem through simulation studies and investigating the optimal sampling regime for a range of estimators. However, the problem with this approach is that the sampling regime recommended may vary due to the hydrological characteristics at each site. Furthermore, the way in which samples are collected may not reflect what should be done theoretically to achieve an estimate of the load that is both accurate and precise.

To illustrate the nature of the bias this type of uncertainty presents, consider the following estimates of bias for sediment and flow recorded at the Euramo site along the Tully River. Flow data is gauged and recorded on average hourly, while total suspended sediment or TSS is recorded less frequently (Figure 3). Table 2 summarises the flow data recorded across eight water years. In this table, n represents the number of concentration records, \bar{q} represents the average flow measured at concentration samples, \bar{Q}_I represents the average predicted flow at regular time intervals using a time series model and \bar{Q} represents the average flow recorded at the gauging station. We computed the bias of the interpolated flow relative to the average gauged flow (B_q) and the bias of the flow recorded only when concentration has been measured, relative to the average gauged flow (B_c). This table shows that the bias from using an interpolated flow record across all 8 water years has some impact and can be up to twice as high as the average flow recorded. The bias incurred from using flow that is only recorded when concentration is measured however, is much more substantial. For example, \bar{q} is 4 times higher than the average gauged flow on some occasions. Not accounting for this bias can lead to serious overestimation or underestimation of the load and highlights the importance of accounting for bias in the loads estimation procedure. The effect of stochastic uncertainty on load estimation will also depend on our knowledge about the flow and concentration processes.

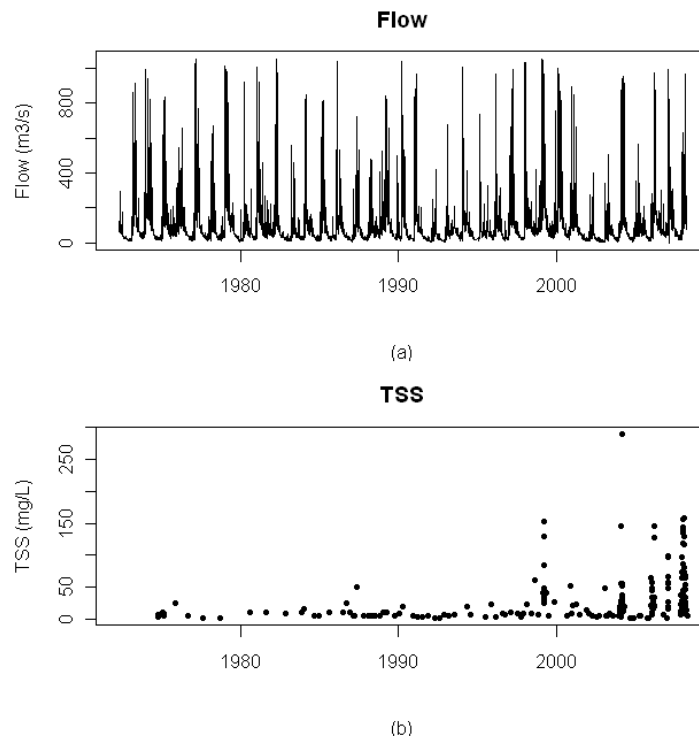


Figure 3: Tully river at Euramo site showing (a) the gauged flow in m^3/s and (b) measured total suspended sediment (TSS) in mg/L from 2000-2008.

Table 2: Illustration of bias in the sampling regime for the Euramo site located along the Tully river. (Data courtesy of Marianna Joo, Department of Environment and Resource Management, QLD.)

Year	n	\bar{q}	\bar{Q}_I	\bar{Q}	B_c	B_q
00/01	6	156.6	202.8	115.8	1.35	1.75
01/02	3	30.2	71.4	44.0	0.69	1.62
02/03	8	51.1	81.0	38.8	1.32	2.09
03/04	28	372.1	210.0	106.1	3.51	1.98
04/05	4	39.4	101.1	60.7	0.65	1.67
05/06	20	260.1	161.9	112.4	2.31	1.44
06/07	12	532.9	185.5	132.9	4.01	1.40
07/08	66	343.9	112.6	112.4	3.06	1.48
Mean	18.4	164.5	149.8	93.1	1.50	1.70

2.3 Knowledge Uncertainty

Knowledge uncertainty arises from our lack of understanding of the underlying hydrological processes and the ensuing choice of load estimation algorithm. It may also be considered a form of bias. In an ideal situation, when there is direct and continuous observation there is no knowledge uncertainty because the load may be measured by the product of the observed concentration and discharge summed across all instances of flow. In circumstances where the sampling and observation is considerably more sparse, there is a need to make assumptions about the underlying processes (e.g. load is proportional to the discharge as assumed for ratio estimators) and incorporate these assumptions along side the observed data to estimate the pollutant load. Knowledge uncertainty is therefore reducible. As we understand more about the nature of the processes and collect data over a range of different years and event types we will build a more complete picture that reduces that source of uncertainty.

In the absence of much knowledge many load estimation methods may be viewed as appropriate, and may give load estimates that can vary widely. For example, Phillips et al. (1999) examined the variation in load estimates for the Rivers Ouse and Swale in England in response to both sampling frequency and the load estimation algorithm. Twenty two load estimation algorithms were considered and a number of replicate analyses or simulations were conducted. While most algorithms produced a median load reasonably close to the reference value, a small number of algorithms deviated significantly from the reference value. As another example, Guo et al. (2002), Etchells et al. (2005) and Tan et al. (2005) tackle knowledge uncertainty through the examination of the variability amongst load methodologies. Incorporating this knowledge uncertainty is difficult though because not all choices of load method are equally likely or supported, and many are highly related. In reality, we usually have existing knowledge, albeit incomplete, that implies that some methods are more appropriate than others. We believe that choosing a single methodology and tackling knowledge uncertainty within this methodology may be able to provide a more comprehensive and accurate estimate of the uncertainty around the load and avoid some of these issues

3 LOADS METHODOLOGY

3.1 Regression based methodology

The loads methodology that we propose takes on a 4 step process as outlined in Algorithm 1. The first step involves predicting flow at regular time intervals using a time series model such that the model captures all of the peak flows. The predicted flow, \hat{q} is then matched to concentration sampling times and used

only when flow was not collected at that specific time interval. The second step involves the prediction of concentration using a predictive model that incorporates all important covariates in an attempt to capture the underlying hydrological processes concerned with the flow and transportation of sediment and nutrient loads. These predictions are made at regular time intervals and matched with \hat{q} at the first stage ensuring that flow is capped and extrapolation does not occur beyond the range of the data. We refer to this part of the estimation process as the *generalised rating curve approach*. We then obtain an estimate of the load, \hat{L} in the third step using the predicted concentration, \hat{c} and predicted flow \hat{q} and incorporating a unit-conversion constant, K for time interval, δ . Standard errors are then computed during the fourth step of this process which incorporate both measurement error and errors due to the spatial location of sampling sites. We believe that this algorithm provides an approach that is capable of adjusting for bias as discussed in Section 2 and can accommodate:

- measurement error through the direct incorporation of error in the estimation phase,
- stochastic uncertainty through the prediction of q and c at regular time intervals, and
- knowledge uncertainty through the inclusion of additional covariates in step 3.

Algorithm 1 Steps for Estimating a Load

1. Estimation steps for flow, \hat{q}
 - Output flow rates at regular time intervals (e.g. hourly, 10 minutes) using a time series model that captures all the peak flows.
 - Output the predicted flow rates at the concentration sampling times using the time series model if the corresponding flow rates are not collected
 2. Estimation steps for concentration, \hat{c}
 - Establish a predictive model for the concentration data which includes all important covariates
 - Output the predicted concentrations at the regular time intervals ensuring that extrapolation does not occur beyond the range of the data.
 3. Obtain an estimate of the load, $\hat{L} = K \sum_{m=1}^M \hat{c}_m \hat{q}_m \delta$
 4. Obtain standard errors, $var(\hat{L})$.
-

We explore some of the important system processes in Section 3.2 and how they can be incorporated into a regression based model in Section 3.3.

3.2 Important system processes for GBR catchments

There are several hydrological phenomena which can be considered in estimating the sediment and nutrient loads of riverine systems. Table 3 summarises these main hydrological processes and how they might be incorporated in a regression model. We describe each of these processes in the following sections in relation to the regression based approach.

Table 3: A summary of the primary hydrological processes affecting the calculation of loads

Phenomena	Process	Description	Representation
1	First Flush	First significant channelised flow is accompanied by high concentrations	Percentile of flow
2	Rising/Falling Limb	Capturing the rise or fall of an event	Categorical variable: measurements located on the rise or fall.
3	Exhaustion	Limited supply of sediments and nutrients due to previous events.	Discounted flow
4	Hysteresis	Complex interactions between flow and concentration with strong historical effects	Non-linear terms for flow
5	Overbank Flow	Flow that goes overbank in flood events	Correction factor

Processes 1 and 3 relate to the antecedent conditions within the catchment prior to a flow event, which can influence the concentration occurring during that event. Processes 2, 4 and 5 relate to systematic temporal trends or changes in concentration observed within individual events. On the other hand, traditional regression models of concentration consider only the discharge at the present moment in time. Present discharge is a good representation for transport capacity, but the other hydrological phenomena listed here relate also to other constraints on pollutant supply.

3.2.1 Phenomena 1: First Flush

What is it?

The "first flush" (Furnas, 2003) is a phenomenon whereby the first significant channelised flow of the wet

season is accompanied by relatively high sediment and nutrient concentrations. Precipitation in GBR catchments occurs predominantly within a well-defined, summer wet season (November to April). The run-off and interflow associated with a wet season's initial, flow-inducing precipitation event tends to pick up unconsolidated, fine sedimentary material and nutrients that have accumulated on or just below the land surface of the catchment. These materials accumulate due to natural weathering, disturbance, anthropogenic activity (e.g. land cultivation) and biomass decay during the relatively long, intervening dry period between wet seasons (Wallace et al., 2008) and are readily entrained by the event runoff.

How do we incorporate it?

The identification of a first flush in a water year is fairly subjective and can vary from system to system. For example, a first flush in a river system residing in a dry catchment like the Burdekin can be quite different to a first flush in a riverine system residing in a wet catchment such as the Tully.

To avoid having to subjectively choose a flow cut-off that represents a first flush, we select a percentile, say the 90th, to represent the flush, Q_p , in a particular water year for a river of interest. The choice of percentile, p can also be considered subjective and may change depending on the river system investigated. Irrespective of this it is perceived to represent a "high" flow for that period, which is used in the creation of other hydrological covariates. We illustrate this concept in Figure 4, which shows the variable that is created from flow records at the Inkerman Bridge site in the Burdekin River. For each yearly period (in this case, a financial year), flush is defined as the 90th percentile ($Q_{0.9}$) for that period. In Figure 4 we see that the 1996/1997 financial year provided the largest flush, which was revisited again in the 1999/2000 financial year.

3.2.2 Phenomena 2: Rising/Falling Limb Sampling Biases

What is it?

The phenomenon of exhaustion explored in Section 3.2.3 leads to a consideration of how samples are taken. Water samples are often retrieved manually several hours, or even days, after the first indication that an event is in progress. This delay typically arises due to travelling time and/or difficulties in accessing a sampling site due to inclement weather conditions. The consequences of such a delay can be that sampling occurs after the peak in sediment/nutrient concentration with the resulting concentration values essentially reflecting exhaustion levels. Without high-resolution sampling across both limbs of the hydrograph it is impossible to know at what point concentrations approach exhaustion levels. However, examining charts of discharge versus TSS, N, and P concentration across several events in the Tully and Murray catchments

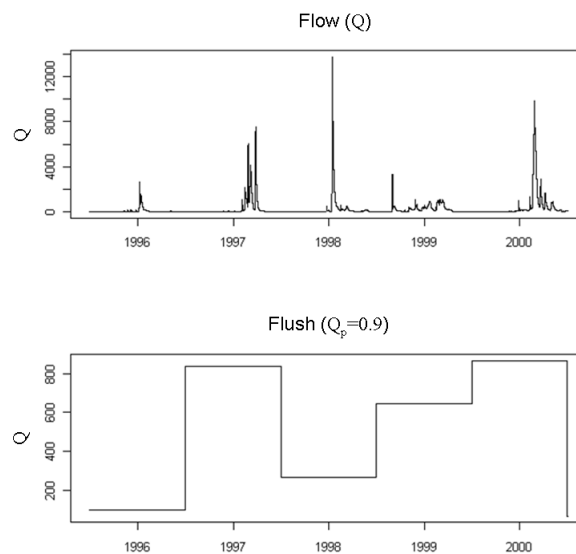


Figure 4: A snapshot from Inkerman Bridge in the Burdekin showing the concept of a "flush" in m³/L which is determined using the 90th percentile for each financial year.

during the 2007/08 wet season (Wallace et al., 2008) it appears that exhaustion, in most cases, is becoming evident by the time the hydrograph peaks. Based on this limited data we believe that it will be useful to identify whether a sample was collected on the rising (prior to exhaustion) or falling limb (indicating exhaustion) of a hydrograph. The other important aspect of this is that different water quality variates may respond differently to the stages of hydrograph. Sediments and nutrients attached to particulates may be mobilised quickly, while other forms may need to dissolve and therefore take longer.

How do we incorporate it?

As concentration is thought to vary during events it makes sense to capture such variabilities through a term that identifies the event and in particular, whether the event and recorded concentration is captured on the rising or falling stages of the hydrograph. Capturing the rise or fall is particularly important in some riverine systems where there is difficulty sampling concentration during an event therefore results in samples being collected on the fall only. It may also be important for different water quality parameters as some are known to respond quickly to flow (e.g. sediment) and closely follow the hydrograph, while others (e.g. dissolved nutrients) may exhibit some lag and possibly show higher concentrations on the falling limb.

Figure 5 shows an example of how we capture the rising and falling stages of an event using a step function that is 1 when flow is on the rise, -1 when flow is decreasing and therefore on the fall and 0 when it is neither for a particular event (or flush as outlined in Section 3.2.1). The exact point at which the event occurs is determined by the flush, Q_p , identified for the water year. So if $Q > Q_p$ then

$$L_i = \begin{cases} 1 & (Q_i - Q_{i-1}) > 0 \\ -1 & (Q_i - Q_{i-1}) < 0 \\ 0 & \text{otherwise} \end{cases}$$

Depending on our definition of an event, we may observe a different pattern for the rising/falling limb. Therefore defining what a flush represents is an important component for the definition of this variable in a model.

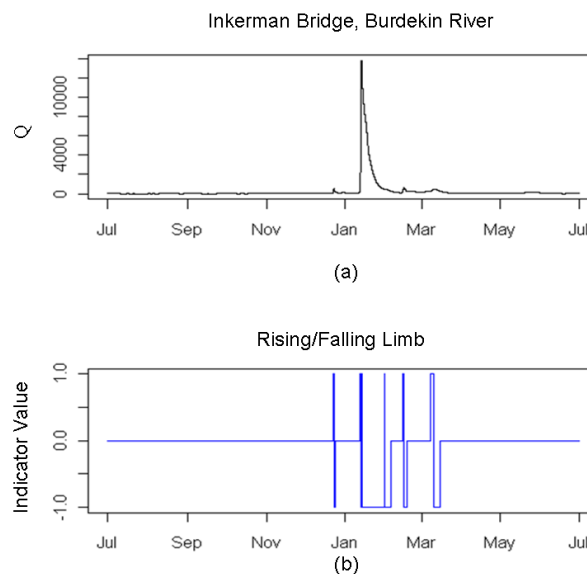


Figure 5: A snapshot from Inkerman Bridge in the Burdekin showing (a) an event for a particular time period and (b) the rising/falling limb is indicated by a step function.

3.2.3 Phenomena 3: Exhaustion

What is it?

The first flush phenomenon described in Section 3.2.1 may occur for fairly small events but is actually part of a broader depletion process that operates and manifests itself as a progressive decline (linear or nonlinear) in concentrations for a given discharge over the season. Events that have occurred after a lengthy dry period will tend to result in higher transportation of sediment and nutrients through a system. This is most evident after the dry season where the conditions lead to the first flush phenomena. Subsequent events throughout the season will continue to move sediment, nutrients and pesticides, though often larger events are required to yield similar concentrations as the season progresses. This occurs because the systems

will reach a point of exhaustion, where despite large events, the amount of load generated is reduced by limitations in supply. Figure 6 illustrates this process for the Myuna site in the Bowen river. In this figure, we see that the maximum turbidity (and TSS concentration) in each event reduces even though the maximum depth (and discharge) increases.

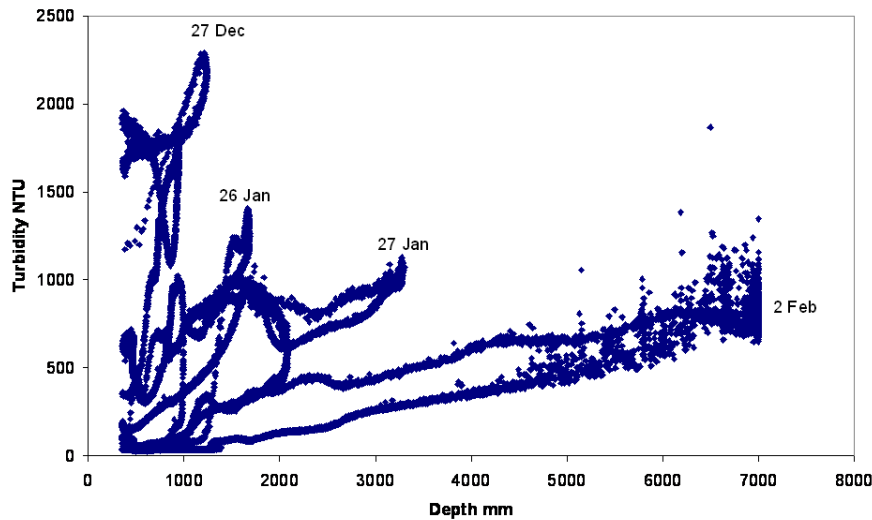


Figure 6: Depth-turbidity relationship in the Bowen river at Myuna for four events in the 2006/07 wet season.

Between events in a given season or year, concentration can generally decline due to depletion of available sediment. This depletion may be caused by transport of material weathered during prior dry seasons and an increase in vegetation cover through the season. Conceptually, the concentration discharge relationship may also be affected by rainfall in prior years, through variations in vegetation cover; thus depletion may occur at two temporal scales. Sediment entrained in rainfall run-off will be derived from two primary pools: A) the pool of readily transportable, unconsolidated material that has accumulated on the ground surface of the catchment (via direct weathering and indirectly via aeolian transport) in the period since the last run-off generating rainfall event, and B) that derived from direct physical erosion of the ground surface by raindrop impact, overland flow etc. During a precipitation event of sufficient intensity to generate run-off, sediment will be entrained from both pools. However, once pool A has been depleted then pool B becomes the predominant supplier of sediment to the runoff. Thus, sediment concentrations are generally higher earlier in a flow event when material is available for transport from both pools and decrease as pool A becomes depleted. This phenomenon is referred to as "exhaustion".

How do we incorporate it?

We attempt to capture the exhaustion phenomena through a discounted flow term, D_i in the regression

model that involves discounting the flow by a factor, d that down weights the contribution of an event based on the time between events and the size of the event, a form of exponential smoothing. In other words we discount yesterday and more the day before. We define the discounted flow, D_i as follows

$$D_i = \frac{(1-d)}{1-d^i} \sum_{m=1}^i d^{i-m} \hat{Q}_m, \quad (i = 1, \dots, T.) \quad (4)$$

where d represents the discount factor ranging between 0 and 1, \hat{Q}_m represents the predicted flow occurring at the (m)-th interval and T represents the length of the time period (across all years). Note that a very small discount (less than 0.1/day, say) is equivalent to using (a smoothed representation of) the current flow while a large discount (more than 0.99/day, say) is essentially equivalent to the cumulative mean flow. Here d may be chosen as 0.95 per day (and hence roughly 0.5 per fortnight) suggesting that about half of the flow occurring two weeks ago is contributing to sediment and nutrient runoff now. The optimal d will depend on the underlying recovery and exhaustion rates of the sediment. In practical terms the discounting will have the effect of reducing the predicted concentrations when there have been recent events in the past. Figure 7 shows the effect of incorporating four different discount factors for flow data collected at the Inkerman Bridge site in the Burdekin over a two month period. We see that as the discount factor increases from 10% to 99%, the flow contribution is shifted by some lag to the right suggesting that the flow occurring in the past is now contributing to sediment runoff in the present. The shift is related strongly to the level of discounting and hence the lag.

3.2.4 Phenomena 4: Hysteresis

What is it?

Hysteresis is the reason why we need to account for hydrological terms such as the first flush, exhaustion, dilution and changes in concentration on the rising or falling limb in a model. There are physical processes which result in non-unique relationships between discharge and concentration at several temporal scales. Within events, there can be hysteresis in the concentration-discharge relationship, such that this relationship varies to form a clockwise or anti-clockwise loop. Frequently, concentration is higher on the rising limb of the hydrograph, due to depletion of sediment availability during the event (Nistor & Church, 2005) and possibly higher rainfall intensity and sediment transport capacity occurring on the rising limb. Water quality concentration data is also observed sequentially in time and is often serially correlated. This infers that past events have some relationship or dependency with present events. Traditional rating curve and regression approaches assume independence. This can ignore the fact that the best predictor of an unobserved concentration may be the observed concentration at a nearby time point. In simplistic terms, the impact

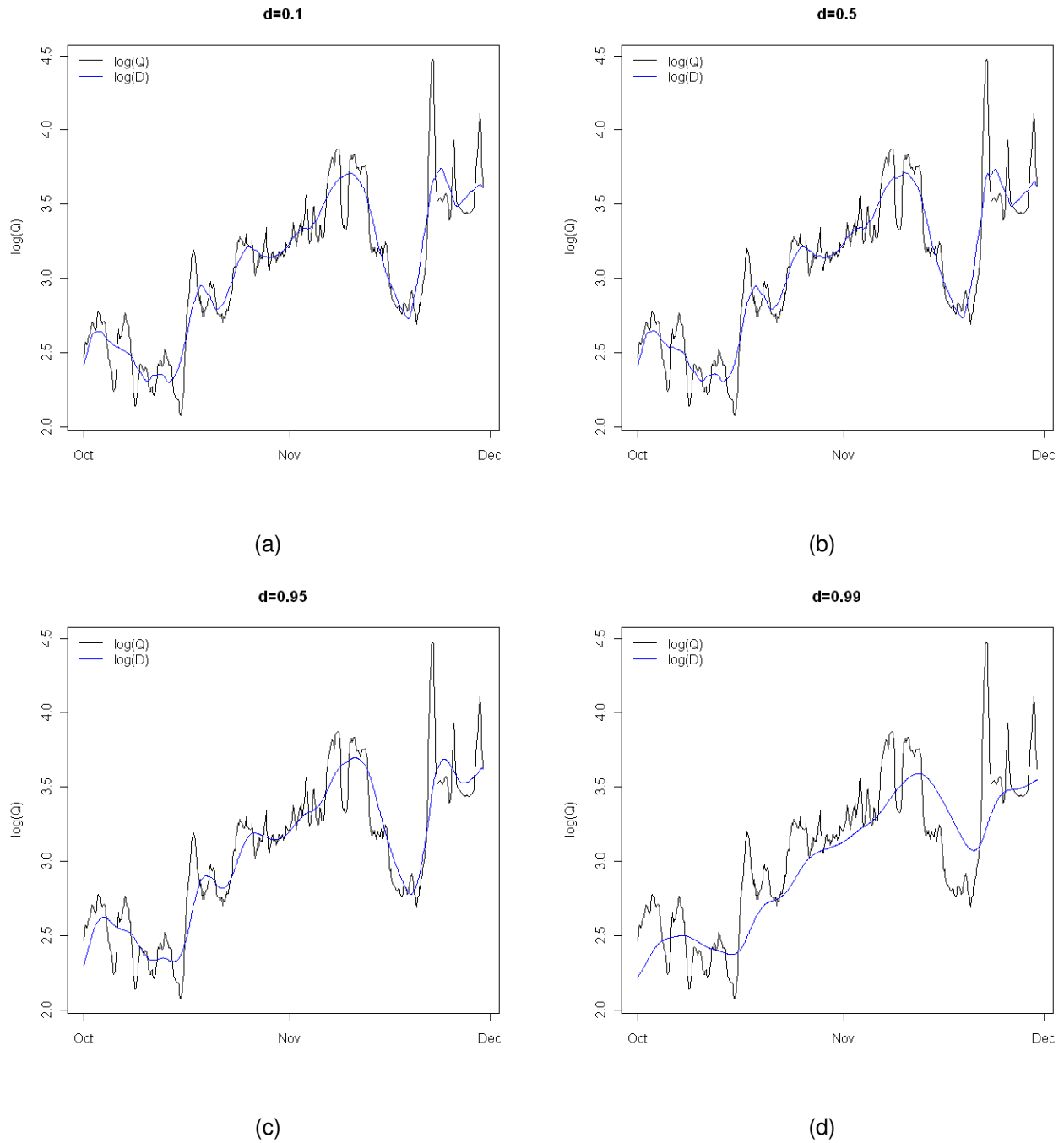


Figure 7: Implications of the discount factor in the calculation of the discounted flow term when (a) $d = 0.1$, (b) $d = 0.5$, (c) $d = 0.95$ and (d) $d = 0.99$.

of the serial dependence in a model is in the standard error calculation and not in the prediction. As the correlation, ρ increases, we typically see larger standard errors in our estimates. Therefore taking into account dependence in these models is important.

How do we incorporate it?

Capturing complex relationships between concentration and flow and in particular hysteresis effects can be achieved by considering non-linear terms for flow (e.g. quadratic or splines) in combination with temporal and seasonal terms (sines and cosine terms) that capture historical processes and seasonal effects respectively. Terms capturing changes in concentration on the rise or fall, exhaustion and dilution which were identified previously can also be considered as part of this process and the importance of serial dependence can also be investigated. With the latter, residual serial dependence is often modelled by assuming that it forms an autoregressive process of order p (denoted AR(p)). This means that the residual, ϵ_i at time t_i depends on the past only through the previous p residuals, $\epsilon_{i-1}, \dots, \epsilon_{i-p}$. In these regression models we assume an AR(1) process, in which case $\epsilon_i = \rho\epsilon_{i-1} + \nu_i$, where ν_i are assumed to be independent Normal random variables and ρ is the lag 1 correlation.

3.2.5 Phenomena 5: Overbank Flow

What is it?

"Breakout flow" or alternatively overbank flow is a hydrological concept that refers to the amount of water leaving a river and going overbank. Flow gauging stations are generally considered to provide a reasonable indication of the flux of water through a particular river cross-section with time. However, if a portion of the boundary between two catchments lies upon a low relief coastal floodplain, then during large, overbank flow-events, where the floodplain is almost entirely inundated, flood water may flow overland and into the adjoining catchment ("breakout flow"), or ocean (e.g. Tully and Murray catchments (Wallace et al., 2008)). If such a breakout of flow occurs upstream of a gauging station, then the gauge will under represent discharge from the catchment.

How do we incorporate it?

In practice this may be difficult to model since the error may not be well observed. Investigations into how to estimate the amount of sediment resulting from overbank discharge is currently underway (Wallace et al., 2008; Kuhnert & Dovers, 2009). This work is attempting to provide a number of correction factors for clusters of rivers exhibiting similar flow and water quality characteristics, which can be used within this modelling

framework to correct for overbank flow. We presently ignore overbank flow in this report but acknowledge that for sites within the Tully, loads may be underestimated.

3.3 The generalised rating curve approach

The generalised rating curve approach attempts to capture the underlying hydrological processes of a load to improve prediction accuracy. The approach we present here is an extension of Cohn et al. (1992) that

- incorporates other factors other than discharge to capture the underlying hydrological processes and reduce knowledge uncertainty, and
- introduces more flexible non-linear functional forms (e.g. quadratics and splines) for the model parameters to improve the accuracy of the prediction.

Based on the covariates discussed in Sections 3.2.1-3.2.5 we consider the following model

$$\log(c_i) = \beta_0 + \sum_{k=1}^7 \beta_k x_{ki} + \epsilon_i, \quad (5)$$

where x_{1i} is $\log(Q)$, x_{2i} is $\log(Q)^2$, x_{3i} is time in days (t), x_{4i} is $\sin(2\pi t/365.25)$, x_{5i} is $\cos(2\pi t/365.25)$, x_{6i} is the limb (1=rising, -1=falling, 0=no flush), and x_{7i} is the discounted flow, D_j , where the discount factor is chosen to be 0.95 per day. Interaction terms may be investigated to allow the effect of the limb to alter according to flow and the discount factor. However, we do not explore them here. In matrix notation, we will write $\log(C) = X_0\beta + \epsilon$, where β is the parameter vector and X_0 is the $n \times 8$ design matrix. The residuals, ϵ_i are assumed to follow an AR(1) process where appropriate. It is important to have the range of x_i covered in the data or spurious predictions may occur. To this end, it may be necessary to impose an upper limit for the concentration to ensure extrapolation does not occur beyond the range of c .

This method represents a general framework for modelling concentration that considers other explanatory variables and attributes of the hydrograph to improve the prediction of concentration. We acknowledge that there may be times when concentration is at best weakly related to discharge. Furthermore, other covariates may be important to include into the model in some circumstances. For example, it may be relevant to consider something that relates rainfall intensity as captured by the rate of the rise in stage height. The model represented by Equation 5 can therefore be as simple or complex as required. In the worst-case scenario, where there is no predictive power, the regression model can be seen to default back to predicting an average concentration and the load estimated according to what is one form for the popular average estimator.

3.4 Estimating pollutant loads from the regression model

Once an appropriate model has been fitted we can form predicted concentrations using the expression (in matrix notation), $(\hat{c}_m)_{(1 \leq m \leq M)} = \exp\{X_1(X_0'X_0)^{-1}X_0z\}$ where X_0 represents the design matrix and X_1 represents the $n \times 8$ design matrix for predicting the n concentrations and $z = \{\log(c_i)\}_{i=1, \dots, n}$. The load estimator is then given by Equation 6 where s^2 and s_m^2 are the estimates of variance of ϵ and $\log(\hat{c}_m)$.

$$\hat{L} = T\delta \sum_{m=1}^M \hat{c}_m \hat{q}_m \exp\{(s^2 - s_m^2)/2\} \quad (6)$$

Note in this expression that we present the bias corrected estimator since $E(C) = E\{\exp(X_1\beta + \epsilon)\} = \exp(X_1\beta + \sigma^2/2)$ and $E(\hat{c}_m) = c_m \exp(\sigma_m^2/2)$ where σ^2 and σ_m^2 are the variances of ϵ and $\log(\hat{c}_m)$ representing measurement error and spatial error respectively. Both of these quantities may be specified subjectively but that they will be based on knowledge of the measurement process (e.g. from replicate sampling) etc. Ferguson (1986) and Koch & Smillie (1986) propose at least three other ways of correcting this estimator. We will not focus on fine tuning such bias because it is relatively small considering the other types of model bias and the associated uncertainties considered by this model. Note that $\exp(s^2/2)$ may be replaced by the smearing estimate, $\sum_{i=1}^n \exp(\hat{\epsilon}_i)/n$ (Duan, 1983) where $\hat{\epsilon}_i$ are the residuals from the regression model.

3.5 Estimating Load Uncertainty

We are interested in establishing the predictive variance of L in which a model error ϵ cannot be eliminated by increasing sample size. The model error, ϵ is assumed to have a variance, σ^2 and correlation matrix $R(\rho)$ with autocorrelation parameter ρ which measures temporal correlation. If we denote the vector of the corrected load estimates at the regular time intervals as L_m , and after some algebra, we have an expression for the variance of \hat{L} :

$$\text{var}(\hat{L}) = \text{trace}\{\text{var}(\hat{\beta})SS^T\} + \alpha_1^2 \left[\sum_m L_m^2 \{1 + \partial f / \partial \log(Q_m)\}^2 \right] + \alpha_2^2 \left[\sum_m L_m \{1 + \partial f / \partial \log(Q_m)\} \right]^2 \quad (7)$$

where $f(\hat{Q})$ is the regression model on the log scale and $\partial f / \partial \log(Q_m) = \beta_1$ for the traditional rating curve model, $S = X_1^T(L_m)_{l \leq m \leq M}$ is a matrix of $K \times M$ (K is the number of parameters), SS^T is a square matrix of $K \times K$ and α_1 and α_2 are the coefficient of variation (CV) of the independent measurement error and spatial/temporal random effects in $\log(Q)$. Note, both α_1 and α_2 are defined in this model and are typically based on published findings or experimental studies investigating errors of this type.

4 CASE STUDY I: BURDEKIN CATCHMENT

4.1 Catchment characteristics

The Burdekin catchment is the second largest catchment draining to the GBR lagoon and it represents the largest in terms of mean gauged annual discharge (Furnas, 2003). The Burdekin river itself drains an area of 130,126 km². The distribution of land use within the catchment is represented primarily by cattle grazing (95%) and other uses, including cropping (5%) (Rayment & Neil, 1996; Furnas, 2003). The geology of the catchment is quite varied containing igneous, sedimentary and metamorphic rock provinces (Fielding & Alexander, 1996; Furnas, 2003) and a wide variety of soil covers. Precipitation within the catchment occurs primarily within a well-defined, summer wet season with higher falls near the coast and declining westwards of the Great Dividing Range (Furnas, 2003; Amos et al., 2004). Area weighted annual rainfall within the catchment is 727 mm (Furnas, 2003). The recorded annual discharge of the Burdekin River is highly variable ranging from 247,110 MI (1930/31, Home Hill) to 54,066,311 MI (1973/74, Clare), representing the end of catchment over the 84 years of the record. Development of the catchment by European settlers began in the mid-1800s with the introduction of sheep and cattle grazing (Lewis et al., 2007) and the commencement of alluvial mining. It is generally accepted that post settlement activities such as these would have increased the annual average flux of sediment to the GBR lagoon (e.g. (Belperio, 1979; Moss et al., 1992; Neil & Yu, 1996; Brodie et al., 2007) and in recent years trace-element analysis of coral cores has provided evidence in support of that proposition (McCulloch et al., 2003; Lewis et al., 2007).

Several attempts have been made to estimate recent annual-average, and event based, sediment fluxes from the Burdekin River to the GBR lagoon. Belperio (1979) estimated annual average load to be 3.45×10^6 tonnes, but Amos et al. (2004) consider this early estimate to be unreliable due to the highly variable seasonal and intra-annual discharge patterns. Amos et al. (2004) estimated a flux of 3.7×10^6 tonnes of suspended sediment and 3×10^5 tonnes of bedload were transported past a monitoring site in the Burdekin River during a 29 day discharge event in February and March 2000. Mitchell & Furnas (1997) monitored suspended sediment transport in the river between 20 December 1995 and 12 February 1996 and obtained a flux of $2.6 - 4.8 \times 10^6$ tonnes over that period. That the two event-based estimates were of similar size but the corresponding peak discharges were of different magnitude ($3166 \text{ m}^3 \text{ s}^{-1}$ vs $11155 \text{ m}^3 \text{ s}^{-1}$) is believed to indicate influence of antecedent weather conditions upon the availability of sediment for transport (Amos et al., 2004).

We applied the methods described in Section 3 to three different sources of data collected in the Burdekin, where the monitoring of total suspended sediment (TSS) and oxidised nitrogen (NO_x) was of interest. These

sites constitute

- Inkerman Bridge, representing the end of catchment for the Burdekin. Data collection at this site was conducted by AIMS, who collected a long term time series of concentration and flow;
- Myuna site at the Bowen River, where data collected automatically represents the sub-catchment scale; and
- Mistake Creek, representing manual community based samples, where data is typically only collected during an event. Therefore data of this type is fairly limited and sparsely recorded across the hydro-graph.

We investigate these three types of datasets to determine if a modelling approach can be used to estimate concentration and therefore allow credible calculation of a load. In terms of modelling, we examined a number of GAM models for predicting concentration which incorporate the covariates outlined in Section 3. The optimal model was determined by assessment of the generalised cross-validation (GCV) score via a backward elimination procedure which begins with a model that includes all covariates. Once the optimal model was identified, we refit the model including an AR1 term (where appropriate) to account for serial correlation and re-estimated the parameters of the final model and evaluated the fit using standard diagnostic tools (e.g. residual plots). Using this model, we predict concentration at regular time intervals and calculate a total load for each water year reflected in the data. We also provide a standard error and corresponding 95% confidence interval for each estimate that incorporates measurement error (α_1) and spatial error (α_2). We explored a range of errors that captured previously published findings as well as some extremes to allow for comparison between different types of errors. These consisted of:

- Error Structure 1: **no** measurement or spatial error ($\alpha_1 = 0, \alpha_2 = 0$)
- Error Structure 2: **mild** measurement and spatial error ($\alpha_1 = 0.1, \alpha_2 = 0.05$)
- Error Structure 3: **moderate** measurement and spatial error ($\alpha_1 = 0.3, \alpha_2 = 0.1$)
- Error Structure 4: **large** measurement and spatial error ($\alpha_1 = 0.5, \alpha_2 = 0.2$)

We also compare the estimates from our model with some of the standard loads based estimators highlighted in the introduction and comment on their applicability to the data at hand.

4.2 Inkerman Bridge

Data collected at Inkerman Bridge was collected by the Australian Institute of Marine Science (AIMS) between 1987 and 2000 as part of their riverine monitoring program for the purpose of calculating annual loads (Mitchell et al., 2006). Flow data was recorded by a Natural Resources and Water (NRW) gauge located at Clare, which resides approximately 20km upstream from the sampling site where concentrations of TSS and NO_x were recorded. Figure 8 shows a plot of flow and concentration collected over the 14 year period. The collection of concentration data appears very sporadic throughout the years, particularly for TSS but becomes more frequent during the later periods.

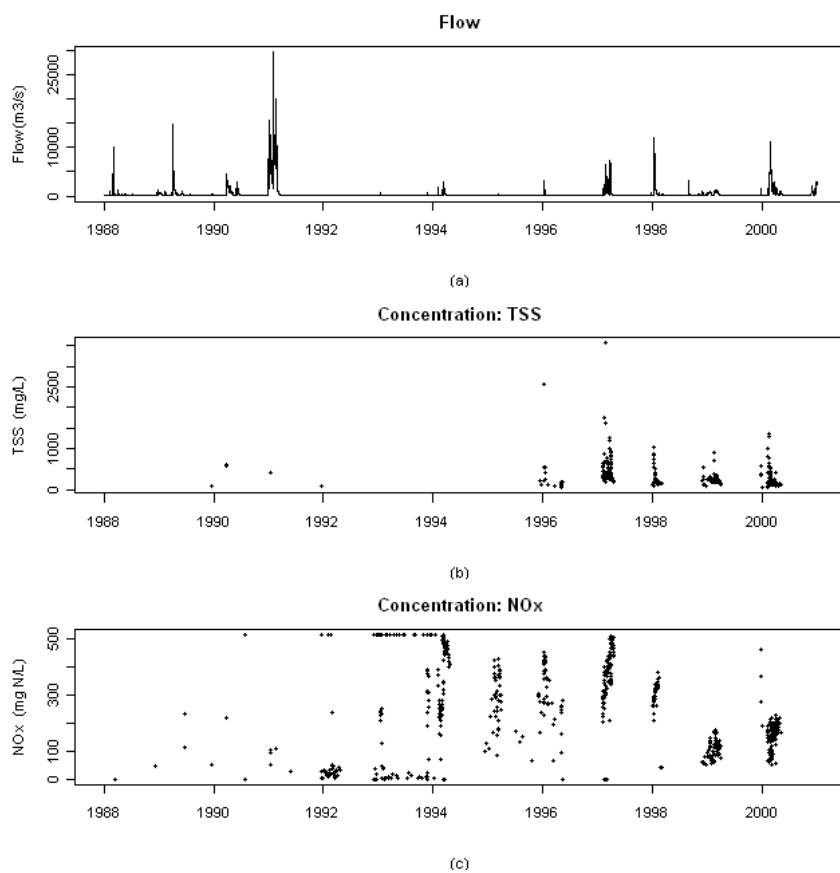


Figure 8: Plot showing (a) flow (m^3/s), (b) TSS (mg/L) and (c) NO_x ($mg N/L$) captured at the Inkerman Bridge site along the Burdekin River.

4.2.1 Total Suspended Sediment (TSS)

As highlighted above, we investigated a number of GAM models and selected the strongest fitting model (lowest GCV score) to use for predicting of TSS at the Inkerman Bridge site. The optimal model for predicting TSS included linear and quadratic terms for flow ($\log(\hat{Q}), \log(\hat{Q})^2$), a term characterising the rising/falling limb and discounted flow (D) which explained 47.3% of the variation in the data. The model is summarised in Table 4 and Figure 9 illustrating the predictive relationship between flow and TSS. Figure 9(b) in particular shows the relationship between the constant (stable) region of the curve produced for D and flow events corresponding to that region and suggests that frequent large events (increase along x -axis of bottom plot) may lead to an exhaustion process. Residual plots are displayed in Figure 10 and indicate the model is fit well to the data.

Table 4: Parameter estimates from the optimal model fit to TSS at the Inkerman Bridge site using 14 years worth of data. The coefficient (β), standard error ($SE(\beta)$) and p-value are shown for each parameter. This model had a GCV score of 0.26 and explained 47.3% of the variation in the data. The estimated serial correlation between adjacent days was 0.802. (bl = baseline reference category.)

Parameter	β	$SE(\beta)$	p-value
Intercept	11.165	1.77	< 0.001
Flow			
$\log(\hat{Q})$	-2.378	0.57	< 0.001
$\log(\hat{Q})^2$	0.220	0.05	< 0.001
Limb (bl=flat)			
Fall	0.135	0.08	0.097
Rise	0.217	0.07	0.002
Smooth Discounted Flow Term			
$s(\log(D))$	EDF=6.825		< 0.001

Specific results from this modelling include:

- 24.2% of TSS on average can be attributed to the rise of an event, while 14.5% are associated with the fall.
- Periods of stability in the discounted cumulated flow term may be linked with periods of exhaustion due to frequent large events as indicated by Figures 9 and 9.
- Increases in flow are indicative of increases in TSS (Figure 9(d)). Although increases are noted with

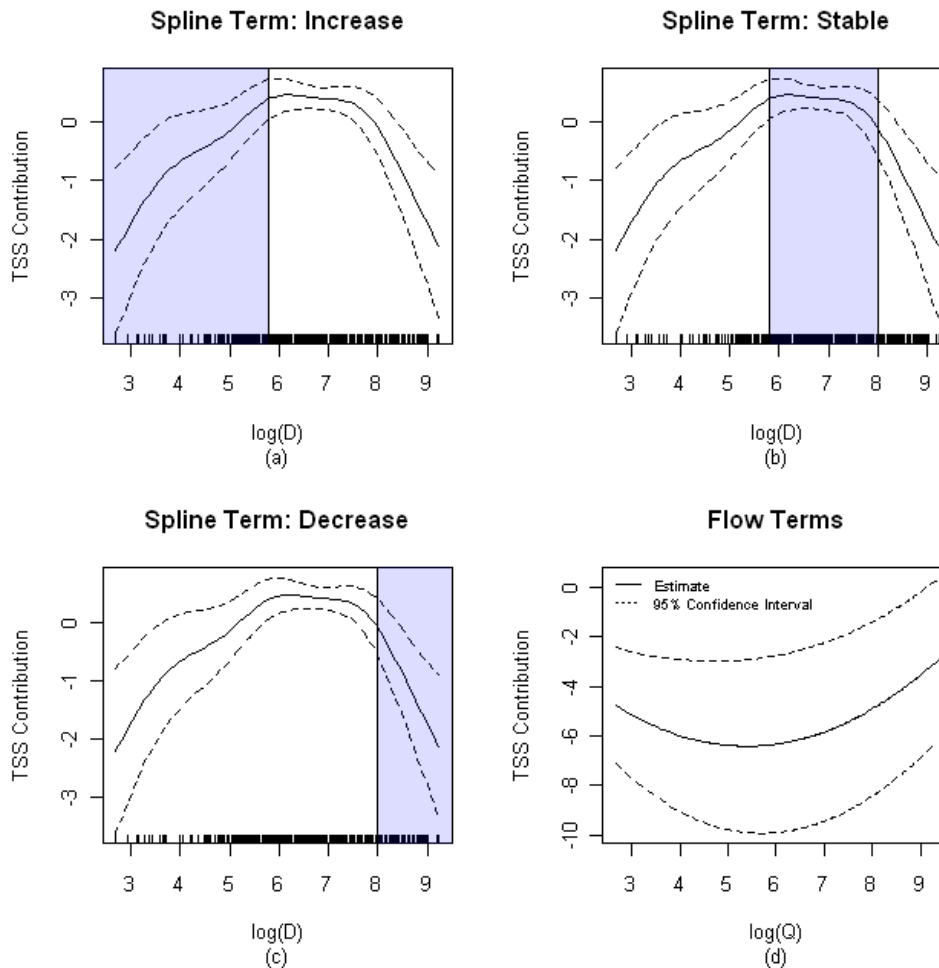


Figure 9: Plots showing the predictive contribution of $\log(D)$ with respect to TSS for the Inkerman Bridge site where (a) illustrates an increase in TSS as $\log(D)$ increases, (b) shows a stable, constant relationship and (c) illustrates a decrease in TSS for large values of $\log(D)$ and (d) highlights the quadratic relationship for flow as expressed in Table 4.

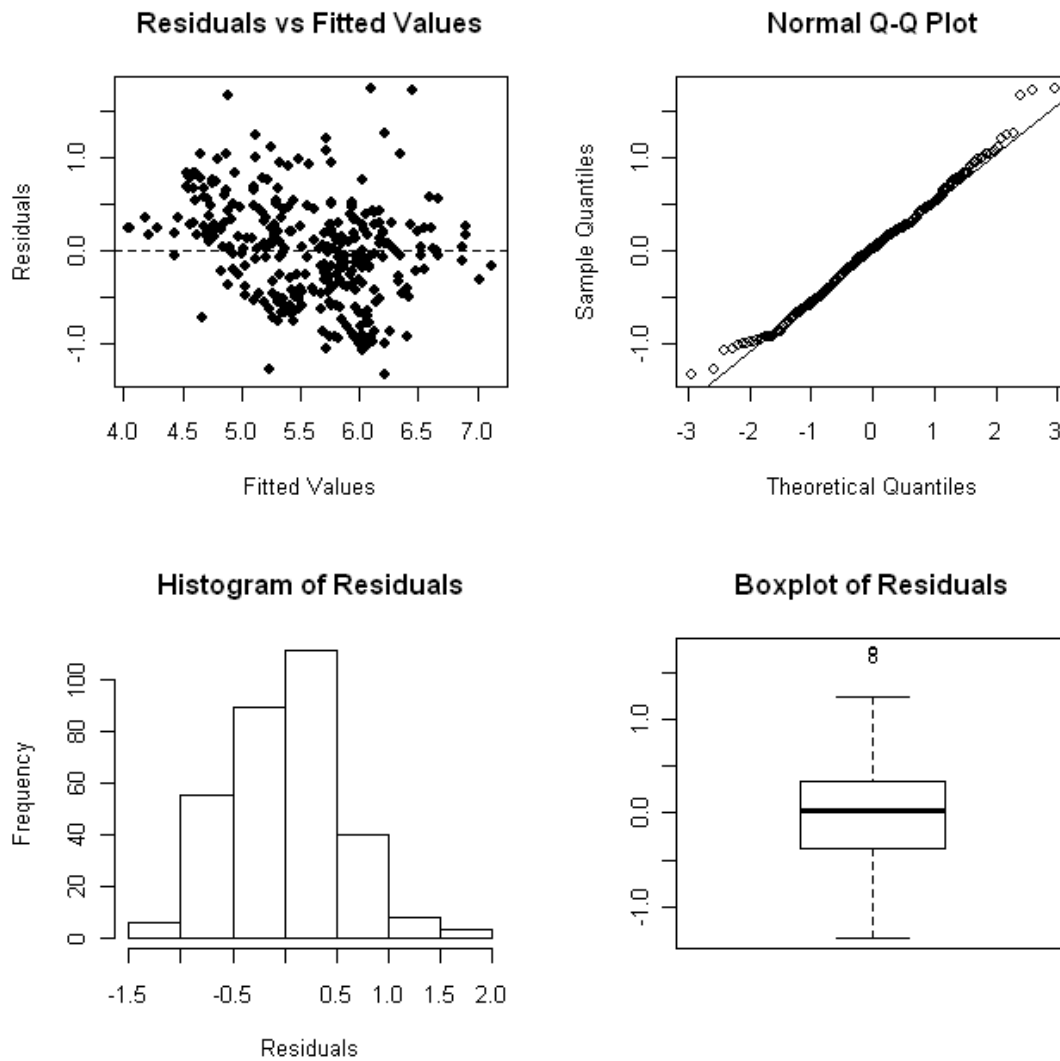


Figure 10: Residual plots examining the fit of the final model for TSS for the Inkerman Bridge site.

low flow events as well. The results may be confounded with D .

Estimates of the total load of TSS for each water year at the Inkerman Bridge site are summarised in Tables 21(a)-24(a) in Appendix A. Figure 11 also summarises the results for each error structure across water years and overlays the Beale Ratio estimator for comparison (red points). Note, the Beale estimator could only be applied when $n > 1$. Results from other estimators are presented in Table 5 for comparison. From these tables and figures, we observe that as the errors increase, the width of the confidence intervals increase, highlighting an increase in the variability in estimates across years. Of all the water years, the 1990/91 water year exhibits the largest standard error which is reflected in the width of the confidence interval and most likely due to the number of samples at that site and the size of the flow measured as can be seen in Figure 8(a). Small loads are predicted for water years encompassing 1991-1996, 1998/99 and 2000/01. Note the ability of this model to estimate a load during water years where no monitoring data has been collected. Although seen as an advantage, care needs to be taken when interpreting these loads estimates, particularly when the time period falls outside the range of the modelled data (e.g. 1987-1989 and 2000/01).

In comparison to the standard load estimators we note that both the average and extrapolation estimators perform the worst, overestimating the load for nearly every water year. Both the ratio and Beale estimators are more comparable to the modelled estimate as can be seen in Figure 11, where the majority of the time, the estimate is within the 95% confidence interval calculated for the load at each water year.

Table 5: Estimates of the total TSS load (Mt) for the average, extrapolation, ratio and Beale estimators for the Inkerman Bridge site.

Water Year	n	\bar{Q}	Standard Estimators			
			Average	Extrapolation	Ratio	Beale
1989/1990	3	296.4	36.48	51.16	5.61	5.62
1990/1991	2	1277.8	115.16	115.16	16.67	16.67
1991/1992	1	16.8	0.03	0.03	0.04	NA
1995/1996	19	68.4	4.05	14.46	2.59	2.83
1996/1997	78	275.2	31.08	48.82	7.53	7.58
1997/1998	39	286.8	24.93	50.61	5.49	5.57
1998/1999	70	190.5	4.68	5.09	1.68	1.68
1999/2000	100	438.0	18.93	26.5	5.04	5.05

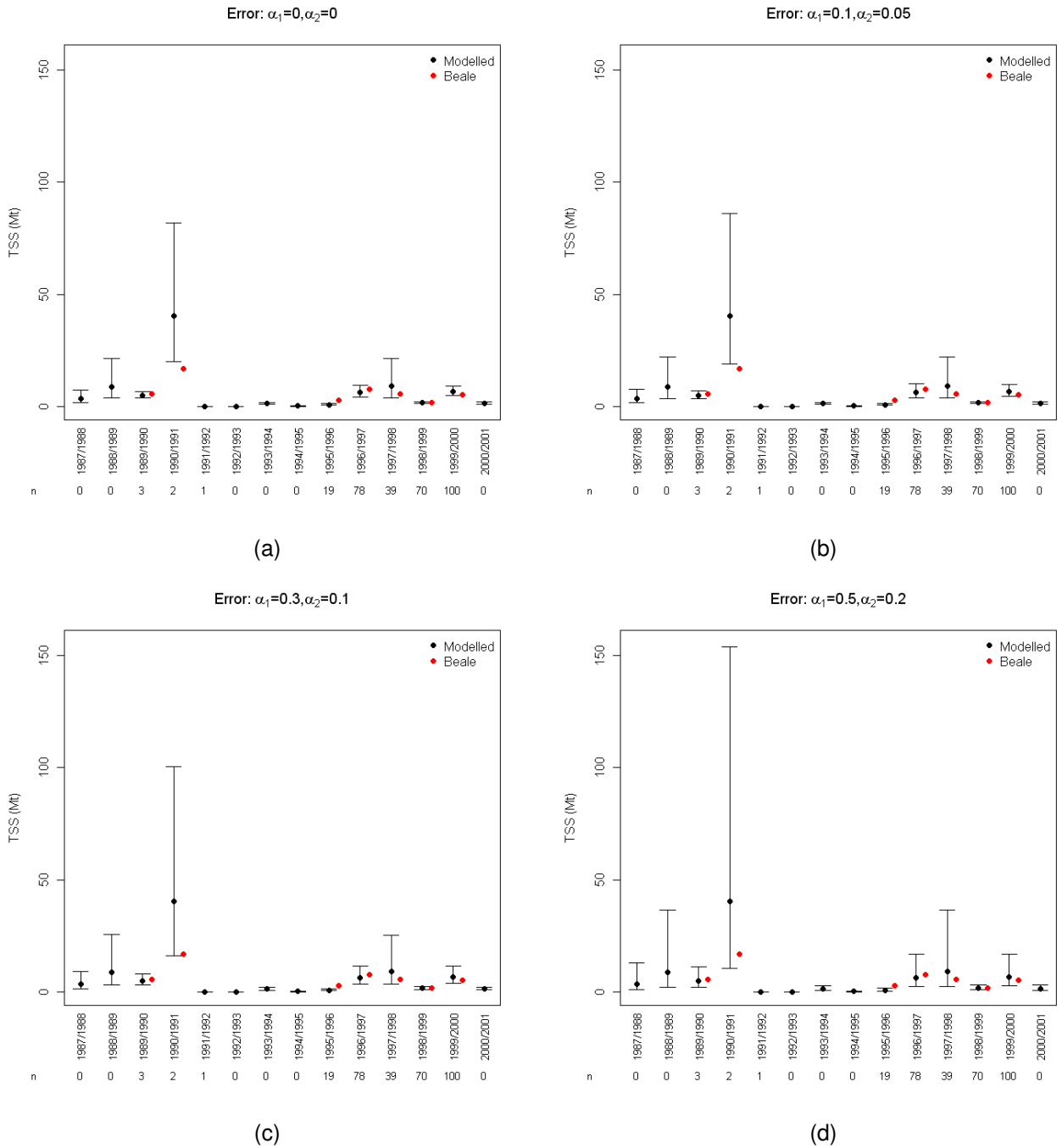


Figure 11: Summary and comparison of loads estimates for Inkerman bridge for TSS assuming (a) error structure 1, (b) error structure 2, (c) error structure 3, and (d) error structure 4. The number of concentration samples collected in each water year (n) is shown along the x -axis.

4.2.2 Oxidised Nitrogen (NOx)

We investigated a number of GAM models and selected the strongest fitting model (lowest GCV score) to use for prediction of NOx at the Inkerman Bridge site. The optimal model for predicting NOx included linear and quadratic terms for flow ($\log(\hat{Q}), \log(\hat{Q})^2$), a periodic term capturing seasonal fluctuations and discounted flow (D) which explained 43.3% of the variation in the data. The model is summarised in Table 6 and Figure 12 which illustrate the predictive relationship between flow and NOx. Residual plots are shown in Figure 14 which examine the adequacy of the model fit to the data. Residual plots suggest that the model provides a reasonable fit.

Figure 12 illustrates an increase in NOx as $\log(D)$ increases suggesting no period where the accumulation of NOx slowed down in the system. A slight decrease in NOx is also noted for higher flows (see Figure 12(a)) suggesting a possible dilution of NOx in the system once flow reaches a certain threshold. The periodic term in the model is explored further in Figure 13 and shows a decrease in NOx from October through to January where a large increase in NOx is noted between January and May (wetter periods) followed by a slight decrease from May through to September.

Table 6: Parameter estimates from the optimal model fit to NOx at the Inkerman Bridge site using 14 years worth of data. The coefficient (β), standard error ($SE(\beta)$) and p-value are shown for each parameter. This model had a GCV score of 0.92 and explained 43.3% of the variation in the data. The estimated serial correlation between adjacent days is 0.897.

Parameter	β	$SE(\beta)$	p-value
Intercept	-2.466	1.23	0.05
Flow			
$\log(\hat{Q})$	0.397	0.42	0.34
$\log(\hat{Q})^2$	-0.058	0.04	0.13
Periodic Term			
c_1	-0.194	0.12	0.11
s_1	0.065	0.20	0.74
c_2	-0.059	0.11	0.60
s_2	-0.032	0.11	0.77
Smooth Discounted Flow Term			
$s(\log(D))$	EDF=4.436		0.004

Specific results from this modelling include:

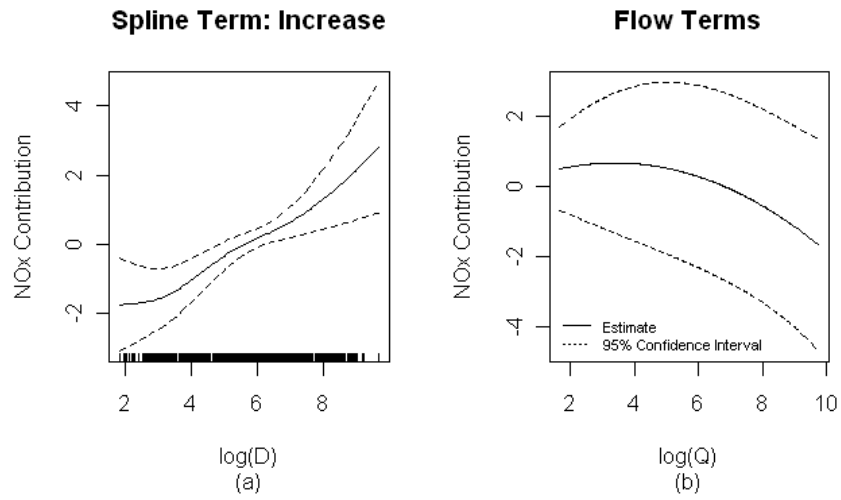


Figure 12: Plots showing the predictive contribution of $\log(D)$ with respect to NOx at the Inkerman Bridge site where (a) illustrates the relationship between NOx and $\log(D)$ and (b) highlights the quadratic relationship for flow as expressed in Table 6.

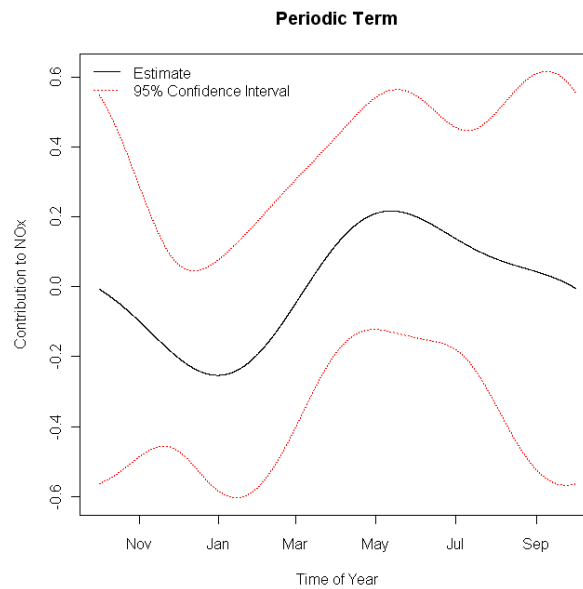


Figure 13: Periodic term fit in the generalised additive model for the Inkerman Bridge site across a water year.

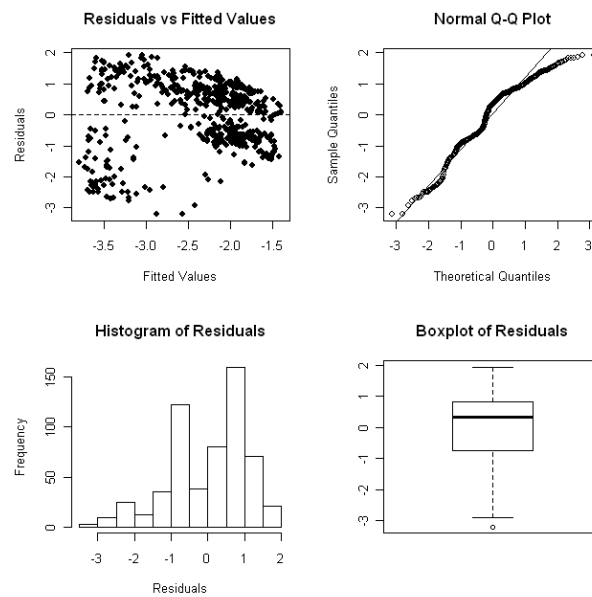


Figure 14: Residual plots examining the fit of the final model for NO_x recorded at the Inkerman Bridge site.

- A possible dilution effect occurring once flow reaches a threshold. This in turn appears to result in an accumulation of NO_x over time as frequent events occur.
- A subtle seasonal effect is noted showing a decrease in NO_x between October and January, an increase between January and May followed by another slight decrease from May through to September.

Estimates of the total load of NO_x for each water year at the Inkerman Bridge site are summarised in Tables 21(b)-24(b) in Appendix A. Figure 15 also summarises the results for each error structure across water years and provides a comparison with the popular Beale ratio estimator. Table 7 presents the results from some of the other standard estimators used to calculate a load. The 1990/91 water year once again is highlighted as having large variability compared to other years which is most likely due to the large recorded annual flow during that period. Some variation is also noted in the estimate produced for the 1999/2000 water year. Irrespective of the error structure implemented we see that some of the Beale estimates underestimate the load and lie outside the 95% confidence interval reported from the model. Once again, the model is able to estimate a load where no concentration data was captured but care must be taken in the interpretation as the 1997/98 and 2000/01 water years lie outside the range of the modelled data.

Load estimates produced using some of the standard loads based estimators are shown in Table 7. Both

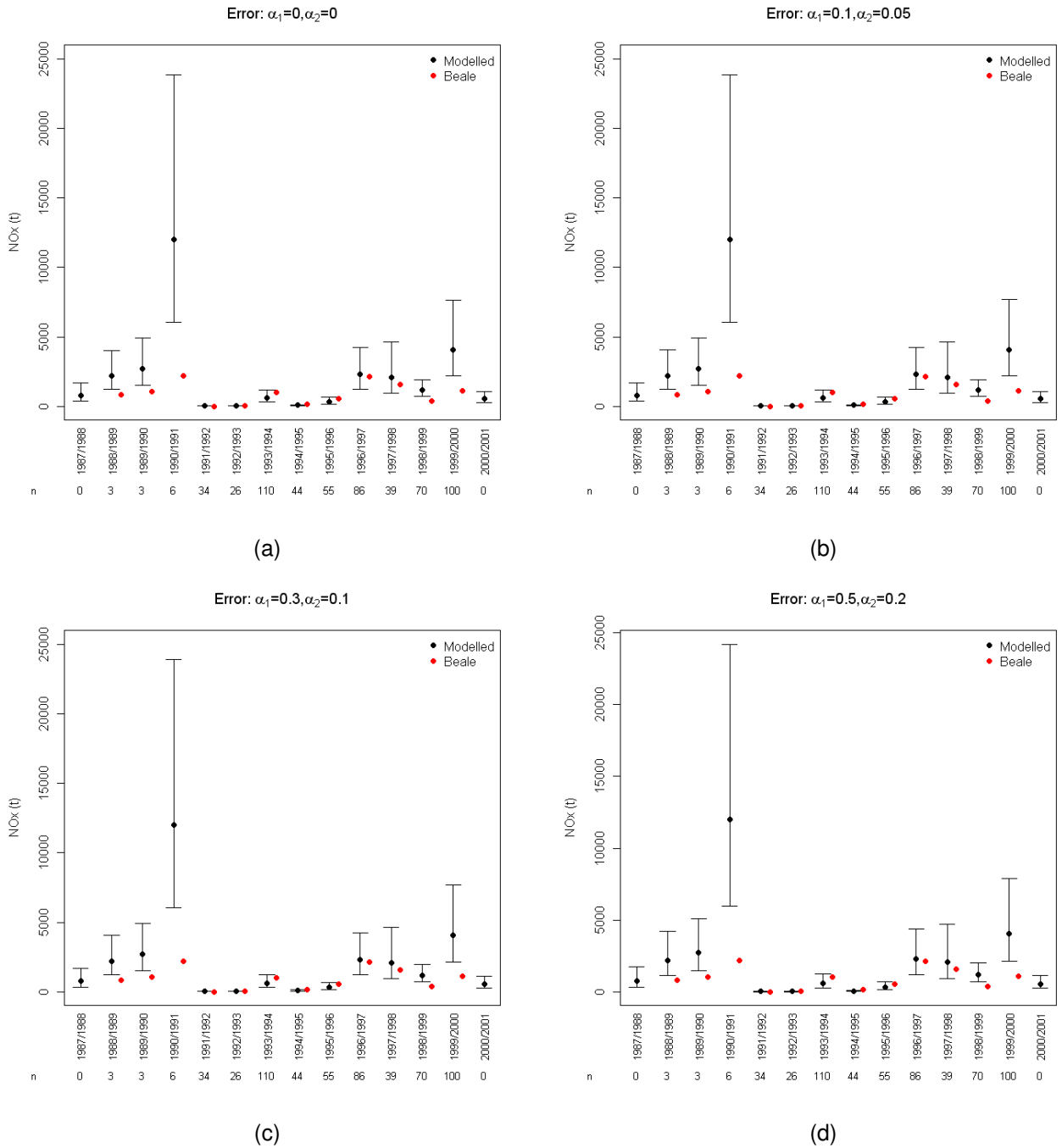


Figure 15: Summary and comparison of loads estimates for Inkerman bridge for NOx assuming (a) error structure 1, (b) error structure 2, (c) error structure 3, and (d) error structure 4. The number of concentration samples collected in each water year (n) is shown along the x -axis.

of the average based estimators overestimate the load substantially for many of the water years, while the Ratio and Beale estimators are more comparable to modelled estimates as shown in Figure 15.

Table 7: Estimates of the total NO_x load (t) for the average, extrapolation, ratio and Beale estimators computed at the Inkerman Bridge site.

Water Year	n	\bar{Q}	Standard Estimators			
			Average	Extrapolation	Ratio	Beale
1988/1989	3	291.2	218.98	279.32	816.62	846.96
1989/1990	3	296.4	7028.72	9672.3	1060.02	1061.65
1990/1991	6	1277.8	11080.31	14032.03	2143.78	2184.61
1991/1992	34	16.8	9.04	12.96	8.79	8.93
1992/1993	26	17.6	28.78	54.07	38.04	39.4
1993/1994	110	92.8	4981.91	6775.88	1022.78	1024.43
1994/1995	44	24.6	364.69	455.4	161.49	162.21
1995/1996	55	68.4	3060.72	3741.77	530.26	529.43
1996/1997	86	275.2	14075.23	13135.37	2161.34	2160.44
1997/1998	39	286.8	14925.05	14566.12	1581.4	1576.31
1998/1999	70	190.5	1109.75	1160.01	382.29	382.45
1999/2000	100	438.0	6150.01	5739.43	1091.25	1092.09

4.3 Bowen River

The Bowen River catchment is 7,200 km^2 in contrast to the much larger Burdekin River catchment which consists of an area of 130,000 km^2 . Data from the Bowen River was collected in the 2005/06 water year and consists of flow collected by NRW at a gauging station at Myuna and recorded hourly (m^3/s), while concentration samples were collected using an ISCO autosampler. Details are provided in Bartley et al. (2007) and references therein. Figure 16 shows a summary of the TSS and NO_x data collected at this site. Although flow samples have been recorded since the start of the water year, concentration measurements were collected from January, 2006 and were quite sporadic resulting in 40 and 41 concentration measurements for TSS and NO_x respectively been taken overall.

The results from modelling TSS and NO_x in the Bowen river are displayed in Table 8 and highlight a linear term for flow and a smooth term for D to be the most important predictors for TSS and an additional periodic term for NO_x. We did not include a correlation term in either model due to the size of the dataset. The model

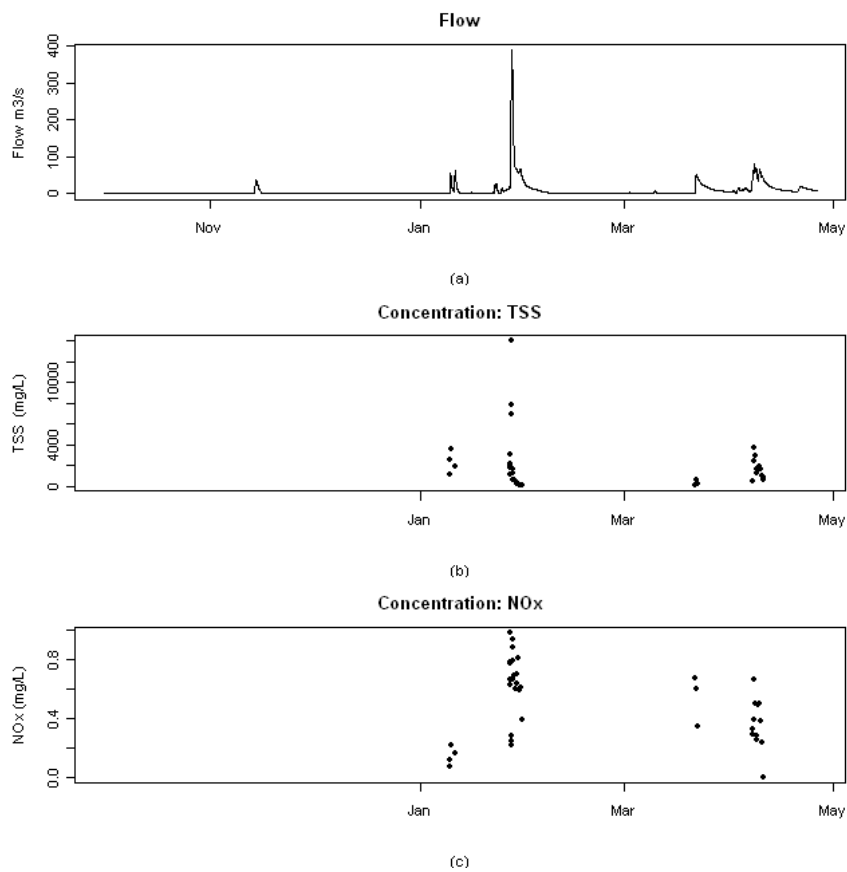


Figure 16: Plot showing flow, TSS and NOx captured at the Myuna site along the Bowen river.

for TSS produced a GCV score of 0.454 and explained 80.5% of the variation in the data while the model for NO_x explained 78.2% of the variation in the data (GCV score = 0.567). A model with just a linear term for flow resulted in under 12% of variation explained by both models, highlighting the importance of the smooth and periodic terms in these models.

Figure 17 shows the smooth relationship for discounted flow and the linear term for flow which were fit in both models. The smooth term shown in Figure 17(a) shows some stability at higher flows where data is represented followed by a decrease in sediment as $\log(D)$ increases whereas for NO_x, this stabilisation remains at higher levels (Figure 17(c)). An increase is observed when flow itself increases linearly for both models, which may also contribute to the exhaustion process. See Figures 17(b) and (d). The periodic term fitted in the NO_x model is shown in Figure 18 and shows increases in the contribution to NO_x from November through to January where the level remains stable through to May.

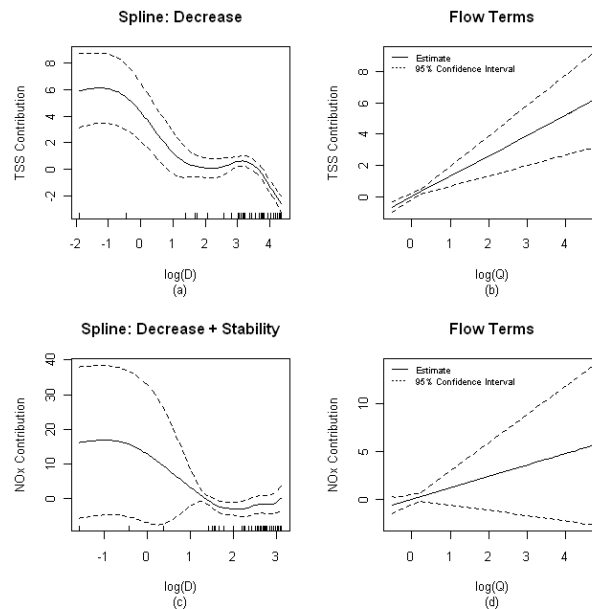


Figure 17: Plots showing the predictive contribution of $\log(D)$ with respect to TSS and NO_x for the Myuna site along the Bowen River, where (a) illustrates the relationship between TSS and $\log(D)$, (b) highlights the linear term for flow, (c) shows the relationship between NO_x and $\log(D)$ and (d) shows the linear term for flow for the model predicting NO_x.

Specific results from this modelling include:

- Some indication of sediment accumulation stabilising although the confidence intervals shown in Figure 17 are quite wide in parts.

Table 8: Parameter estimates from the optimal model fit to TSS and NO_x respectively at the Myuna site in the Bowen River using data collected during the 2005/06 water year. The coefficient (β), standard error ($SE(\beta)$) and p-value are shown for each parameter. This model for TSS had a GCV score of 0.454 and explained 80.5% of the variation in the data while the model for NO_x explained 78.2% of the variation in the data with GCV score of 0.567.

Model for TSS			
Parameter	β	$SE(\beta)$	p-value
Intercept	2.144	1.19	0.081
Flow			
$\log(\hat{Q})$	1.298	0.32	< 0.001
Smooth Discounted Flow Term			
$s(\log(D))$	EDF=5.67		< 0.001
Model for NO_x			
Parameter	β	$SE(\beta)$	p-value
Intercept	-836.4	228.7	0.001
Flow			
$\log(\hat{Q})$	1.20	0.90	0.191
Periodic Term			
c_1	-958.96	266.2	0.001
s_1	661.7	187.3	0.001
c_2	-120.95	37.7	0.003
s_2	325.87	93.7	0.002
Smooth Discounted Flow Term			
$s(\log(D))$	EDF=6.791		0.004

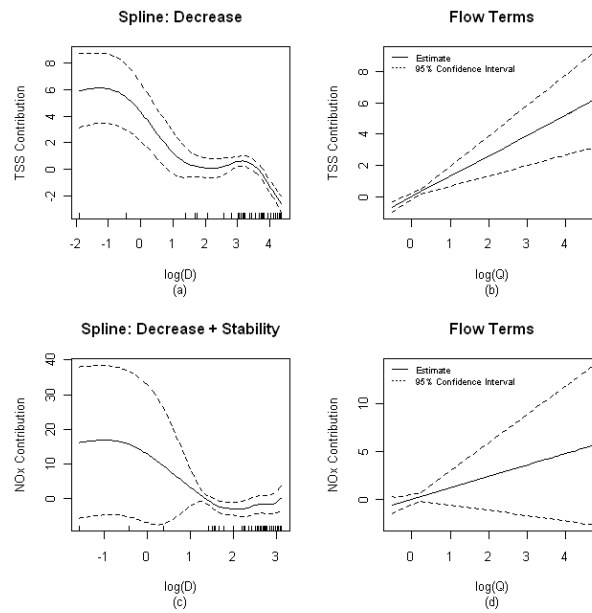


Figure 18: Periodic term fitted to the Myuna dataset showing the contribution to NOx on the y -axis (log-scale) and time on the x -axis.

- Increases in flow are indicative of increases in TSS and NOx (Figure 17(b) and (d)).
- Fitting a quadratic term resulted in some inconsistencies with the fit for both models and large standard errors suggesting that the quadratic term should be dropped. This term is not always appropriate when modelling smaller datasets.
- Serial correlation was not incorporated due to the size and nature of the data and therefore was not considered to be an issue.
- A strong increase in NOx from November through to January which remains stable right through to May.

Estimates of the total load of TSS and NOx for the 2005/06 water year at the Myuna site are summarised in Table 9 along with Figure 20(a) which summarises these results and compares them with the standard ratio estimators. When compared to the standard load estimators both the average and extrapolation estimators overestimated the load whereas the ratio and Beale estimators provided estimates close to the modelled estimates and reside in our calculated 95% confidence interval. See Table 10 and Figure 20(a).

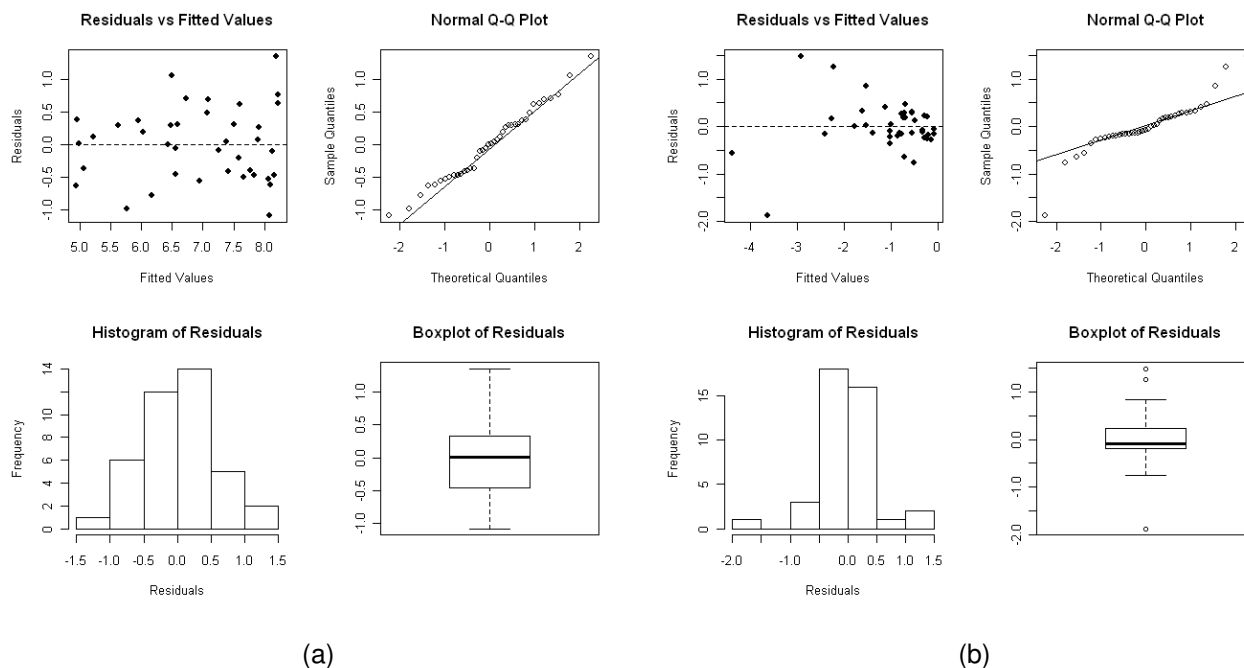


Figure 19: Residual plots for the model fit to (a) TSS and (b) NOx at the Myuna site in the Bowen River.

Table 9: Estimates of the total (corrected, L_c) TSS load (Mt) and NOx load (t) calculated for the Myuna site in the Bowen River and 95% confidence intervals for 4 different error structures. The average flow across the year is $6.73 \text{ m}^3/\text{s}$.

Water Year	Error		\hat{L}	\hat{L}_c	SE	CV (%)	n	CI_L	CI_U
	α_1	α_2							
TSS (Mt)									
2005/06	0	0	1.246	.857	.716	83.5%	40	.17	4.41
2005/06	0.1	0.05	1.246	.857	.724	84.4%	40	.16	4.49
2005/06	0.3	0.1	1.246	.857	.750	87.5%	40	.15	4.76
2005/06	0.5	0.2	1.246	.857	.836	97.5%	40	.13	5.80
NOx (t)									
2005/06	0	0	144.82	69.58	21.69	31.2%	41	37.77	128.19
2005/06	0.1	0.05	144.82	69.58	23.05	33.1%	41	36.35	133.19
2005/06	0.3	0.1	144.82	69.58	26.93	39.7%	41	32.59	148.55
2005/06	0.5	0.2	144.82	69.58	38.26	55.0%	41	23.68	204.42

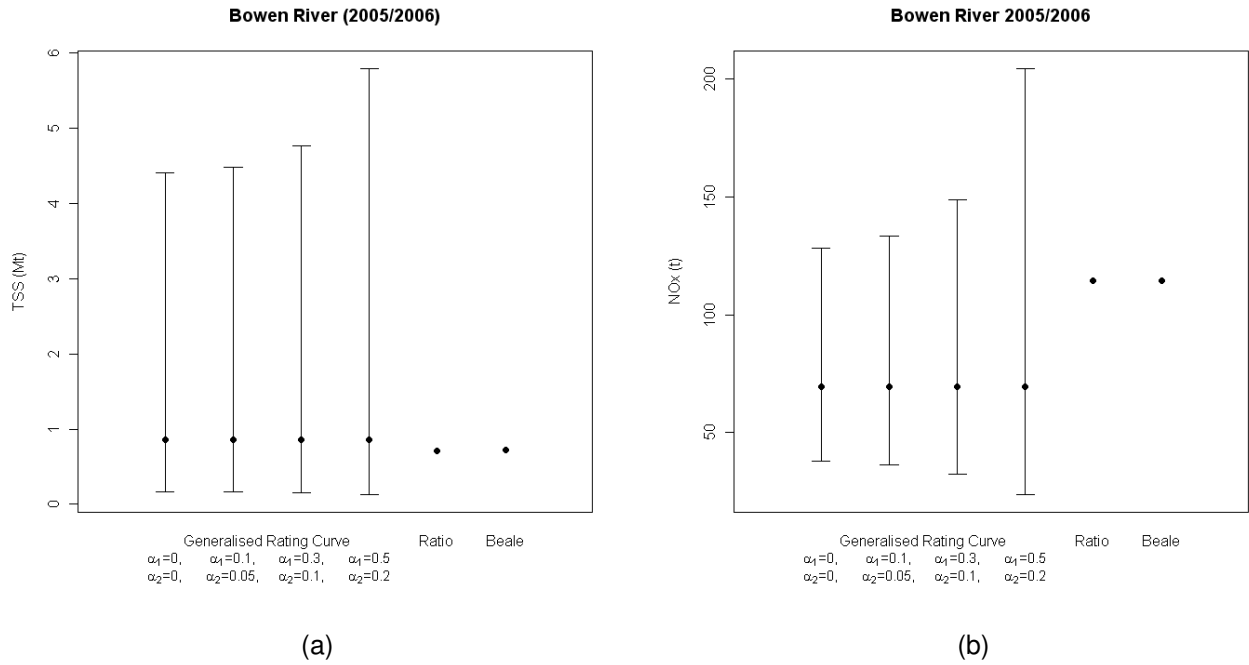


Figure 20: Summary of loads estimates for the Myuna site for (a) TSS and (b) NOx.

Table 10: Estimates of the total TSS load (Mt) and NOx load (t) for the Myuna site in the Bowen River for the average, extrapolation, ratio and Beale estimators.

Water Year	Standard Estimators			
	Average	Extrapolation	Ratio	Beale
TSS (Mt)				
2005/06	6.34	11.10	0.71	0.73
NOx (t)				
2005/06	1575.8	1757.02	114.39	114.32

4.4 Mistake Creek

Community groups actively sample in the Burdekin and visit sites that are difficult for staff to travel to during events or do not have automatic samplers in place. Datasets that capture this type of information can be quite sparse and generally only represent events. Depending on the ease in which samples can be taken, samples arise predominantly on the falling limb, although community groups are encouraged to take samples on both the rise and the fall. Mistake Creek is a site in the Burdekin catchment that represents data collected by a community volunteer. Data consists of events recorded in 2006 only. Figure 21 shows flow, TSS and NO_x data collected at that site. It is clear from these plots that very few samples of concentration were collected ($n = 5$).

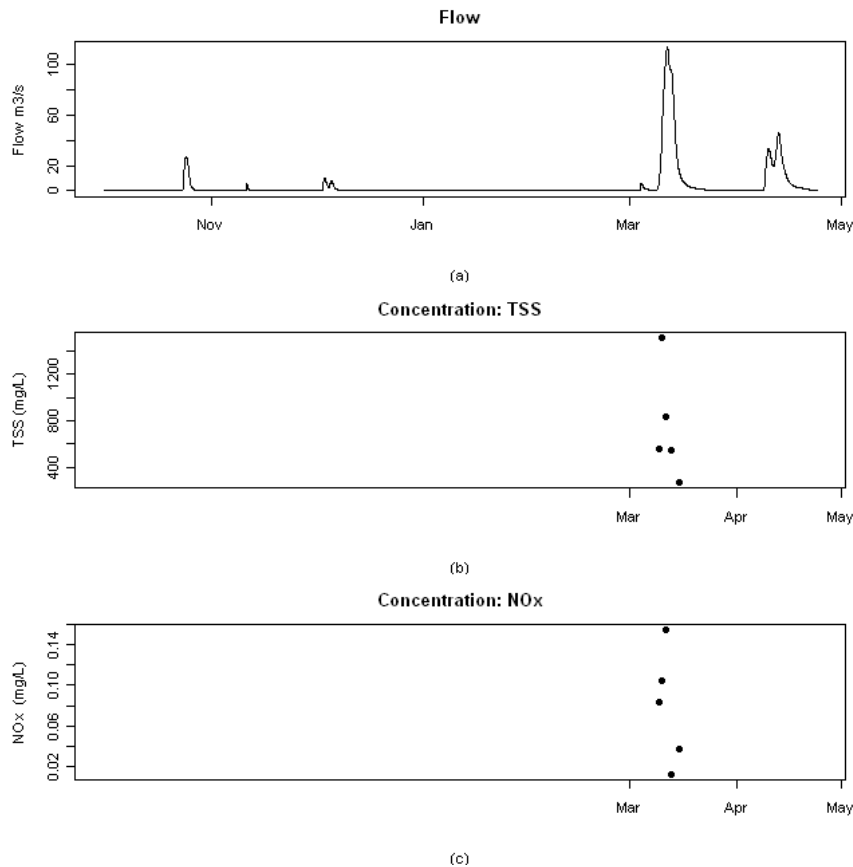


Figure 21: Plot showing (a) flow, (b) TSS and (c) NO_x captured at the Mistake Creek site along the Bowen river.

With very few data points, it is difficult to fit a comprehensive model to both types of concentration datasets with terms that capture hydrological characteristics. In selecting the optimal model, we therefore compared fitting the intercept (equivalent to an average type estimator) with a linear term for flow and/or a discounted

flow term. A seasonal term was not appropriate to consider in addition to the rising/falling limb due to the small sample size. The optimal model for TSS (GCV score of 0.685) was a model that included the intercept and a linear term for the discounted flow which resulted in explaining approximately 22.8% of the variation in the data. The linear term for D suggests that as D increases, a decrease in TSS is observed, however the term is not significant (p -value = 0.42). The strongest model for NO_x however was one that included the intercept term only. Residual plots for both models are displayed in Figure 22 and suggest adequacy of the model fit despite the small number of observations.

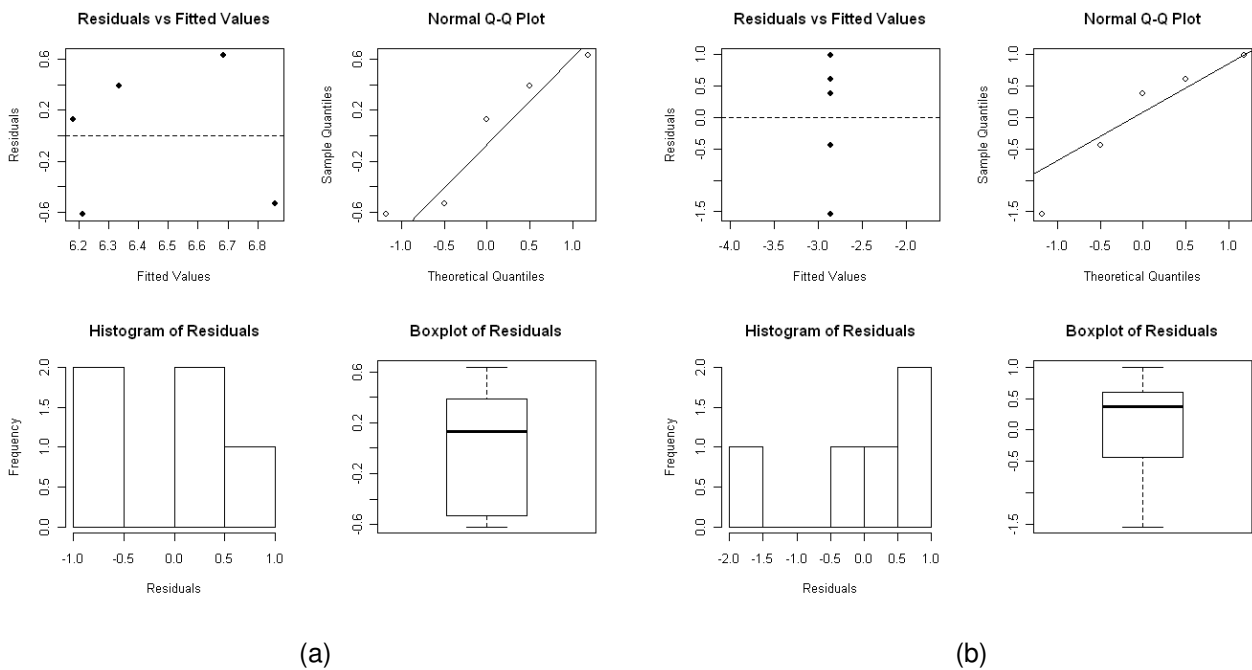


Figure 22: Residual plots for the model fit to (a) TSS and (b) NO_x at the Mistake Creek site in the Burdekin catchment.

Estimates of the total load for both TSS and NO_x are shown in Table 11 and Figure 23 along with the standard estimators in Table 12. Results highlight a coefficient of variation between 29%-35% for NO_x and 45%-50% for TSS resulting in fairly wide confidence intervals for the load estimate. Compared with the standard estimators, the modelled estimates compare reasonably well (estimates within the 95% confidence intervals) with the ratio based estimators. Once again the average estimators tend to overestimate the load.

Table 11: Estimates of the total (corrected, L_c) TSS load (Mt) and NOx load (t) under four different error structures. Corresponding 95% confidence intervals are also presented. The average flow across the year is $3.425 \text{ m}^3/\text{s}$.

Water Year	Error		\hat{L}	\hat{L}_c	SE	CV (%)	n	CI_L	CI_U
	α_1	α_2							
TSS (Mt)									
2005/06	0	0	.038	.043	.012	28.9%	5	.024	.076
2005/06	0.1	0.05	.038	.043	.013	29.3%	5	.024	.076
2005/06	0.3	0.1	.038	.043	.013	30.6%	5	.024	.078
2005/06	0.5	0.2	.038	.043	.015	35.2%	5	.022	.086
NOx (t)									
2005/06	0	0	3.46	5.20	2.36	45.5%	5	2.13	12.68
2005/06	0.1	0.05	3.46	5.20	2.38	45.8%	5	2.12	12.74
2005/06	0.3	0.1	3.46	5.20	2.42	46.6%	5	2.08	12.96
2005/06	0.5	0.2	3.46	5.20	2.59	49.8%	5	1.96	13.79

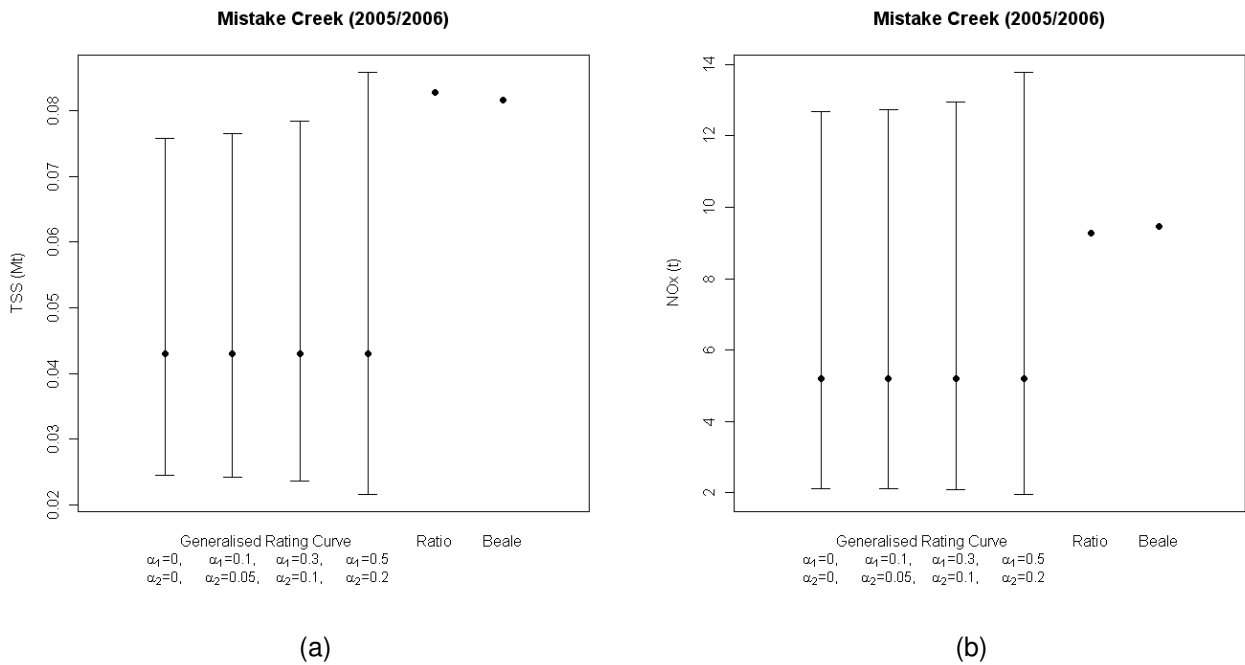


Figure 23: Summary of loads estimates for Mistake Creek for (a) TSS and (b) NOx.

Table 12: Estimates of the total TSS load (Mt) and NOx load (t) at the Myuna site in the Bowen River for the average, extrapolation, ratio and Beale estimators.

Water Year	Standard Estimators			
	Average	Extrapolation	Ratio	Beale
TSS (Mt)				
2005/06	1.178	1.218	0.083	0.082
NOx (t)				
2005/06	123.78	136.4	9.297	9.462

4.5 Summary of Results for the Burdekin Catchment

There are clear advantages from modelling multiple years worth of data. The first and most important advantage is that it builds in history, a time series of flow and concentration characteristics that can be used to predict across the entire time frame. This approach also allows us to observe trends through time (whether seasonal or long term) and it aids in the understanding of concentration and flow relationships and how they might differ for different types of concentrations we are interested in. We could of course fit models to each water year separately. In doing so we may find that a much simpler model is required because the seasonal and long term patterns of flow and concentration are not apparent in a shorter time series, especially where there might be few concentration measurements with which to build the model on.

Tables 13 and 14 summarise the models fit to the three sets of data in the Burdekin catchment. Table 13 indicates the types of terms fit in each model where a (✓) represents that a term was fitted and a (×) indicates the term was omitted. Where crosses are marked for all terms, only the intercept was fit in the model. It is clear from this table that as the size of the dataset decreases, a smaller number of terms are fit in the model. This table also shows that different terms may be applicable for different types of responses. For example, a seasonal term is fit to the Inkerman Bridge dataset for NOx whereas for TSS, the rising/falling limb term is more appropriate. This highlights the importance for investigating a range of models for the data of interest rather than fitting the same suite of terms to all datasets investigated.

In terms of selecting an optimal model for each dataset, we see in Table 14 that fitting additional terms that attempt to mimic important hydrological characteristics is beneficial and provides a much better prediction, and thus a more precise estimate of the load. In particular the % deviance explained for the optimal model compared to fitting a model with just flow or a quadratic term for flow increases substantially.

Table 13: Summary of results for TSS and NOx for the Burdekin catchment

Site	Scale	Concentration Parameter	Important Covariates				
			Linear Flow	Quadratic Flow	Seasonal	Limb	<i>D</i>
Inkerman Bridge	End-of-catchment	TSS	✓	✓	×	✓	✓
		NOx	✓	✓	✓	×	✓
Bowen River	Subcatchment	TSS	✓	×	×	×	✓
		NOx	✓	×	✓	×	✓
Mistake Creek	Local	TSS	×	×	×	×	✓
		NOx	×	×	×	×	×

Table 14: A summary of models fit to the Burdekin data in terms of the % deviance explained. NA's represent models that could not be fit to the data.

Site	Concentration Parameter	% Deviance Explained		
		Optimal Model	Quadratic Flow Only	Linear Flow Only
Inkerman Bridge	TSS	47.3%	33.2%	32.8%
	NOx	43.3%	29.7%	17.2%
Bowen River	TSS	80.5%	5.1%	0.2%
	NOx	78.2%	14.3%	12.1%
Mistake Creek	TSS	22.8%	NA	6.69%

5 CASE STUDY II: TULLY CATCHMENT

5.1 Catchment characteristics

The Tully river in North Queensland, Australia is a small, faster flowing tropical river that extends approximately 130km before discharging into Rockingham Bay. The Tully catchment itself is located in the southern part of the Wet Tropics region in Queensland covering an area of 2790 km^2 when combined with the Murray catchment (Furnas, 2003). Topography of the catchment varies from steep mountainous areas in the west to the low relief floodplain in the east (Karim et al., 2008). Flow discharge within each year is highly variable, peaking between February through to April. As the topography is flat and the location of the Tully and Murray rivers is close, floodwaters have the tendency to merge during floods causing the export of sediment and nutrients to be much higher when compared to the annual average riverine load (Wallace et al., 2008).

5.2 Tully River

Flow records from the Tully were collected during the period 1 July 2000 to 16 April 2008, spanning approximately 8 years and consisting of 51,866 observations. Flow data was collected at irregular time intervals ranging from 0.16 to 34 hours with a mean of 1.32 and a median of 0.66 hours. For some periods flow measurements are taken at intervals of a few days, but for much of the year the flow measurements are only approximately monthly. The total suspended solid concentration data were collected at sporadic time intervals, usually corresponding to an event. Figure 24 shows a plot of flow and concentration records for the 8 years of data collected in the Tully river. Note the increase in concentrations recorded during the later years.

We examined a range of GAM models which considered incorporating a quadratic term for flow, rising/falling limb, a seasonal term and a discounted flow term. The strongest model (GCV score = 0.33) included all of these terms with the exception of the term incorporating the rising/falling limb. The results are displayed in Table 15 and Figure 26. Residual plots examining the fit of the model are shown in Figure 25 and indicate a reasonable fit to the data.

The final model explained 76.3% of the variation in the data, which was much higher compared to a model which just incorporates flow (49.9% explained). Figure 26 summarises the results shown in Table 15 and shows that as flow increases, TSS increases. Furthermore, as large events occur more frequently, TSS tends to decrease indicating possible exhaustion of the system and dilution of material occurring. The

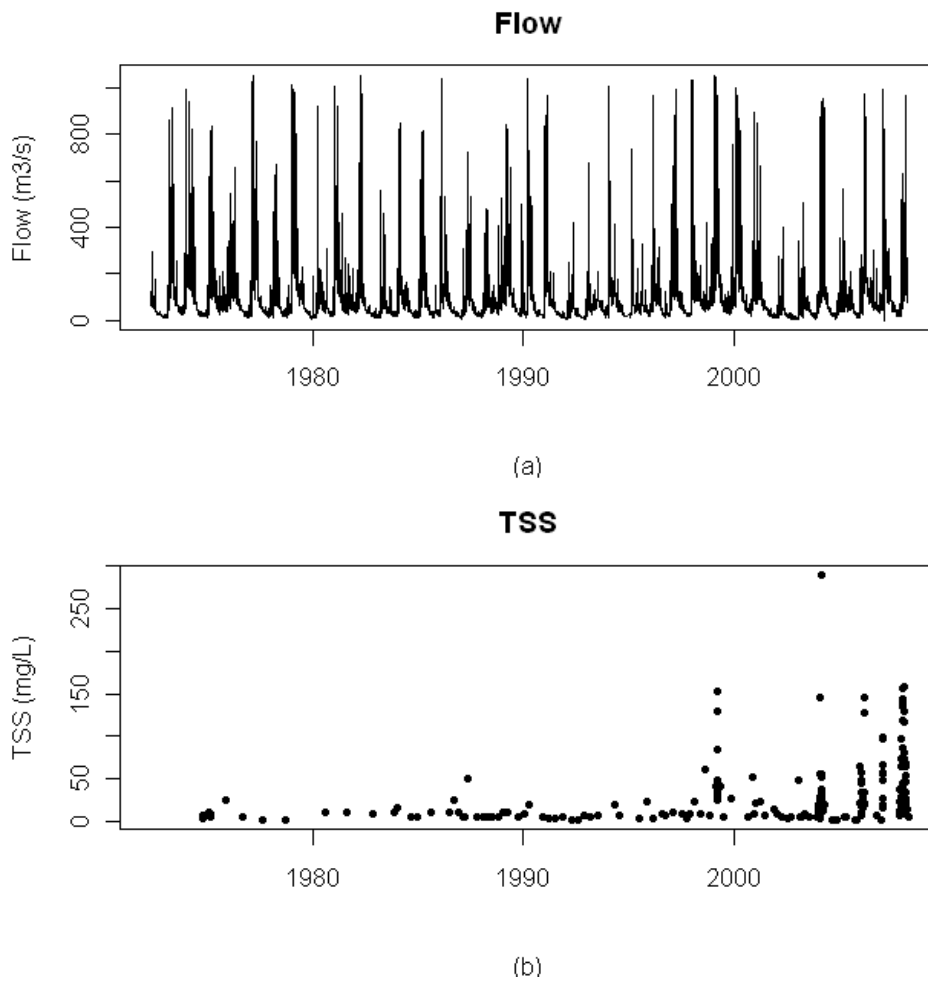


Figure 24: Plot showing (a) flow and (b) TSS captured at the Euramo site along the Tully river.

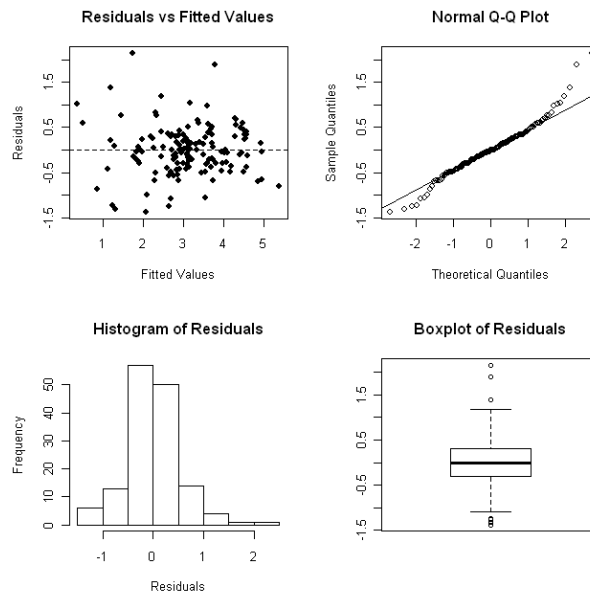


Figure 25: Residual plots for the final GAM model fit to the tully dataset.

periodic term is visualised in Figure 27 and shows increases in TSS in December and January, representing the peak of the wet season with a gradual decrease until September where another increase is observed.

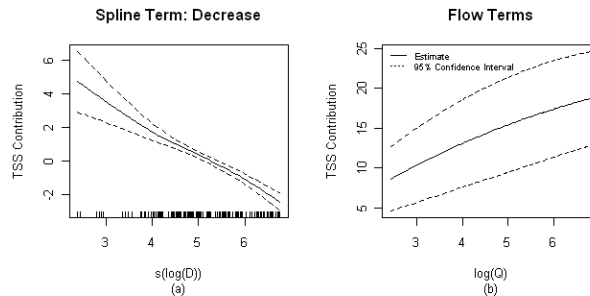


Figure 26: Plots showing the predictive contribution of $\log(D)$ with respect to NO_x for the Euramo site along the Tully River, where (a) illustrates the relationship between TSS and $\log(D)$ and (b) highlights the quadratic relationship for flow as expressed in Table 15.

Estimates of loads produced for the eight years of the Tully are presented in Figure 28 and Tables 25-28 in Appendix B. Standard estimators are presented in Table 16 along with the average flow recorded for each water year. Results indicate some differences between the modelled estimates compared to the Beale estimator represented by the red points in Figures 28. In fact all estimators were quite variable compared to the modelled response. As the measurement and spatial error increases, the error around

Table 15: Parameter estimates from the optimal model fit to TSS at the Euramo site along the Tully river using 8 years worth of data. The coefficient (β), standard error ($SE(\beta)$) and p-value are shown for each parameter. This model had a GCV score of 0.33 and explained 76.3% of the variation in the data. The estimated serial correlation was 0.15.

Parameter	β	$SE(\beta)$	p-value
Intercept	-12.890	2.96	< 0.001
Flow			
$\log(\hat{Q})$	3.992	1.083	< 0.001
$\log(\hat{Q})^2$	-0.182	0.097	0.062
Periodic			
c_1	-0.048	0.16	0.763
s_1	0.290	0.15	0.061
c_2	-0.067	0.11	0.540
s_2	0.135	0.10	0.193
Smooth Flow Term			
$s(\log(D))$	EDF=2.578		< 0.001

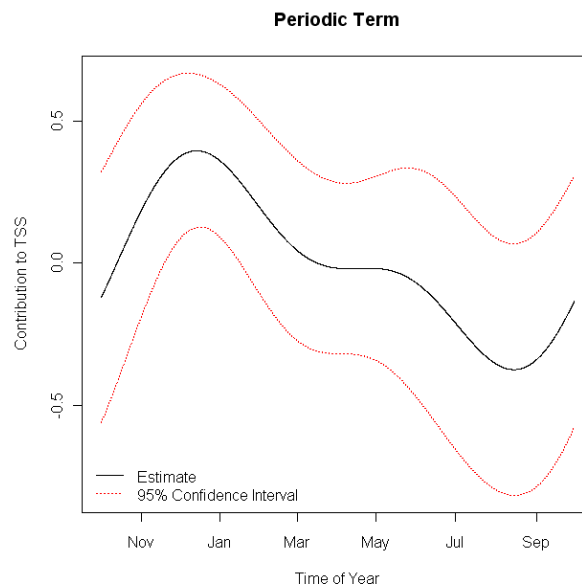


Figure 27: Periodic term fit in the generalised additive model for the Euramo site in the Tully River

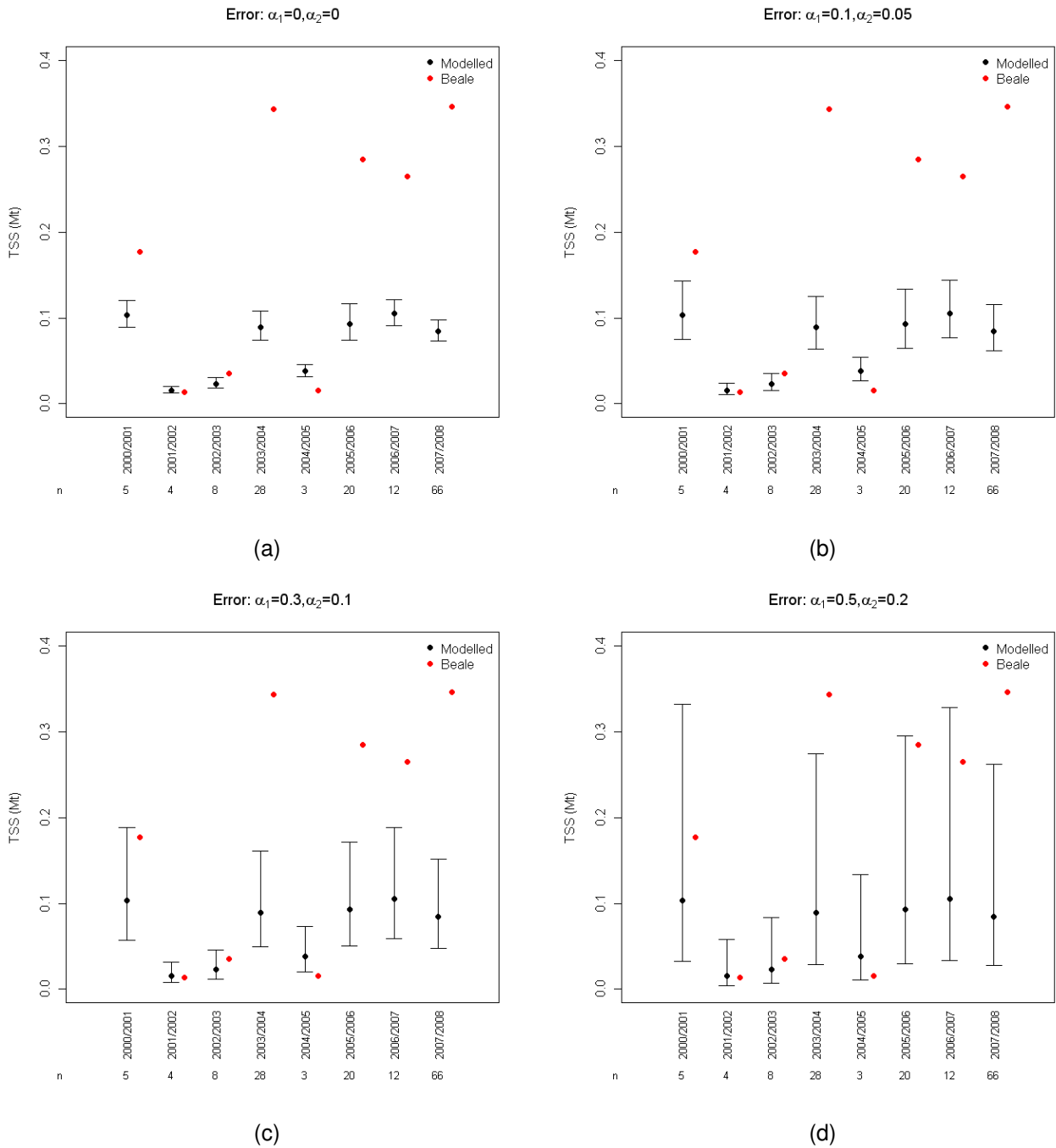


Figure 28: Summary and comparison of loads estimates for the Euramo site along the Tully river for TSS assuming (a) error structure 1, (b) error structure 2, (c) error structure 3, and (d) error structure 4. The number of concentration samples collected in each water year (n) is shown along the x -axis.

the modelled estimates increased and in some cases, these intervals incorporated the Beale estimates. In some instances, the average estimator was more in line with the modelled results (see Table 16, early years). Specific results include:

- Increases in TSS as flow increases in the wetter periods.
- A possible dilution effect occurring due to the frequent high events.
- Low estimates of TSS across the 8 years compared to estimates produced from the Burdekin and compared with the standard estimators.

Table 16: Estimates of the total TSS load (Mt) for the average, extrapolation, ratio and Beale estimators.

Water Year	n	\bar{Q}	Standard Estimators			
			Average	Extrapolation	Ratio	Beale
2000/2001	5	113.5	0.112	0.143	0.171	0.177
2001/2002	4	38.6	0.006	0.006	0.015	0.014
2002/2003	8	46.1	0.023	0.027	0.035	0.035
2003/2004	28	104.5	0.413	0.603	0.34	0.344
2004/2005	3	70.3	0.005	0.006	0.015	0.015
2005/2006	20	115.0	0.309	0.47	0.28	0.284
2006/2007	12	125.2	0.716	0.808	0.265	0.265
2007/2008	66	141.0	0.521	0.612	0.347	0.347

6 VALIDATION OF THE METHOD

A simulation study was constructed to investigate (1) the modelling methodology and its comparison with other existing methods for load estimation and (2) sampling strategies for wet and dry catchments. We will focus initially on a preliminary investigation of (1) and devise a simulation study that examines and compares the proposed loads methodology with standard methods. We will only touch briefly on the second part to this problem and leave the investigation to the final stage of this project in 2009/10.

GBR catchments have not been the focus of intensive, long-term discharge and sediment/nutrient sampling. Long-term, high-resolution discharge/stage height data is available for many catchments, however the frequency of sediment and nutrient sampling has been quite varied and is typically of low temporal resolution (e.g. monthly ambient with more frequent event-based sampling). Ideally, comparison of load estimation

methods is best achieved using a data set where both discharge and sediment and nutrient concentrations have been sampled at a high frequency. Such a dataset can first be used to calculate a 'best-case' load estimate, which can then be degraded into the forms expected under typical sampling regimes and the loads estimated and compared using the various methods under consideration. The results obtained can then be compared with the "best-case" load in order to ascertain the most accurate method.

In the absence of a high-resolution GBR dataset we turned two high resolution United States Geological Survey (USGS) datasets to facilitate the preliminary comparison of the various load estimators. The first dataset is derived from a gauging/sampling site on the San Juan River in New Mexico and represents daily values of discharge and sediment concentration, spanning 36 years (1950-1986) and comprising approximately 13,000 discharge and TSS samples. This site is consistent with sites located in wet catchments of the GBR (see Figure 29(a)). The second site is more typical of a site located in drier parts of the GBR such as the Burdekin, although it represents a much smaller catchment area (117 km^2) and spans 16 years. The site is located in San Juan Creek at San Juan Capistrano in California and exhibits two large events which occur between 1982 and 1983 followed by three smaller flushes (see Figure 30). Note that the wet or flushy site does not present a strong relationship between concentration and flow when compared to the dry site (see Figure 29(b) and Figure 30(b)).

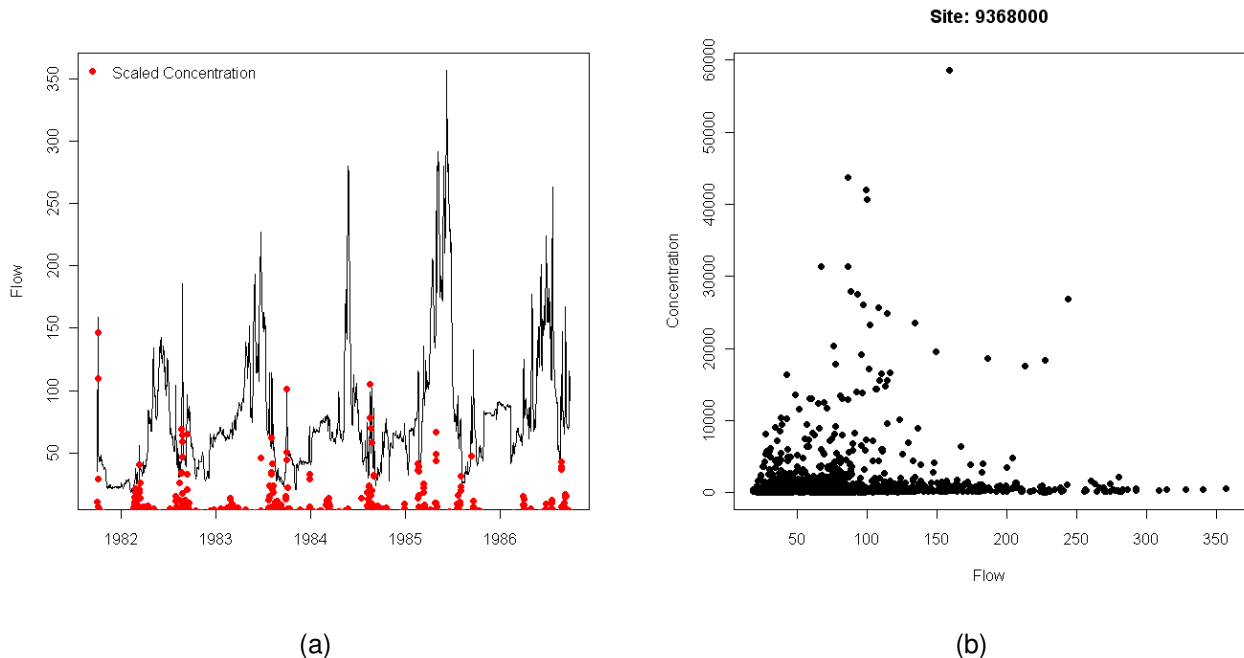


Figure 29: Plots for a wet site (Station 9368000) extracted from the USGS database which show (a) flow and concentration for the last 5 years and (b) the relationship between concentration and flow.

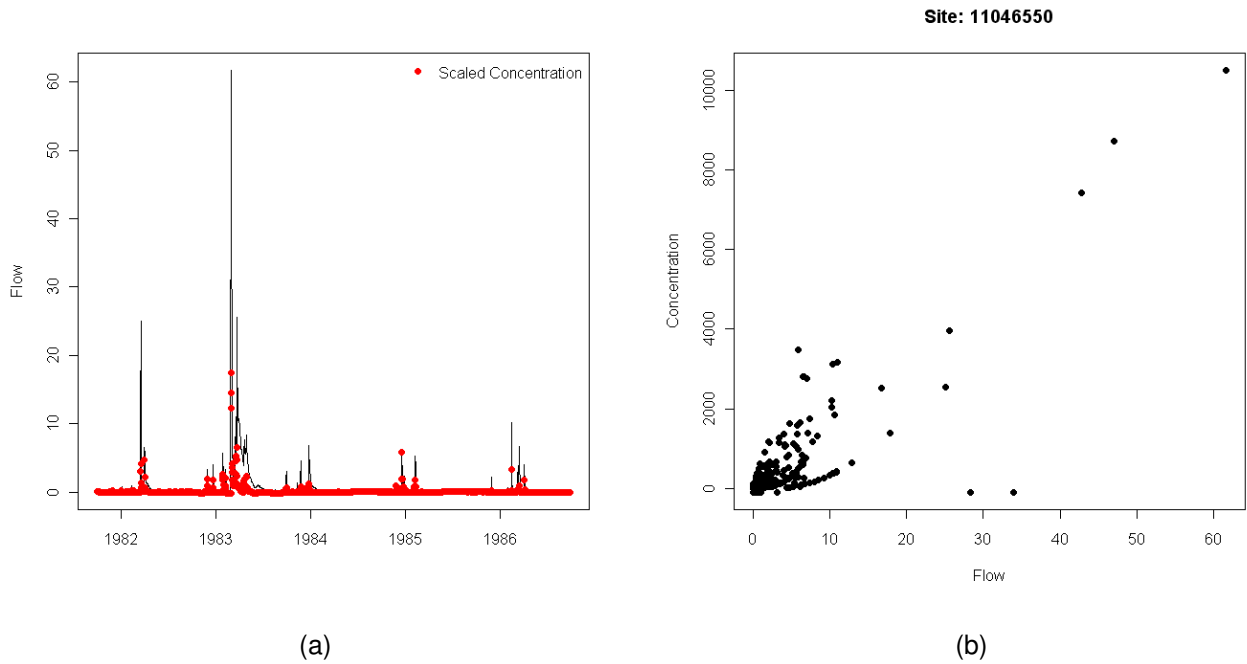


Figure 30: Plots for a dry site (Station 11046550) extracted from the USGS database which show (a) flow and concentration for the last 5 years and (b) the relationship between concentration and flow.

6.1 Simulation Study

We conducted a preliminary simulation study to investigate the performance of the methodology outlined in Section 3 and compared it to four standard loads estimators: Average, Extrapolation, Beale and Ratio estimators. We based the simulation study on the last 5 years worth of data purely for computational convenience. We investigated five different GAM models in this simulation study and these are summarised in Table 17. Note that other models which include interactions could be investigated but we limit the investigation to these 5 models for this study.

Data was simulated probabilistically using the following equation,

$$p_s = (p_H - p_L) \left(\frac{1}{1 + \exp\left\{-\frac{(aQ)}{[Q_{\min} + b(Q_{\max} - Q_{\min})] + a}\right\}} \right) + p_L \quad (8)$$

where p_s represents the probability of the concentration value associated with discharge, Q being retained in the dataset; Q represents the discharge value, Q_{\min} and Q_{\max} represents the minimum and maximum discharge values respectively in the dataset; p_H represents the maximum desired probability of retaining within the dataset a concentration value associated with an "event" grade discharge (i.e. function asymptotes to this value with increasing discharge), represents the minimum desired probability of retaining within the dataset a concentration value associated with an *event* grade discharge (i.e. the function asymptotes

Table 17: Summary of generalised additive models (GAM) fit in the simulation study. A tick indicates that the term was fit in the model.

Model	Intercept	$\log(Q)$	$\log(Q^2)$	Periodic	Rising/Falling Limb	Discounted Flow	Correlation
GAM1	✓	✓	✓	✓	✓	✓	✓
GAM2	✓	✓	✓	✓	✓	✓	
GAM3	✓	✓	✓				
GAM4	✓						
GAM5	✓				✓		

to this value with decreasing discharge); a controls the rate of change of p_s around the inflection point and b controls the location of the inflection point or the *event* threshold. In this study we define an event day as one where flow exceeds the 90th percentile daily discharge. Note this simulation approach results in an n (number of samples) that is variable across the entire set of simulations.

We investigated five scenarios for each site. These scenarios are summarized in Table 18 and represent

1. *stratified sampling*: sampling is stratified such that event-days are sampled more frequently than ambient-flow-days.
2. *event only monitoring*: proportion of *event* class flow-days that are sampled ensuring no ambient sampling is conducted.
3. equal rates of ambient and event based monitoring
4. ambient only monitoring
5. community based sampling: reflects the way in which community samples are undertaken (i.e. few samples taken at large events).

Table 18: Parameters used to simulate the five different scenarios investigated in the simulation study.

Sampling Scenario	p_H	p_L	a	b
Stratified (80/10)	0.8	0.1	10	0.2
Event Only (100/0)	1	0	10	0.2
Stratified (50/50)	0.5	0.5	10	0.2
Ambient Only (0/3.3)	0	0.033	150	0.2
Community	1	0	10	0.2

For each type of catchment we conducted 1000 simulations, from which, we calculated the mean square error (MSE) for each of the GAMs models shown in Table 17 and the four standard estimators investigated. We assume measurement error is zero for all simulations for the purpose of making comparisons. We summarise the results for each simulation scenario below.

6.1.1 Simulations of a wet site

Figure 31 and Figure 32(a) summarises the five sampling scenarios investigated for the wet site chosen from the USGS dataset (samples are shown in blue along the time series). The ambient only scenario selects on average 46 samples across the 5 years or 12 per year. Note, we would typically expect 60 samples to be selected on average as it represents monthly sampling however part of 1987 was not available. The event only scenario selects on average 260 samples across the 5 year period while stratified (80/3.3) sampling selects on average 445 samples while the stratified (20/20) selects approximately 338 samples. Community based monitoring selects approximately 46 samples across the 5 year period due to the number of *flushes* that occur throughout the period.

We summarise the results from the simulation in Table 19 and Figures 33 and 34 which highlights the best models as indicated by the mean square error calculated across the 1000 simulations. Results are presented by water year and to simplify results we placed a tick in the table cell where a group of models was found to perform well (i.e. have a low MSE). The groups correspond to G (Any of the GAM models presented in Table 17), R (either the ratio or Beale estimator) and A (either the average or extrapolation estimators). If any of the models in these groups was found to perform well, a tick was placed in the cell of the table otherwise it was left blank.

The results show some variability between years, sampling scenarios and methods however, it is clear that across most years the generalised additive models investigated perform reasonably well and in fact, for event only scenarios outperform the ratio and average based estimators. It is hardly surprising that the majority of methods perform well in ambient only situations. In this scenario we find the GAM4 (equivalent to average based estimator) and GAM5 models to give comparable results to the average and ratio based estimators.

6.1.2 Simulations of a dry site

Figure 35 and Figure 32(b) summarise the five sampling scenarios investigated for the dry site chosen from the USGS dataset (samples are shown in blue along the time series). The ambient only scenario selects on

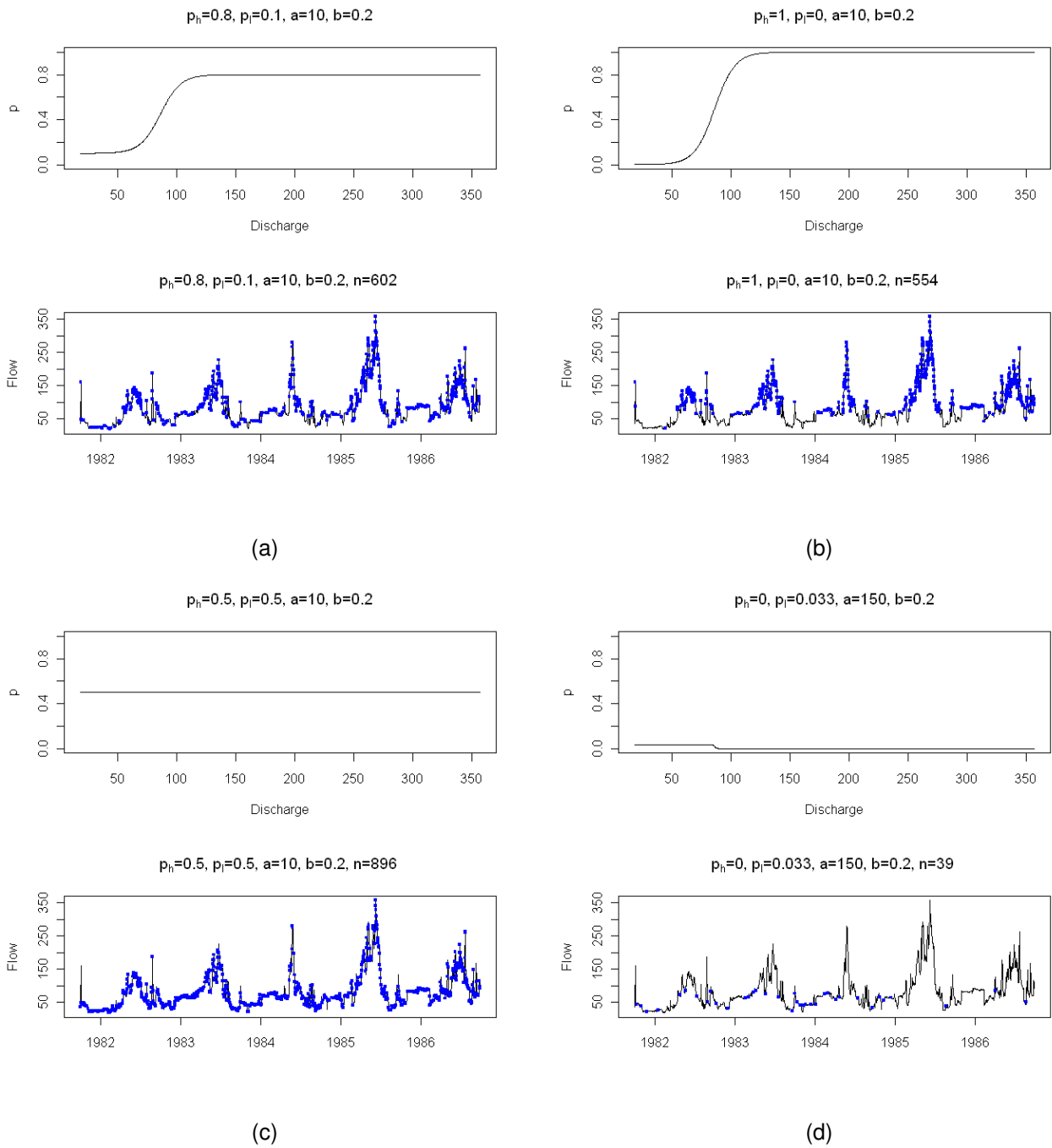


Figure 31: Sampling scenarios generated for a wet catchment site using the USGS data based on (a) stratified (80/10), (b) event only, (c) stratified (50/50) and (d) ambient only sampling.

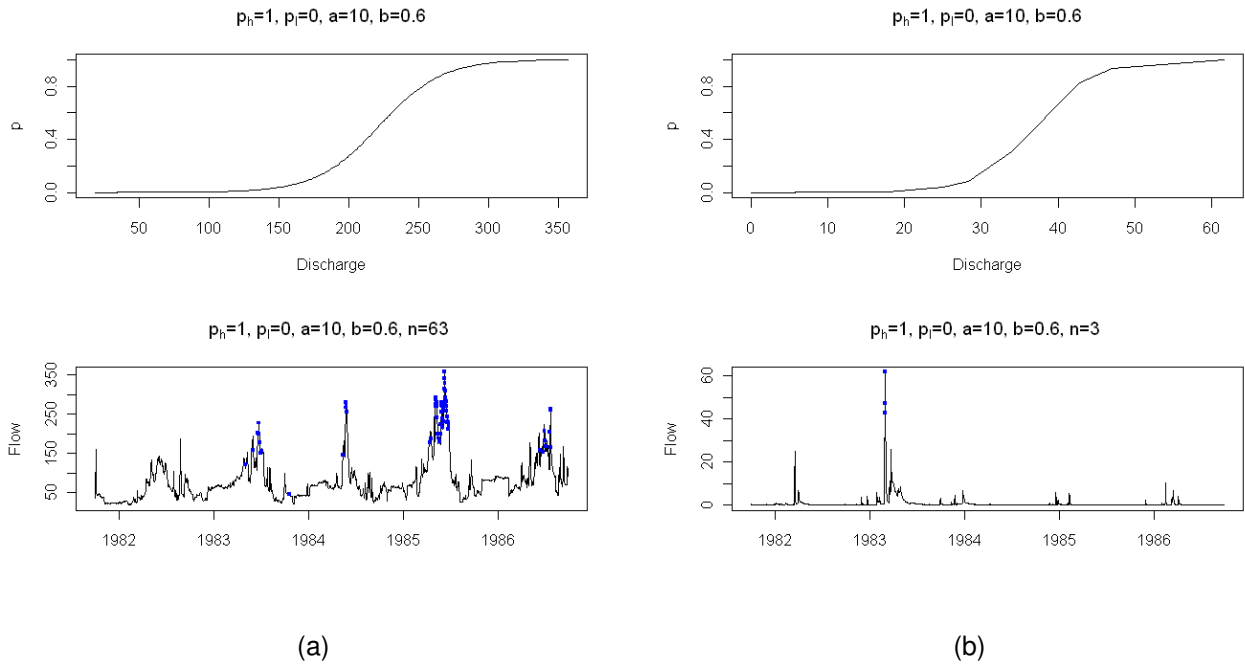


Figure 32: Sampling scenarios generated for (a) a wet catchment site and (b) a dry catchment site using the USGS data based on community sampling

Table 19: Summary of results by year from the wet catchment scenarios where we highlight the *best models* representing those with low mean square errors reported from the simulation study. Models are grouped into 3 types: GAM (G), Ratio (R) and Average (A).

Sampling Scenario	Year														
	81/82			82/83			83/84			84/85			85/86		
	G	R	A	G	R	A	G	R	A	G	R	A	G	R	A
Stratified (80/3.3)	✓			✓	✓		✓	✓		✓					✓
Event Only (50/0)	✓			✓			✓			✓					✓
Stratified (20/20)	✓		✓			✓			✓			✓			✓
Ambient Only (0/3.3)	✓	✓	✓	✓	✓	✓	✓		✓	✓	✓				✓
Community	✓			✓				✓			✓				✓

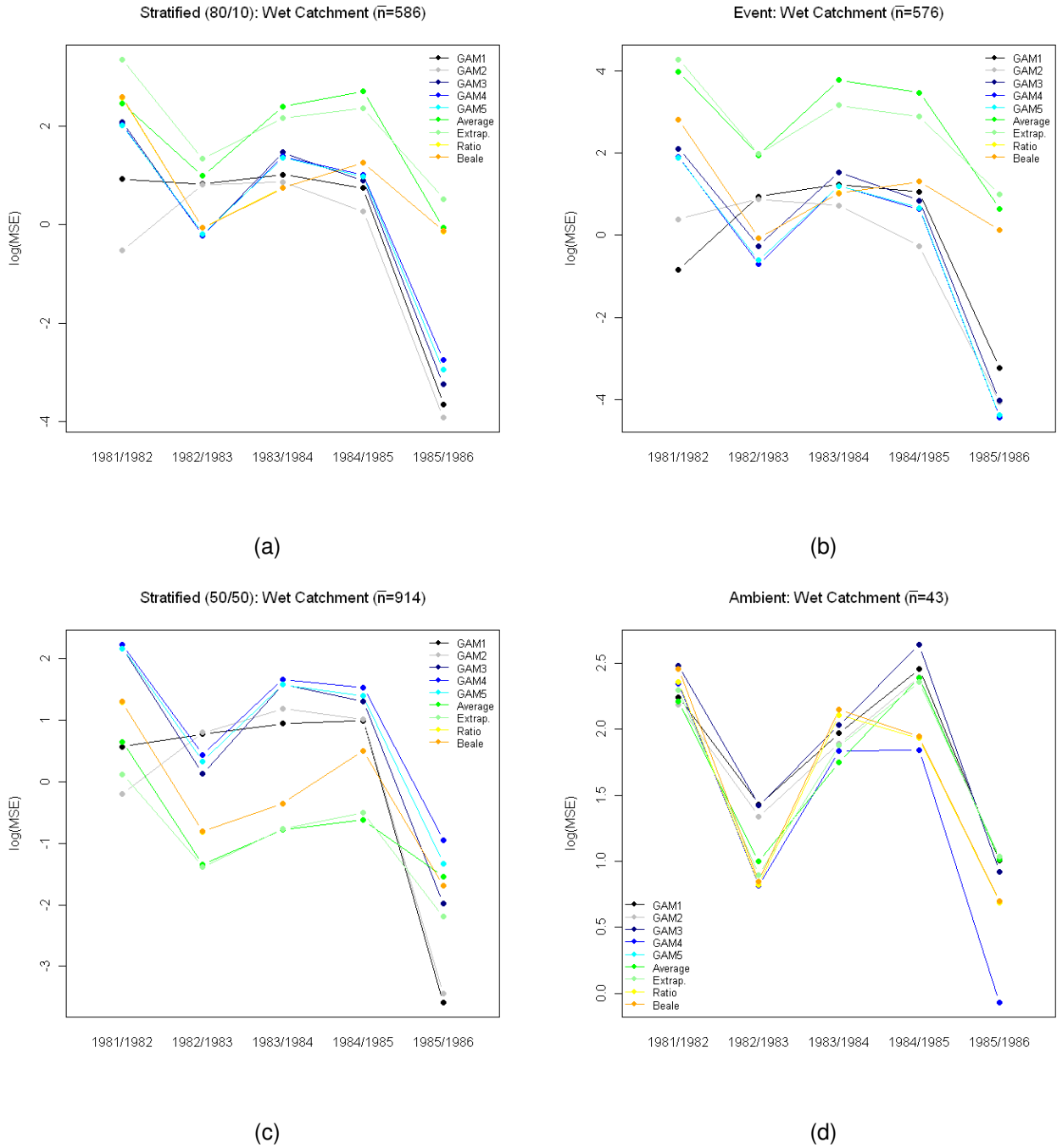


Figure 33: Plots showing the MSE (on the log scale) from all models fitted in (a) the stratified (80/10), (b) event only, (c) stratified (20/20) and (d) ambient only scenarios for the wet catchment.

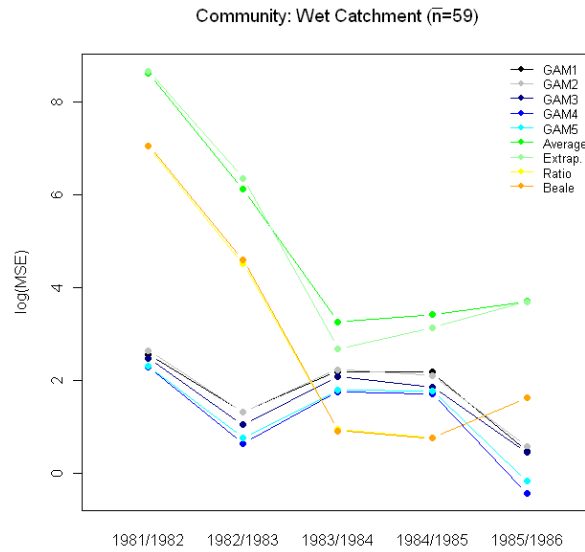


Figure 34: Plots showing the MSE (on the log scale) from all models fitted in the community sampling scenario for the wet catchment.

average 60 samples across the 5 years or 12 per year as it represents monthly sampling, while the event based scenario for this site targets approximately 12 samples across the 5 year period due to the small number of "events" that occurred. Stratified (80/10) sampling selects on average 190 samples while the stratified (50/50) selects approximately 913 samples. Community based monitoring selects approximately 3 samples across the 5 year period. These samples tend to be related to the large event in 1983 as shown in Figure 30.

We summarise the results from the simulation in Table 20 and Figures 36 and 37 which highlights the best models as indicated by the mean square error calculated across the 1000 simulations. Results are presented by water year similar to those presented for the wet site, i.e. we placed a tick in the table cell where a group of models was found to perform well (i.e. have a low MSE).

The results for the dry catchment are quite contrasting to the wet catchment. Little variability is shown between years, sampling scenarios and methods, apart from the event only and community sampling scenarios. Overall, the majority of methods perform well. In event only situations however, the GAM and ratio methods performed the best.

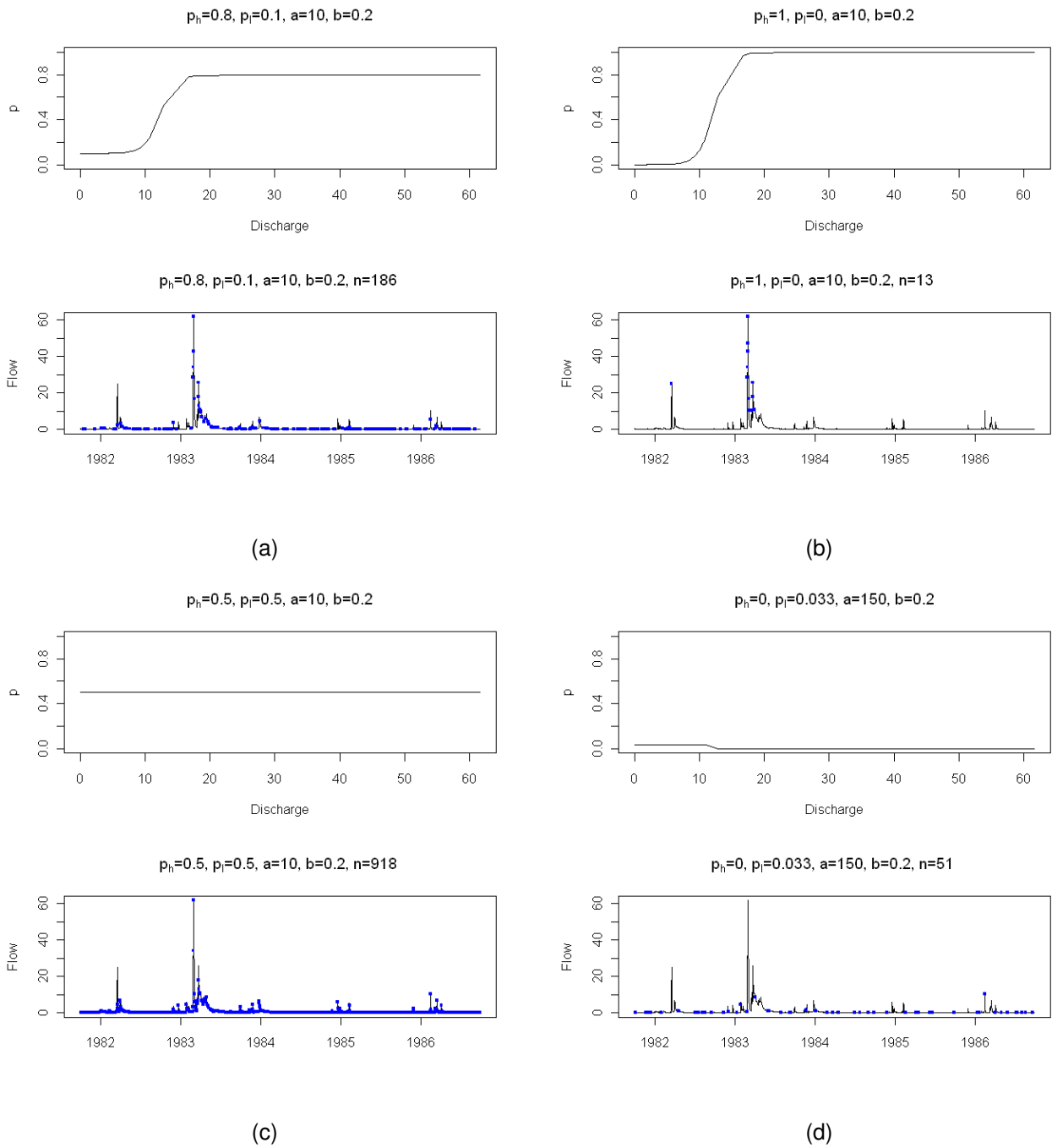


Figure 35: Sampling scenarios generated for a dry catchment site using the USGS data based on (a) stratified 80/10, (b) event only, (c) stratified 50/50 and (d) ambient only sampling.

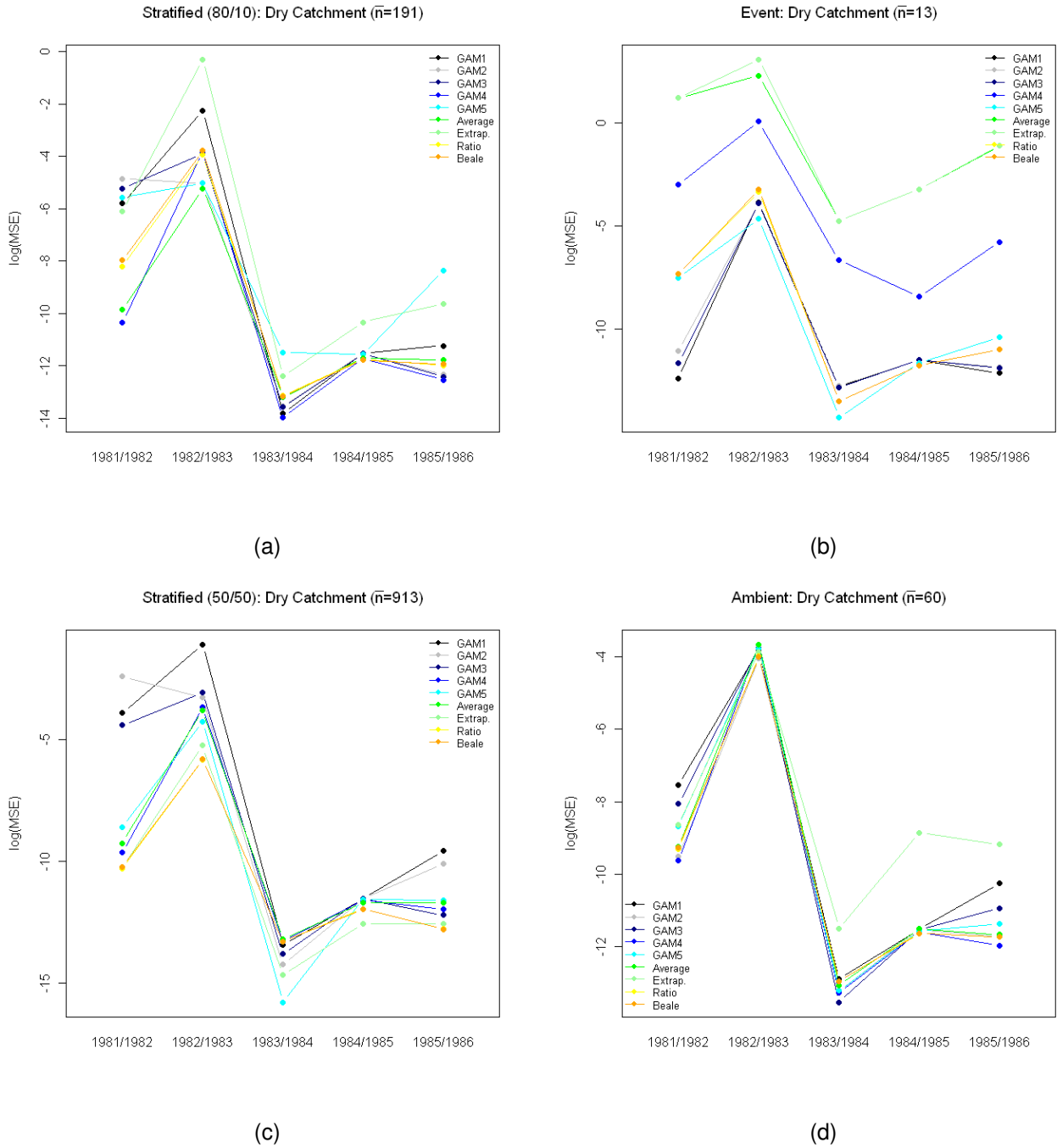


Figure 36: Plots showing the MSE (on the log scale) from all models fitted in (a) the stratified (80/10), (b) event only, (c) stratified (50/50) and (d) ambient only scenarios for the dry catchment.

Table 20: Summary of results by year from the dry catchment scenarios where we highlight the *best models* representing those with low mean square errors reported from the simulation study. Models are grouped into 3 types: GAM (G), Ratio (R) and Average (A).

Sampling Scenario	Year														
	81/82			82/83			83/84			84/85			85/86		
	G	R	A	G	R	A	G	R	A	G	R	A	G	R	A
Stratified (80/10)	✓		✓	✓		✓	✓	✓	✓	✓	✓	✓	✓		
Event Only (100/0)	✓			✓	✓		✓	✓		✓	✓		✓	✓	
Stratified (50/50)	✓	✓	✓		✓	✓	✓	✓	✓	✓	✓	✓	✓	✓	✓
Ambient Only (0/3.3)	✓	✓		✓	✓	✓	✓	✓	✓	✓	✓	✓	✓	✓	✓
Community	✓	✓		✓	✓		✓	✓	✓	✓	✓	✓	✓	✓	

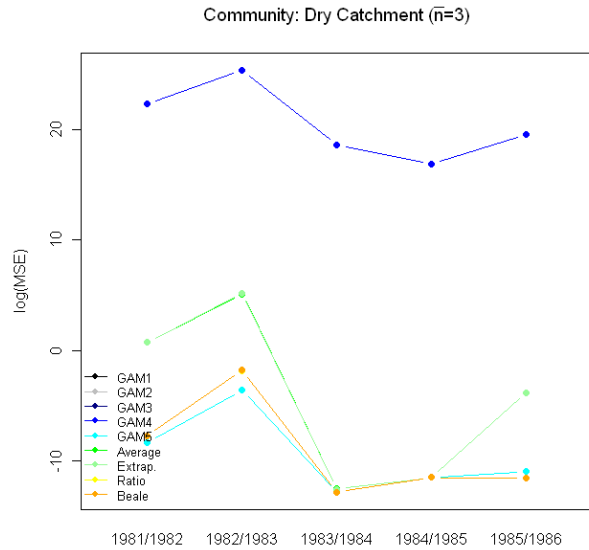


Figure 37: Plots showing the MSE (on the log scale) from all models fitted in the community sampling scenario for the wet catchment.

6.2 Conclusions

This simulation study presents work in progress and requires some further investigation and fine tuning of the approach. In particular,

- We need to obtain confirmation about the sites chosen in the USGS that adequately reflect wet and dry sites in the GBR so adequate comparisons can be made.
- We need to obtain confirmation about the data simulation scenarios that are chosen to reflect different types of sampling regimes used in practice to ensure our results and conclusions about methodologies are realistic.

Once these items are assured we can adequately comment on current sampling designs and make some recommendations regarding the frequency and number of samples to take at a site that is characterised by the intensity of flow (i.e. wet or dry). Initial results are promising as the new methodology seems to work well if not better than standard loads estimators, particularly for wet catchments.

7 DISCUSSION

In this final report, we have developed and demonstrated a regression approach through simulation and application that appears to be flexible enough for predicting concentration and calculating a load for a range of datasets with varying flow and concentration characteristics.

It is clear from the models fit to the Tully and Burdekin sites that there is no one regression model that can be fit to all datasets. The relationship between flow and concentration and the nature of the sampling undertaken will dictate the type of model required. In some situations, a model with flow and concentration only will provide an adequate model, however in other situations, although there may not be an obvious relationship between flow and discharge, other variables such as the discounted flow or rising/falling limb may be important. For sites with limited sampling a linear term for flow may be suitable. These terms need to be thoroughly investigated in any modelling exercise undertaken and it is recommended that standard diagnostics plots in addition to examining the GCV score and % deviance explained from the model is required to ensure the model fit is adequate and problems such as overfitting are not experienced.

As identified in earlier reports (Kuhnert et al., 2008), regression estimators can be highly biased, especially if systematic sampling is used in an event responsive system (Preston et al., 1992). Preston et al. (1989) also found that estimates of load produced via a regression approach can be less accurate than those produced by the ratio estimator if a small number of samples are collected and the relationship is not well understood. However, in these examples, other covariates were not explored and the models were based predominantly on functions of flow. Despite this, regression-based estimates improve when adequate sampling has been undertaken over a vast range of conditions, thus providing the best estimates with low error.

Some may argue in instances where the regression based estimators are estimating a load similar to the standard load based estimators that there is no need to change to a regression based estimator. However, the focus of this report has not only been around the load based estimator and the actual estimate of total load, but the corresponding estimate of the uncertainty around that load. In our investigations, we have been able to demonstrate a method that is able to include and account for different forms of error to produce a confidence interval for the load. Furthermore, in situations where multiple years worth of data have been collected for a site, the GAM model has the capacity to incorporate all data, incorporate trend and seasonal terms as well as other terms that capture some of the common hydrological characteristics of these river systems. Interpretation of these characteristics can then be visualised and inferences can be drawn accordingly.

8 CONCLUSIONS AND FUTURE WORK

The following conclusions can be drawn from this analysis:

1. Depending on the nature of the sampling and assumptions about measurement and spatial error, the coefficient of variation CV can be as low as 5% (heavily sampled) and as high as 80% (community based datasets).
2. We found that loads estimates were similar to standard ratio based estimators at sites where sampling bias was minimal (e.g. Inkerman Bridge, Burdekin) but much smaller when the bias was large (e.g. Tully). The regression based methodology offers a novel way of capturing all forms of bias and uncertainty that we believe leads to a more robust estimate of the load compared to other estimators. The average based estimators consistently estimated a higher load compared to the modelled based estimators except when samples were taken at regularly based intervals and the only significant term fitted in the model was the constant term (e.g. Mistake Creek).
3. The generalised regression based approach is general enough to incorporate a range of different models from models involving just flow to more complicated models that incorporate other covariates (e.g. rising/falling limb, discounted cumulative flow) and possibly interaction terms. Different covariates may be important in different catchments because the underlying hydrological and catchment processes vary and their contribution in a model can be graphically explored to determine the reason why a large load has been estimated in any particular water year. This represents a novel feature of the regression based approach not offered by standard load based estimators.
4. Serial correlation may also be an issue and needs to be accounted for where appropriate as high correlations can lead to larger standard errors.
5. Sites with small numbers of concentration samples can also be modelled, although the number and type of covariates incorporated into the model are limited. At worst, the model defaults to the popular average type estimator.
6. Stochastic uncertainty is adequately dealt with by predicting concentration at regular flow intervals and estimating the load accordingly. This eliminates unwanted bias effectively.
7. The regression approach allows us to borrow strength across years to characterise relationships better and improve the estimation of loads, particularly in years where sampling is poor.
8. The framework presented here is general enough to be applied to all GBR catchments.

We have targeted a number of areas of future work which will help to operationalise the methodology presented here. These are outlined below.

- **[TASK1]** Further validation of the methodology through simulation is required. We have performed a preliminary investigation of the methodology through a simulation exercise in this report but some further fine tuning of parameters are required (e.g. choice of discounting, percentile for defining a "flush", evaluating redundancy and whether all process representations are required, additional covariates). Selection of suitable datasets for simulation also requires discussion with key stakeholders (QDERM and JCU) to ensure they are representative of catchments in the GBR and whether other Australian longterm datasets are available may be more suitable, or whether "true load" measurements are available with which to validate the sample-based modelling methods (eg continuous turbidity for sediment).
- **[TASK2]** Investigate how new data consisting of new sites over other monitoring years can be incorporated into the analysis and how well existing models can predict concentration at these sites.
- **[TASK3]** Investigate computational issues for the standard error calculation. Currently for large datasets, the standard error calculation involves inverting a large matrix. Approaches that speed up the calculation of the standard error are of interest.
- **[TASK4]** Expand the simulation approach to investigate and inform current sampling regimes with the aim of having direct input into future monitoring schemes in the GBR.
- **[TASK5]** Operationalise methods through workshops and interactions with key stakeholders (QDERM and JCU) using case studies in the GBR (e.g. Burdekin & Tully).
- **[TASK6]** Focus on the interpretation of the model outputs and the reporting of loads.
- **[TASK7]** Publishing results in a number of applied and theoretical publications to provide greater confidence in the methods via peer review. Currently we have one publication in the Modelling and Simulation (MODSIM) conference and a second paper in the pipeline that outlines the methodology intended for submission into *Water Resources Research*.

References

Amos, K., Alexander, J., Horn, A., Pocock, G. & Fielding, C. (2004), 'Supply limited sediment transport in a high discharge event of the tropical Burdekin River, North Queensland Australia', *Sedimentology* **51**, 145–162.

- Bainbridge, Z. (2006), GBR catchments water quality monitoring (field, lab and loads) methodology workshop, a joint initiative between wqsip, actfr/csiro collaboration project and the reef water quality partnership, Technical report, Riverglenn Conference Centre.
- Bartley, B., Hawdon, A. & Keen, R. (2007), Sediment and nutrient loads at the Myuna gauge in the Bowen catchment (2006/07). client report, Technical report, CSIRO Land and Water, Brisbane Australia.
- Baun, K. (1982), 'Alternative methods of estimating pollutant loads in flowing water'.
- Belperio, A. (1979), 'The combined use of wash load and bed material load rating curves for the calculation of total load: an example from the Burdekin River, Australia.', *Catena* **6**, 317–329.
- Brodie, J., De'ath, G., Devlin, M., Furnas, M. & Wright, M. (2007), 'Spatial and temporal patterns of near-surface chlorophyll a in the Great Barrier Reef lagoon', *Marine and Freshwater Research* **58**(4), 342–353.
- Cohn, T., Caulder, D., Gilroy, E., Zynjuk, L. & Summers, R. (1992), 'The validity of a simple statistical model for estimating fluvial constituent loads: an empirical study involving nutrient loads entering Chesapeake Bay', *Water Resources Research* **28**(9), 2353–2363.
- Degens, B. & Donohue, R. (2002), Sampling mass loads in rivers: a review of approaches for identifying evaluating and minimising estimation errors, Technical report, Aquatic Science Branch, Resource Science Division, Water and Rivers Commission.
- Duan, N. (1983), 'Smearing estimate: A nonparametric retransformation method'.
- Etchells, T., Tan, K. & Fox, D. (2005), Quantifying the uncertainty of nutrient load estimates in the shepparton irrigation region, in A. Zerger & R. Argent, eds, 'MODSIM 2005 International Congress on Modelling and Simulation', Modelling and Simulation Society of Australia and new Zealand, Melbourne Australia, pp. 170–176.
- Ferguson, R. I. (1986), 'Hydraulics and hydraulic geometry'.
- Fielding, C. & Alexander, J. (1996), 'Sedimentology of the upper Burdekin River of North Queensland, Australia an example of a tropical, variable discharge river.', *Terra Nova* **8**, 447–457.
- Fox, D. (2004), Statistical considerations for the modelling and analysis of flows and loads, Technical report, Australian Centre for Environmetrics.
- Fox, D. (2005), Protocols for the optimal measurement and estimation of nutrient loads: Error approximations, Technical report, Australian Centre for Environmetrics.

- Furnas, M. (2003), *Catchments and corals: Terrestrial runoff to the Great Barrier Reef*, Australian Institute of Marine Science, Townsville, Queensland, Australia.
- Guo, Y. P., Markus, M. & Demissie, M. (2002), 'Uncertainty of nitrate-n load computations for agricultural watersheds', *Water Resources Research*.
- Harmel, R., Cooper, R., Slade, R., Haney, R. & Arnold, J. (2006), 'Cumulative uncertainty in measured streamflow and water quality data for small watersheds', *Transactions of the American Society of Agricultural and Biological Engineers* **49**, 689–701.
- Johnes, P. (2007), 'Uncertainties in annual riverine phosphorus load estimation: Impact of load estimation methodology, sampling frequency, baseflow index and catchment population density', *Journal of Hydrology* **332**, 241–258.
- Karim, F., Wallace, J., Henderson, A. & Wilkinson, S. (2008), Assessment of sediment and nutrient transport across the Tully-Murray floodplain using the SedNet and ANNEX models, science report no 60/08, Technical report, CSIRO Land and Water.
- Koch, R. W. & Smillie, G. M. (1986), 'Comment on "river loads underestimated by rating curves" by r. i. ferguson'.
- Kuhnert, P. & Dovers, E. (2009), Clustering rivers in the Great Barrier Reef Catchments using flow and water quality metrics, preliminary report, Technical report, CSIRO Mathematical and Information Sciences.
- Kuhnert, P., Peterson, E., Rustomji, P., Henderson, B., Wang, Y.-G., Joo, M., De Hayr, R. & Catzikiris, S. (2008), Statistical methods for the estimation of annual pollutant loads from monitoring data: Review and synthesis for Great Barrer Reef Catchments, mtsrf 07/08 final report, Technical report, CSIRO.
- Letcher, R. A., Jakeman, A. J., Calfas, M., Linforth, S., Baginska, B. & Lawrence, I. (2002), 'A comparison of catchment water quality models and direct estimation techniques', *Environmental Modelling and Software* **17**(1), 77–85.
- Lewis, S., Shields, G., Kamber, B. & Lough, J. (2007), 'A multi-trace element coral record of land-use changes in the Burdekin River catchment, NE, Australia', *Palaeogeography, Palaeoclimatology, Palaeoecology* **246**, 471–487.
- McCulloch, M., Fallon, S., Wyndham, T., Hendy, E., Lough, J. & Barnes, D. (2003), 'Coral record of increased sediment flux to the inner Great Barrier Reef since European settlement', *Nature* **421**, 727–730.

- Mitchell, A. & Furnas, M. (1997), Terrestrial inputs of nutrients and suspended-sediments to the GBR lagoon., *in* 'The Great Barrier Reef: Science, Use and Management A National Conference', Vol. 1, James Cook University of North Queensland, Townsville, Australia, pp. 59–71.
- Mitchell, A., Furnas, M., De'Ath, G., Brodie, J. & Lewis, S. (2006), A report into the water quality condition of the Burdekin River and surrounds based on the AIMS end-of-catchment sampling program, Technical report, ACTFR Report 06/06.
- Moss, A., Rayment, G., Reilly, N. & Best, E. (1992), A preliminary assessment of sediment and nutrient exports from Queensland coastal catchments., Technical report, Queensland Government.
- Neil, D. & Yu, B. (1996), Fluvial sediment yield to the Great Barrier Reef lagoon: Spatial patterns and the effect of land use, *in* H. Hunder, A. Eyles & G. Rayment, eds, 'Downstream Effects of Land Use', Department of Natural Resources, Queensland Australia, pp. 281–286.
- Nistor, C. & Church, M. (2005), 'Suspended sediment transport regime in a debris-flow gully on Vancouver Island, British Columbia', *Hydrological Processes* **19**(4), 861–885.
- Olsen, M., Farrow, R. & Jolly, P. (2004), Report on the accuracy of hydsys generated flow data for gauging stations in the Daly River catchment, Technical report, Northern Territory Department of Infrastructure, Planning and Environment.
- Phillips, J., Webb, B., Walling, D. & Leeks, G. (1999), 'Estimating the suspended sediment load of rivers in the LOIS study area using infrequent samples', *Hydrological Processes* **13**, 1035–1050.
- Preston, S., Bierman, J. V. & Silliman, S. (1992), 'Impact of flow variability on error in estimation of tributary mass loads', *Journal of Environmental Engineering* **118**, 402–418.
- Preston, S., Bierman, V. & Silliman, S. (1989), 'An evaluation of methods for the estimation of tributary mass loads'.
- Rayment, G. & Neil, D. (1996), Sources of material in river discharge, *in* 'The Great Barrier Reef: Science, Use and Management a National Conference', Vol. 1, James Cook University of North Queensland, Townsville, Australia., pp. 42–58.
- Rustomji, P. & Wilkinson, S. (2008), 'Applying bootstrap resampling to quantify uncertainty in fluvial suspended sediment loads estimated using rating curves', *Water Resources Research* **44**, doi:10.1029/2007WR006088.

- SOQ (2003), Reef water quality protection plan: For catchments adjacent to the Great Barrier Reef world heritage area, Technical report, The State of Queensland and Commonwealth of Australia, Queensland Department of Premier and Cabinet.
- Tan, K., Fox, D. & Etchells, T. (2005), 'GUMLEAF: Generator for uncertainty measures and load estimates using alternative formulae, user guide and reference manual'.
- Tarras-Wahlberg, N. & lane, S. (2003), 'Suspended sediment yield and metal contamination in a river catchment affected by el nino events and gold mining activities: the Puyango River basin, southern Ecuador', *Hydrological Processes* **17**, 3101–3123.
- Thomas, R. & Lewis, J. (1995), 'An evaluation of flow-stratified sampling for estimating suspended sediment loads', *Journal of Hydrology* **170**(1-4), 27–45.
- Wallace, J., Stewart, L., Hawdon, A. & Keen, R. (2008), 'The role of coastal floodplains in generating sediment and nutrient fluxes to the Great Barrier Reef lagoon in australia'.
- Walling, D. & Webb, B. (1981), 'The reliability of suspended sediment load data'.

A Loads Estimates for Inkerman Bridge, Burdekin Catchment

Estimates of TSS and NO_x are presented from the Inkerman Bridge site in the Burdekin catchment for a range of error structures. In each table we present the estimated load, \hat{L} , the corrected load, \hat{L}_c (corrected for bias), the standard error, SE of the corrected load, the coefficient of variation, CV represented as a percentage, the number of concentration records observed, n and the lower (CI_L) and upper (CI_U) 95% confidence intervals. The error structures investigated for α_1 (measurement error) and α_2 (spatial error) are as follows:

1. Error Structure 1: No measurement or spatial error ($\alpha_1 = 0, \alpha_2 = 0$)
2. Error Structure 1: Mild measurement and spatial error ($\alpha_1 = 0.1, \alpha_2 = 0.05$)
3. Error Structure 1: Moderate measurement and spatial error ($\alpha_1 = 0.3, \alpha_2 = 0.1$)
4. Error Structure 1: Large measurement and spatial error ($\alpha_1 = 0.5, \alpha_2 = 0.2$)

A LOADS ESTIMATES FOR INKERMAN BRIDGE, BURDEKIN CATCHMENT

Table 21: Estimates of (a) the total TSS load (Mt) and (b) NOx load (t) assuming error structure 1 ($\alpha_1 = 0, \alpha_2 = 0$).

Water Year	\hat{L}	\hat{L}_c	SE	CV (%)	n	CI_L	CI_U
1987/1988	3.148	3.497	1.35	38.5	0	1.64	7.44
1988/1989	8.323	8.804	3.98	45.2	0	3.63	21.36
1989/1990	4.230	4.827	0.72	14.9	3	3.60	6.47
1990/1991	37.786	40.198	14.54	36.2	2	19.78	81.69
1991/1992	0.049	0.055	0.01	19.1	1	0.04	0.08
1992/1993	0.053	0.059	0.01	18.5	0	0.04	0.09
1993/1994	1.035	1.189	0.21	17.4	0	0.85	1.67
1994/1995	0.078	0.089	0.01	15.2	0	0.07	0.12
1995/1996	0.684	0.784	0.15	19.6	19	0.53	1.15
1996/1997	5.557	6.301	1.33	21.0	78	4.17	9.52
1997/1998	8.612	9.132	3.93	43.1	39	3.93	21.24
1998/1999	1.412	1.630	0.19	11.6	70	1.30	2.05
1999/2000	5.831	6.677	1.04	15.6	100	4.92	9.07
2000/2001	1.153	1.326	0.23	17.2	0	0.95	1.86

(a)

Water Year	\hat{L}	\hat{L}_c	SE	CV (%)	n	CI_L	CI_U
1987/1988	461.962	775.856	308.86	39.8	0	355.57	1692.95
1988/1989	1316.849	2220.766	676.3	30.5	3	1222.58	4033.92
1989/1990	1603.689	2723.637	815.32	29.9	3	1514.74	4897.34
1990/1991	7220.078	12028.916	4196.74	34.9	6	6070.82	23834.49
1991/1992	18.38	31.009	7.67	24.7	34	19.09	50.37
1992/1993	21.012	35.47	10.28	29	26	20.1	62.6
1993/1994	353.695	605.492	211.24	34.9	110	305.59	1199.7
1994/1995	42.02	71.681	20.34	28.4	44	41.11	125
1995/1996	192.963	329.376	116.24	35.3	55	164.92	657.82
1996/1997	1341.801	2286.486	716.51	31.3	86	1237.16	4225.84
1997/1998	1249.699	2079.621	850.38	40.9	39	933.06	4635.08
1998/1999	699.026	1197.151	286.12	23.9	70	749.39	1912.45
1999/2000	2397.393	4081.377	1312.13	32.1	100	2173.44	7664.19
2000/2001	317.6	537.993	193.21	35.9	0	266.12	1087.62

(b)

Table 22: Estimates of (a) the total TSS load (Mt) and (b) NOx load (t) assuming error structure 2 ($\alpha_1 = 0.1, \alpha_2 = 0.05$).

Water Year	\hat{L}	\hat{L}_c	SE	CV (%)	n	CI_L	CI_U
1987/1988	3.148	3.497	1.42	40.6	0	1.58	7.76
1988/1989	8.323	8.804	4.16	47.2	0	3.49	22.21
1989/1990	4.23	4.827	0.86	17.9	3	3.4	6.86
1990/1991	37.786	40.198	15.65	38.9	2	18.75	86.2
1991/1992	0.049	0.055	0.01	19.1	1	0.04	0.08
1992/1993	0.053	0.059	0.01	18.6	0	0.04	0.09
1993/1994	1.035	1.189	0.23	19.5	0	0.81	1.74
1994/1995	0.078	0.089	0.01	15.3	0	0.07	0.12
1995/1996	0.684	0.784	0.17	21.4	19	0.52	1.19
1996/1997	5.557	6.301	1.5	23.8	78	3.95	10.05
1997/1998	8.612	9.132	4.12	45.2	39	3.77	22.13
1998/1999	1.412	1.63	0.22	13.6	70	1.25	2.13
1999/2000	5.831	6.677	1.28	19.1	100	4.59	9.72
2000/2001	1.153	1.326	0.26	19.6	0	0.9	1.95

(a)

Water Year	\hat{L}	\hat{L}_c	SE	CV (%)	n	CI_L	CI_U
1987/1988	461.962	775.856	309.684	39.9	0	354.83	1696.47
1988/1989	1316.849	2220.766	679.324	30.6	3	1219.32	4044.71
1989/1990	1603.689	2723.637	818.74	30.1	3	1511.02	4909.41
1990/1991	7220.078	12028.916	4202.367	34.9	6	6065.26	23856.34
1991/1992	18.38	31.009	7.842	25.3	34	18.89	50.91
1992/1993	21.012	35.47	10.425	29.4	26	19.94	63.1
1993/1994	353.695	605.492	212.052	35	110	304.79	1202.86
1994/1995	42.02	71.681	20.594	28.7	44	40.82	125.88
1995/1996	192.963	329.376	116.748	35.4	55	164.43	659.79
1996/1997	1341.801	2286.486	718.904	31.4	86	1234.62	4234.51
1997/1998	1249.699	2079.621	851.826	41	39	931.8	4641.39
1998/1999	699.026	1197.151	288.954	24.1	70	745.92	1921.35
1999/2000	2397.393	4081.377	1315.775	32.2	100	2169.64	7677.62
2000/2001	317.6	537.993	193.871	36	0	265.48	1090.24

(b)

A LOADS ESTIMATES FOR INKERMAN BRIDGE, BURDEKIN CATCHMENT

Table 23: Estimates of (a) the total TSS load (Mt) and (b) NOx load (t) assuming error structure 3 ($\alpha_1 = 0.3, \alpha_2 = 0.1$).

Water Year	\hat{L}	\hat{L}_c	SE	CV (%)	n	CI_L	CI_U
1987/1988	3.148	3.497	1.66	47.6	0	1.38	8.89
1988/1989	8.323	8.804	4.77	54.2	0	3.05	25.45
1989/1990	4.23	4.827	1.21	25	3	2.96	7.88
1990/1991	37.786	40.198	18.78	46.7	2	16.09	100.45
1991/1992	0.049	0.055	0.01	19.1	1	0.04	0.08
1992/1993	0.053	0.059	0.01	18.6	0	0.04	0.09
1993/1994	1.035	1.189	0.3	25.1	0	0.73	1.94
1994/1995	0.078	0.089	0.01	15.6	0	0.07	0.12
1995/1996	0.684	0.784	0.21	26.4	19	0.47	1.32
1996/1997	5.557	6.301	1.95	31	78	3.43	11.57
1997/1998	8.612	9.132	4.74	51.9	39	3.3	25.27
1998/1999	1.412	1.63	0.3	18.4	70	1.14	2.34
1999/2000	5.831	6.677	1.82	27.3	100	3.91	11.4
2000/2001	1.153	1.326	0.34	25.5	0	0.8	2.19

(a)

Water Year	\hat{L}	\hat{L}_c	SE	CV (%)	n	CI_L	CI_U
1987/1988	461.962	775.856	312.19	40.2	0	352.59	1707.25
1988/1989	1316.849	2220.766	688.4	31	3	1209.59	4077.25
1989/1990	1603.689	2723.637	829.01	30.4	3	1499.89	4945.83
1990/1991	7220.078	12028.916	4219.36	35.1	6	6048.49	23922.48
1991/1992	18.38	31.009	8.33	26.9	34	18.32	52.49
1992/1993	21.012	35.47	10.85	30.6	26	19.47	64.62
1993/1994	353.695	605.492	214.52	35.4	110	302.36	1212.52
1994/1995	42.02	71.681	21.35	29.8	44	39.98	128.52
1995/1996	192.963	329.376	118.28	35.9	55	162.94	665.82
1996/1997	1341.801	2286.486	726.13	31.8	86	1226.99	4260.84
1997/1998	1249.699	2079.621	856.24	41.2	39	927.93	4660.72
1998/1999	699.026	1197.151	297.34	24.8	70	735.75	1947.9
1999/2000	2397.393	4081.377	1326.77	32.5	100	2158.21	7718.27
2000/2001	317.6	537.993	195.87	36.4	0	263.55	1098.21

(b)

A LOADS ESTIMATES FOR INKERMAN BRIDGE, BURDEKIN CATCHMENT

Table 24: Estimates of (a) the total TSS load (Mt) and (b) NOx load (t) assuming error structure 4 ($\alpha_1 = 0.5, \alpha_2 = 0.2$).

Water Year	\hat{L}	\hat{L}_c	SE	CV (%)	n	CI_L	CI_U
1987/1988	3.148	3.497	2.31	66	0	0.96	12.74
1988/1989	8.323	8.804	6.38	72.5	0	2.13	36.47
1989/1990	4.23	4.827	2.05	42.6	3	2.1	11.12
1990/1991	37.786	40.198	27.54	68.5	2	10.49	153.97
1991/1992	0.049	0.055	0.01	19.2	1	0.04	0.08
1992/1993	0.053	0.059	0.01	18.8	0	0.04	0.09
1993/1994	1.035	1.189	0.47	39.8	0	0.54	2.59
1994/1995	0.078	0.089	0.01	16.7	0	0.06	0.12
1995/1996	0.684	0.784	0.31	40	19	0.36	1.72
1996/1997	5.557	6.301	3.13	49.7	78	2.38	16.68
1997/1998	8.612	9.132	6.44	70.6	39	2.29	36.41
1998/1999	1.412	1.63	0.5	30.9	70	0.89	2.99
1999/2000	5.831	6.677	3.15	47.1	100	2.65	16.81
2000/2001	1.153	1.326	0.55	41.1	0	0.59	2.97

(a)

1987/1988	461.962	775.856	321.86	41.5	0	344.08	1749.46
1988/1989	1316.849	2220.766	723.34	32.6	3	1172.87	4204.92
1989/1990	1603.689	2723.637	868.59	31.9	3	1457.77	5088.74
1990/1991	7220.078	12028.916	4286.14	35.6	6	5983.03	24184.2
1991/1992	18.38	31.009	10.03	32.3	34	16.45	58.45
1992/1993	21.012	35.47	12.42	35	26	17.86	70.44
1993/1994	353.695	605.492	223.98	37	110	293.24	1250.22
1994/1995	42.02	71.681	24.14	33.7	44	37.05	138.69
1995/1996	192.963	329.376	124.11	37.7	55	157.38	689.36
1996/1997	1341.801	2286.486	754.06	33	86	1197.97	4364.05
1997/1998	1249.699	2079.621	873.36	42	39	913.07	4736.56
1998/1999	699.026	1197.151	328.62	27.5	70	699.01	2050.28
1999/2000	2397.393	4081.377	1369.49	33.6	100	2114.38	7878.25
2000/2001	317.6	537.993	203.56	37.8	0	256.27	1129.41

(b)

B Loads Estimates for the Tully River at Euramo

Estimates of TSS and NO_x are presented from the Euramo site along the Tully River for a range of error structures. In each table we present the estimated load, \hat{L} , the corrected load, \hat{L}_c (corrected for bias), the standard error, SE of the corrected load, the coefficient of variation, CV represented as a percentage, the number of concentration records observed, n and the lower (CI_L) and upper (CI_U) 95% confidence intervals. The error structures investigated for α_1 (measurement error) and α_2 (spatial error) are as follows:

1. Error Structure 1: No measurement or spatial error ($\alpha_1 = 0, \alpha_2 = 0$)
2. Error Structure 1: Mild measurement and spatial error ($\alpha_1 = 0.1, \alpha_2 = 0.05$)
3. Error Structure 1: Moderate measurement and spatial error ($\alpha_1 = 0.3, \alpha_2 = 0.1$)
4. Error Structure 1: Large measurement and spatial error ($\alpha_1 = 0.5, \alpha_2 = 0.2$)

Table 25: Estimates of the total TSS load (Mt) assuming error structure 1 ($\alpha_1 = 0, \alpha_2 = 0$).

Water Year	\hat{L}	\hat{L}_c	SE	CV (%)	n	CI_L	CI_U
2000/2001	0.09	0.104	0.008	7.7	5	0.09	0.12
2001/2002	0.014	0.016	0.002	12.8	4	0.01	0.02
2002/2003	0.021	0.024	0.003	13.6	8	0.02	0.03
2003/2004	0.078	0.09	0.009	9.5	28	0.07	0.11
2004/2005	0.034	0.038	0.004	9.2	3	0.03	0.05
2005/2006	0.082	0.093	0.011	11.6	20	0.07	0.12
2006/2007	0.092	0.105	0.008	7.2	12	0.09	0.12
2007/2008	0.074	0.085	0.006	7.3	66	0.07	0.1

Table 26: Estimates of the total TSS load (Mt) assuming error structure 2 ($\alpha_1 = 0.1, \alpha_2 = 0.05$).

Water Year	\hat{L}	\hat{L}_c	SE	CV (%)	n	CI_L	CI_U
2000/2001	0.09	0.104	0.017	16.6	5	0.07	0.14
2001/2002	0.014	0.016	0.003	20.5	4	0.01	0.02
2002/2003	0.021	0.024	0.005	20.8	8	0.02	0.04
2003/2004	0.078	0.09	0.015	17	28	0.06	0.12
2004/2005	0.034	0.038	0.007	18.2	3	0.03	0.05
2005/2006	0.082	0.093	0.017	18.4	20	0.07	0.13
2006/2007	0.092	0.105	0.017	16.1	12	0.08	0.14
2007/2008	0.074	0.085	0.014	16	66	0.06	0.12

Table 27: Estimates of the total TSS load (Mt) assuming error structure 3 ($\alpha_1 = 0.3, \alpha_2 = 0.1$).

Water Year	\hat{L}	\hat{L}_c	SE	CV (%)	n	CI_L	CI_U
2000/2001	0.09	0.104	0.03	30.5	5	0.06	0.19
2001/2002	0.014	0.016	0.01	34.7	4	0.01	0.03
2002/2003	0.021	0.024	0.01	34.5	8	0.01	0.05
2003/2004	0.078	0.09	0.03	29.8	28	0.05	0.16
2004/2005	0.034	0.038	0.01	32.9	3	0.02	0.07
2005/2006	0.082	0.093	0.03	31.1	20	0.05	0.17
2006/2007	0.092	0.105	0.03	29.7	12	0.06	0.19
2007/2008	0.074	0.085	0.03	29.6	66	0.05	0.15

Table 28: Estimates of the total TSS load (Mt) assuming error structure 4 ($\alpha_1 = 0.5, \alpha_2 = 0.2$).

Water Year	\hat{L}	\hat{L}_c	SE	CV (%)	n	CI_L	CI_U
2000/2001	0.09	0.104	0.06	59.4	5	0.03	0.33
2001/2002	0.014	0.016	0.01	65.6	4	0	0.06
2002/2003	0.021	0.024	0.02	64.5	8	0.01	0.08
2003/2004	0.078	0.09	0.05	57.2	28	0.03	0.27
2004/2005	0.034	0.038	0.02	63.7	3	0.01	0.13
2005/2006	0.082	0.093	0.05	58.7	20	0.03	0.3
2006/2007	0.092	0.105	0.06	58	12	0.03	0.33
2007/2008	0.074	0.085	0.05	57.6	66	0.03	0.26

For further information:

CSIRO Mathematical and Information Sciences

Petra Kuhnert

Phone: +61 7 3826 7187

Email: Petra.Kuhnert@csiro.au

Web: www.csiro.au

Contact Us

Phone: 1300 363 400

+61 3 9545 2176

Email: enquiries@csiro.au

Web: www.csiro.au

Your CSIRO

Australia is founding its future on science and innovation. Its national science agency, CSIRO, is a powerhouse of ideas, technologies and skills for building prosperity, growth, health and sustainability. It serves governments, industries, business and communities across the nation.